Vol. 68 • No. 1

January 2025

Microwave® Journal

horizon house®
Founded in 1958
mwjournal.com

DORADO JQL FERROCOM

JQL ISOLATORS, CIRCULATORS, CERAMIC WAVEGUIDE FILTERS FOR RADAR

JQL had designed Isolators, Circulators & Waveguide ceramic filters with advanced materials & process in various topologies for enhanced radar system accuracy, range and reliability and to meet complex environment.

Critical Parameters

- High Power Handling Capability
- High Rejection for WG Cereamic Filters
- Low Insertion Loss
- Small Foot Print

Quality Management For Aerospace & Defense

- AS 9100 : 2016
- ISO 9001: 2015

Environment Management

- ISO 14001 : 2015

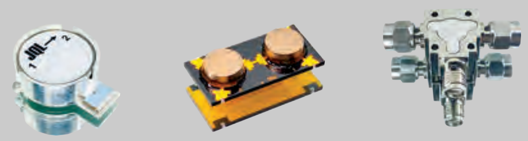

ISOLATORS & CIRCULATORS

SURFACE MOUNT, MICROSTRIP, DROP-IN, COAXIAL & WAVEGUIDES

MADE IN USA

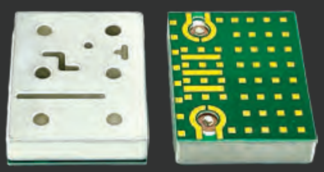

FILTERS & MULTIPLEXERS

CERAMIC WAVEGUIDE

US Operations
1255 Armour Blvd.,
Mundelein, IL 60060
USA

JQLTECHNOLOGIES.COM
DORADO-INTL.COM
FERROCOMRF.COM
SALES@JQLTECHNOLOGIES.COM

European Operations
Via Palazetti, 22
40068 San Lazzaro di Savena BO
ITALY

DC TO 110 GHz

RF & Microwave Test Accessories

One-Stop Shopping from R&D to Production

LEARN MORE

ADAPTERS
Coax & Waveguide

AMPLIFIERS
DC to 110 GHz

ATTENUATORS
DC to 65 GHz

GAUGES, CAL KITS & WRENCHES

BIAS TEES
0.1 MHz to 54 GHz

CABLES
Test Leads
& System Cables

COUPLERS
0.005 MHz to 65 GHz

DC BLOCKS
0.1 MHz to 65 GHz

EQUALIZERS
DC to 40 GHz

FILTERS
DC to 86 GHz

HYBRIDS, 90° & 180°
0.01 to 4200 MHz

IMPEDANCE MATCHING PADS
DC to 3000 MHz

LIMITERS
0.2 to 8200 MHz

MIXERS
0.0005 MHz to 65 GHz

MODULATORS & DEMODULATORS
1 to 200 MHz

MULTIPLIERS
0.05 MHz to 20 MHz

PHASE DETECTORS
1 MHz to 100 MHz

PHASE SHIFTERS
250 MHz to 430 MHz

POWER DETECTORS
10 MHz to 43.5 GHz

POWER SPLITTERS & COMBINERS
DC to 67 GHz

SWITCHES
DC to 67 GHz

TERMINATIONS
DC to 65 GHz

TRANSFORMERS & BALUNS
DC to 2500 MHz

Mini-Circuits®

Microwave Journal

CONTENTS

January 2025
Vol. 68 • No. 1
Radar & Antennas
mwjournal.com

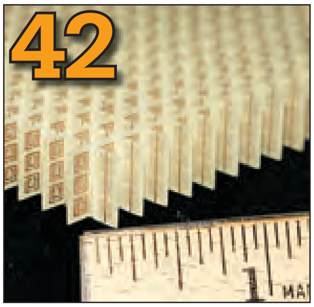

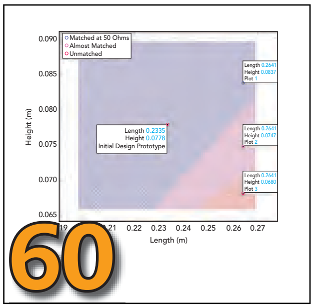

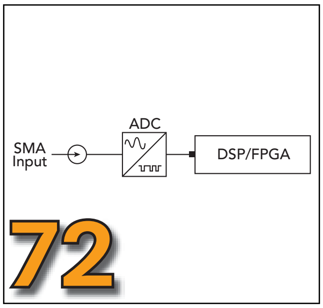

Cover Feature

Special Reports

Application Note

Tutorial

ACCESS NOW!
digital.microwavejournal.com

eXclusive Digital Content ›››

68 YEARS OF PUBLISHING EXCELLENCE

MILLER MMIC

AI Powered RFIC Design Platform

RapidRF

Revolutionizing RFIC Design with AI-Driven Innovation.
Our AI driven design platform is redefining the future of the RFIC design industry. We automate the design of RFICs for the next generation of wireless communication, accelerating innovation for a smarter future.

AI-Driven Design Automation – Multiplying Engineers Productivity

- Technology Independent: GaAs, GaN, and Silicon proven
- Fast and reliable: more than 100x faster than an experienced design engineer
- AI-Driven Layout Optimization: cutting down costs, maximizing performance

Reference Design Done by Experienced Engineer

≈10 Days/Design

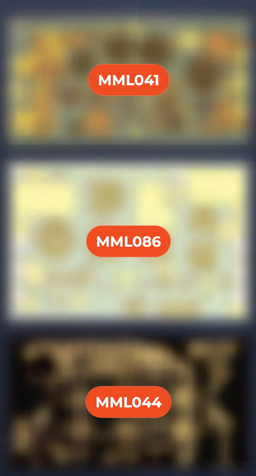

AI MMIC Design Process

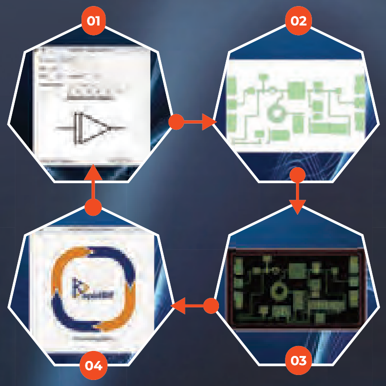

1. Set Design Target
2. Schematic & Layout Generation & Optimization
3. GDS Generation
4. Learning

Design Done by RapidRF AI Platform

≈5 Hours/Design

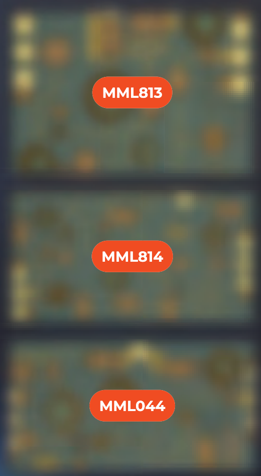

Performance Comparisons: RapidRF AI vs Human Engineer Designs

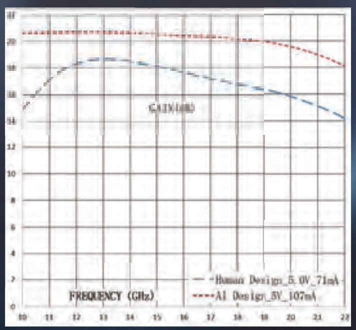

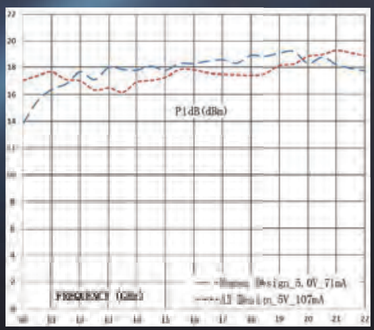

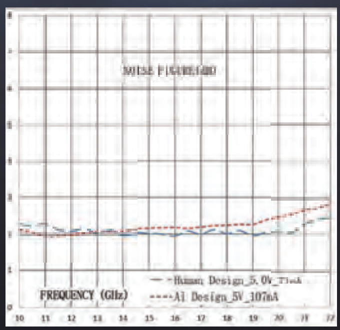

Microwave Journal

CONTENTS

mwjournal.com

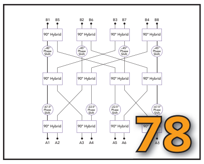

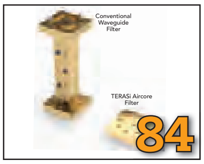

Product Features

Tech Briefs

Departments

Microwave Journal (USPS 396-250) (ISSN 0192-6225) is published monthly by Horizon House Publications Inc., 685 Canton St., Norwood, MA 02062. Periodicals postage paid at Norwood, MA 02062 and additional mailing offices.

POSTMASTER: Send address corrections to Microwave Journal, PO Box 1028, Lowell, MA 01853 or e-mail mwj@e-circ.net.com. Subscription information: (978) 671-0446. This journal is issued without charge upon written request to qualified persons working in the RF & microwave industry. Other subscriptions are: domestic, $130.00 per year, two-year subscriptions, $200.00; foreign, $225.00 per year, two-year subscriptions, $400.00; back issues (if available) and single copies, $20.00 domestic and $30.00 foreign. Claims for missing issues must be filed within 90 days of date of issue for complimentary replacement.

STAFF

EXECUTIVE EDITORIAL OFFICE
685 Canton Street, Norwood, MA 02062
Tel: (781) 769-9750
FAX: (781) 769-5037
e-mail: mwj@mwjournal.com

EUROPEAN EDITORIAL OFFICE
16 Sussex Street, London SW1V 4RW, England
Tel: Editorial: +44 207 596 8730 Sales: +44 207 596 8740
FAX: +44 207 596 8749

SUBSCRIPTION SERVICES
Send subscription inquiries and address changes to:
Tel: (978) 671-0446
e-mail: mwj@e-circ.net

www.mwjournal.com

Printed in the USA

Microwave Journal ONLINE .COM

E LEARNING CENTER

Access webinars on-demand from the archived webinars and events page at www.mwjournal.com/events

Catch *Frequency Matters*, the industry update from *Microwave Journal*,
microwavejournal.com/ FrequencyMatters

WHITE PAPERS

Coilcraft

qorvo
all around you

Radar Royale: How UWB Steals the Spotlight in Cars, IoT, and Beyond!

Executive Interview

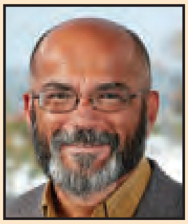

Chet Babla, Senior Vice President of Strategic Marketing at **indie**, discusses his background, the company's product portfolio and focus, along with indie's vision for the future.

Join Us Online

Follow us
@Pathindle
@MWJEric
@MWJEditor

Join us at the RF and Microwave Community

Become a fan at facebook.com/ microwavejournal

Visit us @ mwjournal.com

LISTEN NOW

Microwave Journal podcasts include the RF/microwave update series, Frequency Matters, plus interviews with industry experts and executives.

https://podcasts.microwavejournal.com

DC TO 50 GHz

MMIC Amplifiers

300+ Models Designed in House

Options for Every Requirement

CATV (75Ω)

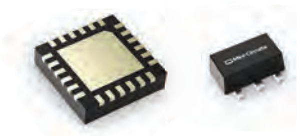

Supporting DOCSIS® 3.1 and 4.0 requirements

Dual Matched

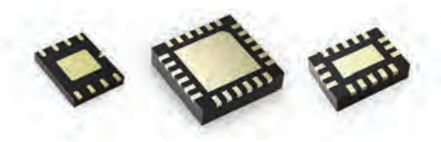

Save space in balanced and push-pull configurations

Hi-Rel

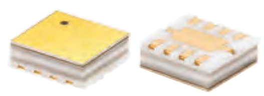

Rugged ceramic package meets MIL requirements for harsh operating conditions

High Linearity

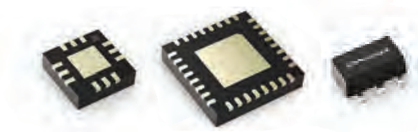

High dynamic range over wide bandwidths up to 45 GHz

Low Noise

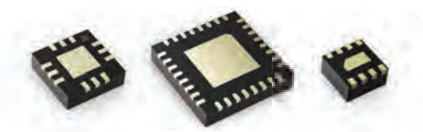

NF as low as 0.38 dB for sensitive receiver applications

Low Additive Phase Noise

As low as -173 dBc/Hz @ 10 kHz offset

RF Transistors

<1 dB NF with footprints as small as 1.18 x 1.42mm

Variable Gain

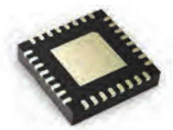

Up to 31.5 dB digital gain control

Wideband Gain Blocks

Flat gain for broadband and multi-band use

Mini-Circuits®

MARK YOUR CALENDAR

JANUARY 2025

7-10
CES 2025
Las Vegas, Nev.
www.ces.tech

19-22
104th ARFTG
San Juan, Puerto Rico
https://arftg.org/104-conference/

28-30
DesignCon 2025
Santa Clara, Calif.
www.designcon.com

FEBRUARY

19-21
iWAT
Cocoa Beach, Fla.
https://attend.ieee.org/iwat-2025

MARCH

1-8
IEEE Aerospace Conference
Big Sky, Mont.
www.aeroconf.org

3-6
MWC
Barcelona, Spain
www.mwcbarcelona.com

10-13
Satellite 2025
Washington, DC
www.satshow.com

15-20
IPC APEX EXPO 2025
Anaheim, Calif.
www.ipcapexexpo.org

25-27
EMV
Stuttgart, Germany
https://emv.mesago.com/events/en.html

30-4/4
EuCAP 2025
Stockholm, Sweden
www.eucap2025.org

APRIL

8-9
IEEE Texas Symposium
Waco, Texas
https://texassymposium.org

Register online at signalintegrityjournal.com

ONLINE PANEL SERIES

3/14
Using AI in the Design of Electronic Systems

Call for Papers Deadlines

1/13 IEEE EMC+ SIPI 2025

2/7 WAMICON

FOR DETAILS VISIT MWJOURNAL.COM/EVENTS

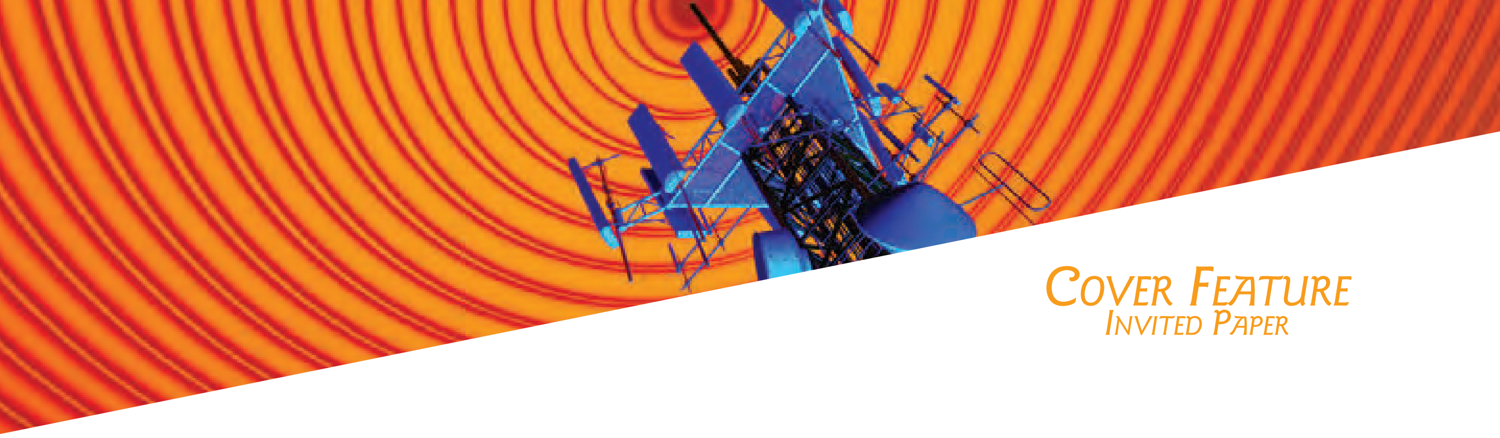

COVER FEATURE
INVITED PAPER

Evaluating Antenna Testing Options

Andrew Laundrie
Eravant (formerly Sage Millimeter Inc.), Torrance, Calif.

Over the past several years, rapid changes have taken place in the field of antenna testing. With more antenna types and new applications emerging at higher frequencies, there is increased urgency to refine established test strategies and develop new ones. For those who are new to antenna testing or are just getting reacquainted after several years away from the practice, it can be instructive to brush up on the fundamentals of antenna testing and study recent trends.

THE BASICS

The basic methods of antenna testing have not changed substantially, but the options for how and where to test antennas have shifted. The options enable various levels of cost, convenience, accuracy and sophistication. In particular, compact antenna test ranges (CATRs) are more widely available and operate at higher frequencies, up to 330 GHz or beyond.

For antenna measurements above 100 GHz, many CATR designs can be customized for specific waveguide bands by selecting different vector network analyzer (VNA) frequency extender modules and suitable feed antennas. For example, Eravant offers an open CATR with reflector options of 300 × 300 mm or 600 x 600 mm, as shown in ***Figure 1***. These CATRs are available with VNA frequency extenders and feed antennas operating up to 330 GHz.

MilliBox has developed a series of CATR designs using modular anechoic enclosures. The MBX32CTR CATR from MilliBox provides measurement solutions for frequencies up to 330 GHz, as well. An example of their test range is shown in ***Figure 2***.

Rohde & Schwarz provides a selection of mmWave CATR designs that feature shielded anechoic environments. ***Figure 3*** shows a Rohde & Schwarz CATR with a shielded enclosure surrounding an anechoic chamber. Other commercially available antenna ranges include many traditional far-field ranges, as well as a variety of near-field (NF) scanning systems. ***Figure 4*** shows a planar NF system from ASYSOL. The ASYSOL systems, along with others, typically operate at frequencies from microwave to mmWave bands.

For those requiring only occa-

Fig. 1 **Eravant CATR.**

Fig. 2 **MilliBox MBX32CTR CATR.**


The only
QPL Certified
MECHANICAL
SWITCH
House!
Quick Turn
RF FILTER
Prototypes
are in our DNA!
Huge Library
of PASSIVES
with Best in Show
HIGH POWER
COUPLER
offering!
L-4241A
S/N 2206001
RUGGED & RELIABLE
AGILE & ADAPTIVE
HIGH POWER & VARIETY
RLC
RF MECHANICAL SWITCHES,
RF FILTERS & RF PASSIVES
AS9100 CERTIFIED, MADE IN USA
High Performance Precision Microwave Components
Serving the world-wide aerospace & defense community since 1959
Robust Catalog Portfolio - no hassle, quick turn, custom solutions our specialty
RLC Electronics | 83 Radio Circle, Mt. Kisco, NY 10549 | 914-241-1334 | sales@rlcelectronics.com | www.rlcelectronics.com

Fig. 3 Rohde & Schwarz ATS1800C CATR.

sional antenna tests, one of the most common strategies is to use someone else's antenna range. At first glance, this can seem like an inconvenient and expensive option

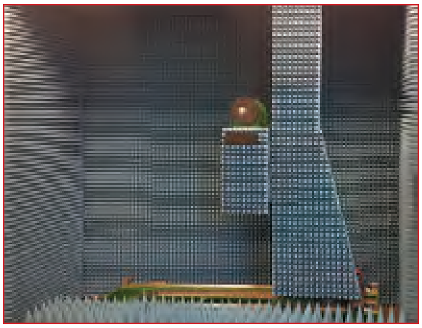

Fig. 4 ASYSOL planar near-field system.

until the time and cost of acquiring and maintaining a suitable antenna range is appreciated. Gaining experience using a variety of antenna ranges is one of the best ways to become familiar with current practices and equipment. Many companies offer economical antenna testing services, with some bringing their test equipment to the antenna rather than the other way around. For example, Quadsat provides airborne antenna measurement services for high gain outdoor antennas with drones. A Quadsat drone that provides these services is shown in ***Figure 5***.

At the high end of the cost and complexity spectrum, complete an-

Fig. 5 Quadsat drone for airborne antenna measurement services.

tenna test ranges are available with fully engineered anechoic chambers, positioning systems, computer platforms, software and test equipment. A wide variety of configuration options can tailor antenna ranges to meet specific needs. Configuring a complete antenna range requires a team with advanced knowledge to perform tasks related to design, planning, construction, calibration, operation and maintenance.

Less complicated and lower-cost solutions are also available. Antenna range components like anechoic chambers, positioning systems, test equipment and software can be developed in-house or purchased individually. A list of companies in

TABLE 1

ANTENNA TESTING COMPANIES AND CAPABILITIES

	Products & Services					
Company	Antenna Test Ranges	Anechoic Chambers	Scanning System Components	Control & Analysis Software	Antenna Test Instrumentation	Measurement Services
Antenna Systems Solutions	■	■	■	■	■	■
AP Americas		■				
Chamber Services Inc.		■				
Comtest Engineering		■				
Delta Sigma Company	■	■	■			
Eravant	■				■	■
ETS-Lindgren Inc.	■	■	■		■	
JEM Engineering					■	■
Keysight	■				■	
Microwave Vision Group	■	■	■	■		■
MilliBox	■	■	■			
Next Phase Measurements	■	■	■	■		
NSI-MI Technologies	■		■	■		
Rohde & Schwarz	■		■	■	■	
TDK RF Solutions		■	■			■

this space, along with the products and services offered by these companies, is shown in ***Table 1***. Companies that supply these components can provide expert advice based on specific testing needs and they may refer customers to existing facilities to serve as points of reference. In general, the antenna testing community is open and cooperative on all levels, making it one of the most rewarding career paths available. Its participants span a diverse range of skills and interests.

At any level of knowledge and resources, there is no substitute for experimentation to learn about antenna measurements. There are many sources of useful information for understanding established practices as well as the underlying electromagnetic and signal-processing theories. Some companies, such as NSI-MI, offer online short courses that cover introductory and advanced topics related to antenna measurements, NF theory and compact range design.[1] Additionally, professional organizations such as the Antenna Measurement Techniques Association offer introductory boot camps for those who are new to the field.[2]

IEEE practice standards are some of the best sources of information on the topic. IEEE Std 149-2021, "Recommended Practice for Antenna Measurements," underwent a significant overhaul in 2021. Recognizing that no measurement is truly complete without a statement of uncertainty, the standard provides a comprehensive treatment of antenna measurement uncertainty.[3] As an illustrative example, the recommended uncertainty analysis is applied to a hypothetical compact antenna test range.

IEEE Std 149-2021 covers a wide range of theoretical and practical topics. However, it no longer includes NF antenna measurements, which are now covered by IEEE Std 1720-2012, "Recommended Practice for Near-Field Antenna Measurements."[4,5] Updates to this standard are underway, with the next release expected in 2025.

Physical standards are also being developed to enable different measurement groups to evaluate and compare test results. One such

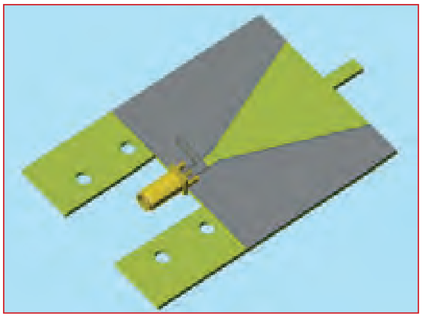

Fig. 6 A wideband antenna measurement standard to compare test results.

standard is an antenna that was first established as a benchmark for computational electromagnetics.[6] With an operating bandwidth of approximately 4 to 12 GHz, the antenna shown in ***Figure 6*** was developed for UWB applications. It is easily fabricated using an FR-4 substrate with a single metal layer and the design can serve as a common measurement standard. The design is being shared among a diverse collection of antenna test facilities to compare test measurement results across different antenna ranges.[7]

ANTENNA MEASUREMENT METHODS

One of the most straightforward ways to measure the gain of an antenna is to compare its response to a known standard. In this gain transfer method, a total of three antennas are required: One serves as the transmit antenna, another as a reference antenna and the third as the antenna under test (AUT). Two measurements are needed, with the first establishing a calibration response through the reference antenna. The other measurement has the AUT inserted in place of the reference antenna.

A number of complications can arise when using the gain transfer method. If the antennas are not far enough apart, multiple reflections between the antennas can introduce significant error terms. If the "quiet zone" established by the transmit antenna is not sufficiently quiet, meaning it is not adequately low in amplitude and phase variations, additional errors are introduced. Sources of error can also include multipath interference caused by nearby surfaces or cables, electrical loading of antennas by support structures, interference signals (equipment leakage), antenna mismatch errors, the limited accuracy of test equipment or antenna alignment errors. Ultimately, gain uncertainty for the AUT cannot be better than that of the gain standard used.

Another common gain measurement technique is direct or absolute measurement. This approach requires two identical antennas or three antennas that are not identical but have certain restrictions on their polarization. The test system is calibrated by recording the receiver's response when it is connected to the signal source directly or through a calibrated shorting cable. The two-antenna method measures transmission loss with two identical antennas separated by a known distance. The Friis transmission equation yields the combined gain of the antenna pair. The gain of either antenna is the square root of the antenna gain product.

The three-antenna method measures the gain product for three different antenna pairs. The gain of each antenna is computed from a system of three equations with three unknowns. Both the two- and three-antenna methods assume that the antennas are separated by far-field distances, which are often regarded as greater than $2D^2/\lambda$ where D is the effective aperture width and λ is the wavelength. However, at this distance, the interaction between directional antenna pairs may be enough to raise gain uncertainty to an unacceptable level. Distances of at least $32D^2/\lambda$ are often recommended to limit proximity effects adequately.

At mmWave frequencies, far-field separation can be problematic if there is insufficient signal power to overcome transmission losses. The problem may be aggravated if gain patterns must be measured over a significant dynamic range. Greater signal strength may also be necessary if antenna polarization must be measured as well.

A variety of enhanced measurement methods have been developed to extrapolate far-field antenna gain from measurements obtained at NF distances.[8,9] Extrapolated gain is a well-known strategy for accurately calibrating standard gain antennas, with uncertainties of ±0.1 dB achievable with sufficient

effort. Both the amplitude and phase of antenna pair responses are required to perform gain extrapolation, necessitating the use of a vector signal analyzer.

During gain extrapolation tests, signal transmission between antenna pairs is measured over a range of separation distances. The result is a set of S_{21} data with increasing attenuation over distance. Rather than a smooth amplitude curve that follows a 1/d trend, the data usually contains additional features caused by multiple reflections between the antennas and various other proximity effects. When third-order reflections between the antennas are dominant, the amplitude data contains periodic variations with a spatial period of $\lambda/2$.

Extrapolated gain data can be analyzed to produce a best-fit mathematical expression for the coupled signal versus distance, normalized to 1/d. The form of the expression is a power series with each summation term a constant multiplied by $1/d^n$, where d is distance and n indicate the n^{th} term. The first-order term in the series, for which n = 0, represents the far-field gain product of the antenna pair when d is extrapolated to infinity.

To mathematically derive the first-order term in the power series, traditional gain extrapolation techniques require large sets of S_{21} measurements. These measurements are obtained at intervals of about one-tenth of a wavelength over distances spanning 200 to 300 wavelengths. This amount of data is typically necessary to produce accurate high-order terms in the signal versus distance power series.

A recently demonstrated gain extrapolation method offers a new approach that dramatically reduces the number of S_{21} samples needed while compressing the span of measurement distances.[10] The technique involves accurately locating the positions of successive minima and maxima in signal amplitude, with one S_{21} sample taken at each location. The paired measurements are repeated about a dozen times at regularly spaced intervals over a span of about 40 wavelengths. Demonstrated results are comparable to those achieved using traditional methods that require thousands of S_{21} measurements. One caveat is that multipath effects must be negligible, making the new method best suited for directional antennas and well-controlled test environments.

NF SCANNING

NF antenna ranges are widely regarded as providing the best measurements in terms of accuracy and versatility. However, they typically have higher hardware costs and greater measurement times compared to other range types. NF theory states that when electromagnetic fields are measured with sufficient accuracy and resolution over a closed surface surrounding a transmitting antenna, it is possible to compute the fields at any arbitrary point outside of the antenna's reactive zone.[11] The computations are complex and require significant computing resources and specialized software to perform functions such as field transformations, spatial filtering and probe correction.

Depending on the surfaces they scan, NF systems are categorized as either spherical (SNF), cylindrical

Leading the way

In RF/Microwave PCB Manufacturing Solutions

At Teledyne Labtech, we have over 40 years of expertise in the thermal management of complex RF/Microwave printed circuit boards (PCBs). As one of the few companies in the world capable of producing large format PCBs, we provide extensive antenna manufacturing capabilities, along with comprehensive assembly and testing services. This unique combination makes Teledyne Labtech the only company in Europe offering a complete one-stop PCB manufacturing solution.

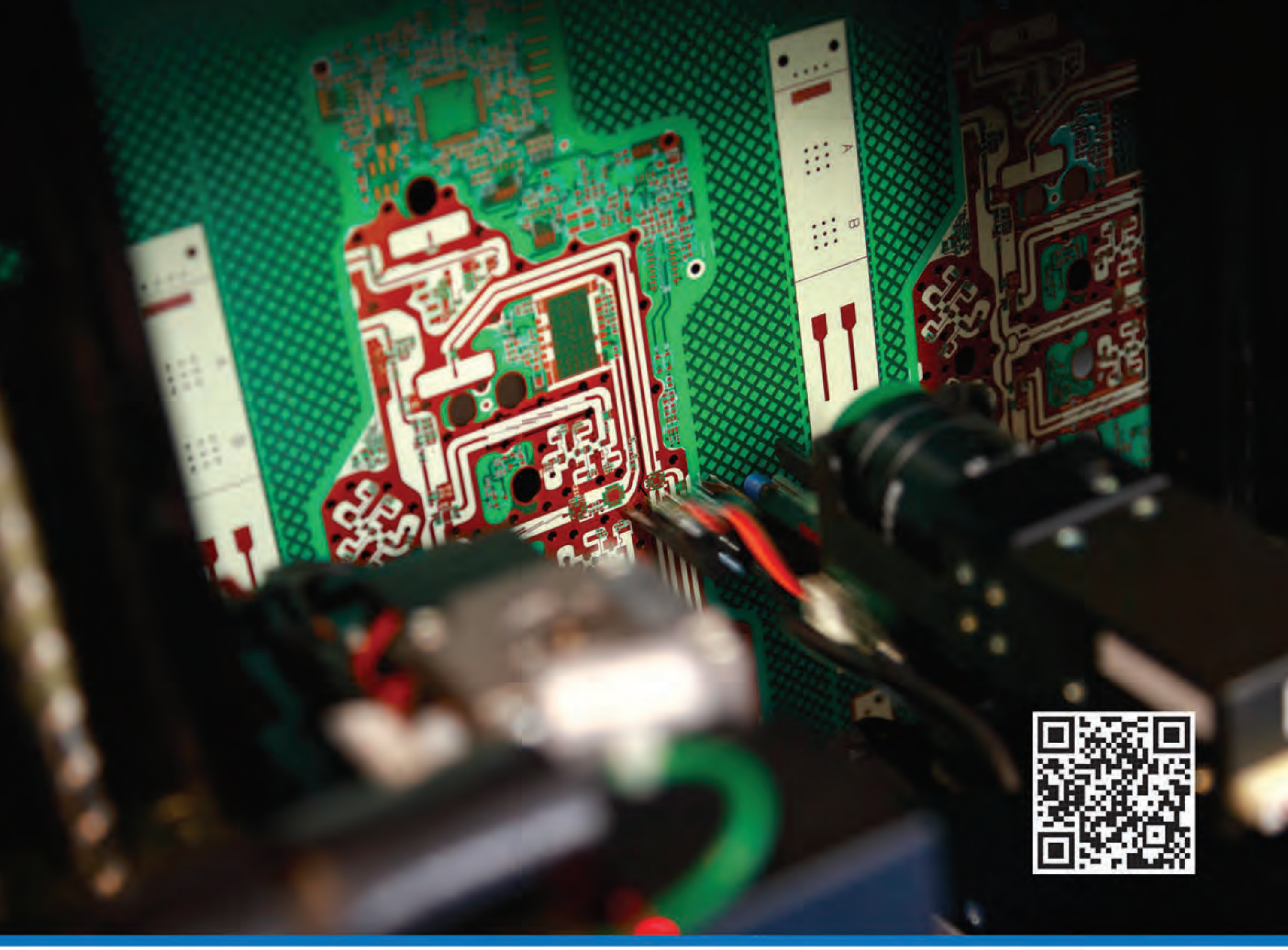

Aerospace and Defense Electronics | Teledyne Labtech
TeledyneLabtech.com

TELEDYNE

(CNF) or planar (PNF). PNF systems are widely used for directional radiators such as horn, lens and reflector antennas, as well as antenna arrays. CNF scanners are often realized within a PNF system by adding a positioner that rotates the AUT.

PNF and CNF systems cannot probe an entire closed surface unless multiple scans are performed with different antenna orientations. When significant fields exist outside of the scanned area, their omission from far-field gain calculations contributes to computational errors. SNF data can be easier to process mathematically, and probe corrections are generally more straightforward. As a result, many SNF ranges provide better performance for similar levels of cost and effort when compared to other NF systems.

At mmWave frequencies, many antennas are small enough to be scanned using a commercially available six-axis robot. Such robots can manipulate field probes over a range of surface profiles, including planar, cylindrical and spherical. They can also perform extrapolated gain measurements and other tests using the same antenna and probe configurations as those used for NF scans.

At frequencies above 100 GHz, significant challenges face designers and operators of NF systems. In general, NF techniques require probe positioning uncertainties of λ/50 or less. At 100 GHz, this corresponds to 60 microns. This level of mechanical precision stretches the capabilities of many robotic systems as well as the dimensional probes and laser trackers required for calibration. As a result, NF measurements at frequencies above 300 GHz will remain only marginally practical until robotic systems with greater accuracy and speed are developed. However, ongoing efforts are addressing these challenges.

At the National Institute of Standards and Technology (NIST), researchers are pushing NIST-developed NF scanning techniques to frequencies as high as 500 GHz. The Configurable Robotic MilliMeterwave Antenna facility (CROMMA) is one of the most advanced positioning systems currently in use for precision NF measurements.[12] The facility has successfully profiled antennas operating at 183 GHz and can perform NF measurements as high as 500 GHz. NF measurements being performed at this facility are shown in ***Figure 7***.

CROMMA uses a six-axis COTS robot to manipulate field probes with repeatability and accuracy of approximately 25 microns. The range of motion for field probes is roughly 4 m vertically and 5 m horizontally. To calibrate the system, the probe carrier is moved throughout the robot's reach while laser trackers scan targets located on the carrier. When a field probe is mounted onto the carrier, a separate calibration fixture uses high-resolution cameras to find the center of the probe aperture and determine its position and orientation relative to reference points on the carrier assembly.[13]

Some commercially available NF systems are reported to be usable at frequencies reaching 110 GHz or higher. Unfortunately, the suppliers of NF ranges are hesitant to indicate expected accuracies at such frequen-

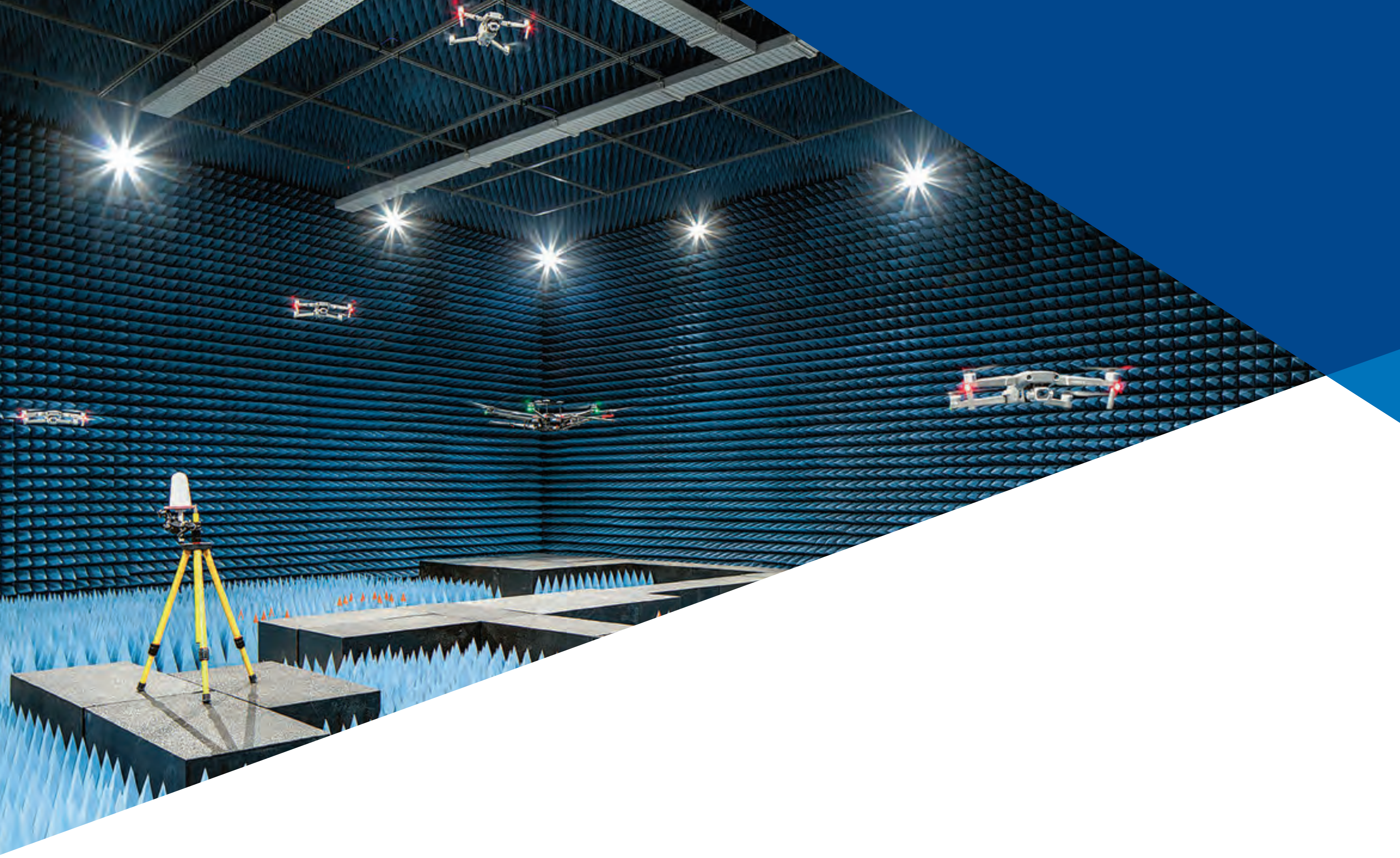

cies because measurement results depend significantly on how their systems are used in specific situations. As more NF test results are reported for sub-THz wavelengths, the capabilities of these antenna test systems should become more apparent.

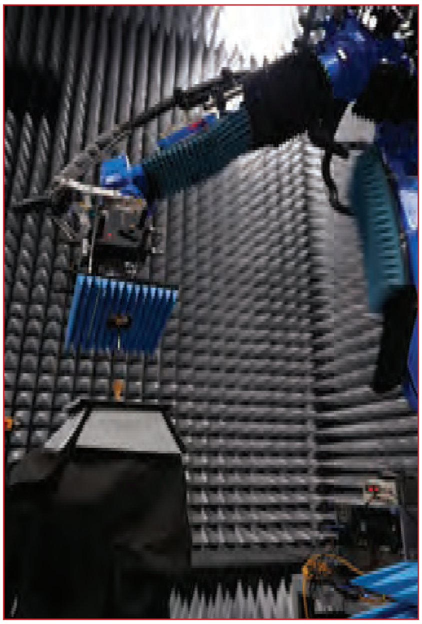

▲ Fig. 7 CROMMA performs NF measurements. (*Photo used with permission.* Rebecca Jacobson, National Institute of Standards and Technology.)

CONCLUSION

Commercial and defense applications are moving higher in frequency to provide better performance to the end user. This means that test techniques and equipment must lead the charge to support a wide range of new, higher frequency components and systems. This article has presented an overview of some of the techniques, products, services and companies that will make the vision of higher frequency systems a reality. ■

References

1. Short Course, *NSI-MI Technologies*, Web: www.nsi-mi.com/news-and-events/short-course.
2. Antenna Measurement Techniques Association, Web: www.amta.org.
3. "IEEE Recommended Practice for Antenna Measurements," *IEEE Std 149-2021*, Feb. 2022.
4. "IEEE Recommended Practice for Near-Field Antenna Measurements," *IEEE Std 1720-2012*, Dec. 2012.
5. L. J. Foged, V. Rodriguez, J. Fordham, J. Dobbins and V. Monebhurrun, "Revision Progress 2024: IEEE Std 1720," *2024 Antenna Measurement Techniques Association Symposium (AMTA)*, Cincinnati, Ohio, U.S.
6. V. Monebhurrun, S. Chakrabarti and R. Quoi, "A 5G NR FR1 UWB Antenna as Benchmark for the Development of IEEE Standard P2816," *2023 Antenna Measurement Techniques Association Symposium (AMTA)*, Renton, Wash., U.S.
7. V. Monebhurrun, J. Fordham and L. Foged, "Application of IEEE Std 149-2021: International Antenna Measurement Campaign," *2024 Antenna Measurement Techniques Association Symposium (AMTA)*, Cincinnati, Ohio, U.S.
8. A. Newell, R. Baird and P. Wacker, "Accurate Measurement of Antenna Gain and Polarization at Reduced Distances by an Extrapolation Technique," *IEEE Transactions on Antennas Propagation*, Vol. AP-21, No. 4, July 1973.
9. Z. Chen, Y. Wang and D. Lewis, "Examination of Antenna Calibration Methodologies in an Extrapolation Range," *2022 16th European Conference on Antennas and Propagation (EuCAP)*, Madrid, Spain.
10. J. A. Gordon and B. L. Moser, "Enhanced Gain Extrapolation Technique: A Third-Order Scattering Approach For High-Accuracy Antenna Gain, Sparse Sampling, At Fresnel Distances," *2024 Antenna Measurement Techniques Association Symposium (AMTA)*, Cincinnati, Ohio, U.S.
11. A. Ludwig, "Near-field Far-field Transformations using Spherical-wave Expansions," *IEEE Transactions on Antennas and Propagation*, Vol. 19, No. 2, 1971, pp. 214–220.
12. "Configurable Robotic MilliMeter-wave Antenna (CROMMA)," *NIST*, Web: www.nist.gov/ctl/configurable-robotic-millimeter-wave-antenna-cromma.
13. "Single-Pixel Touchless Laser Tracker Probe (Pixel Probe)," NIST, Web: www.nist.gov/ctl/single-pixel-touchless-laser-tracker-probe-pixel-probe.

RF Amplifiers and Sub-Assemblies for Every Application

Delivery from Stock to 2 Weeks ARO from the catalog or built to your specifications!

- Competitive Pricing & Fast Delivery
- Military Reliability & Qualification
- Various Options: Temperature Compensation, Input Limiter Protection, Detectors/TTL & More
- Unconditionally Stable (100% tested)

ISO 9001:2000 and AS9100B CERTIFIED

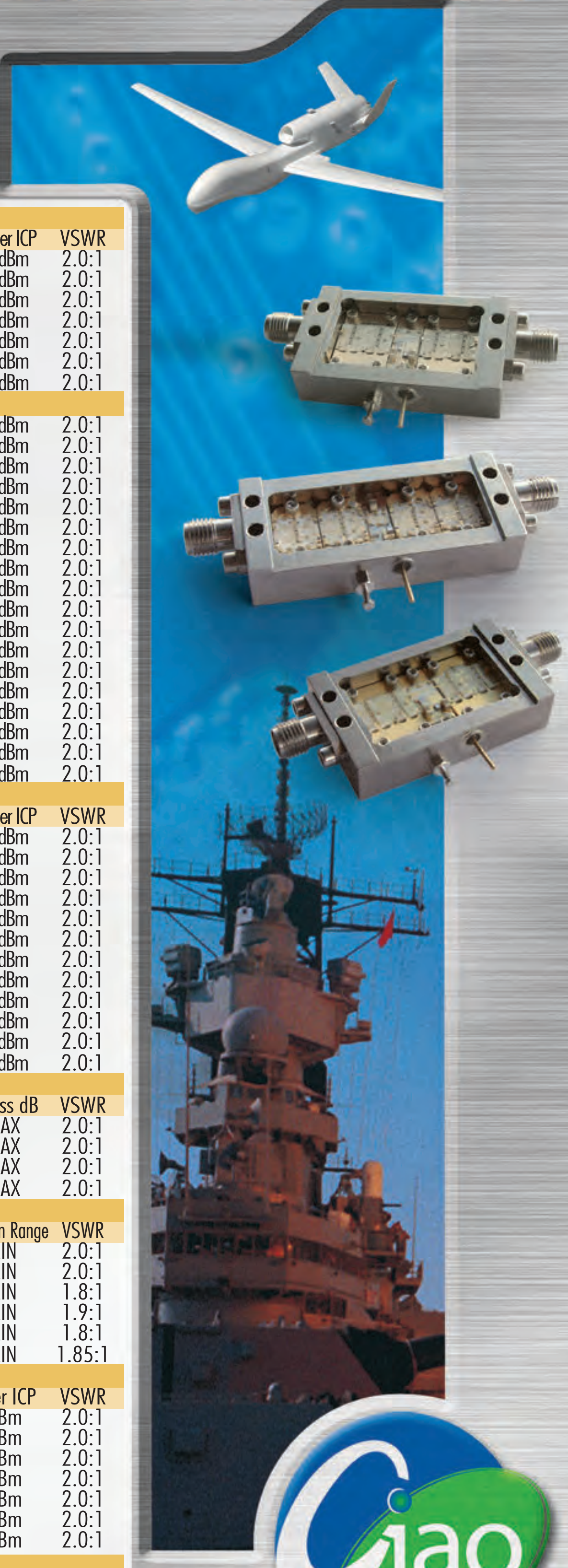

OCTAVE BAND LOW NOISE AMPLIFIERS

Model No.	Freq (GHz)	Gain (dB) MIN	Noise Figure (dB)	Power-out @ P1-dB	3rd Order ICP	VSWR
CA01-2110	0.5-1.0	28	1.0 MAX, 0.7 TYP	+10 MIN	+20 dBm	2.0:1
CA12-2110	1.0-2.0	30	1.0 MAX, 0.7 TYP	+10 MIN	+20 dBm	2.0:1
CA24-2111	2.0-4.0	29	1.1 MAX, 0.95 TYP	+10 MIN	+20 dBm	2.0:1
CA48-2111	4.0-8.0	29	1.3 MAX, 1.0 TYP	+10 MIN	+20 dBm	2.0:1
CA812-3111	8.0-12.0	27	1.6 MAX, 1.4 TYP	+10 MIN	+20 dBm	2.0:1
CA1218-4111	12.0-18.0	25	1.9 MAX, 1.7 TYP	+10 MIN	+20 dBm	2.0:1
CA1826-2110	18.0-26.5	32	3.0 MAX, 2.5 TYP	+10 MIN	+20 dBm	2.0:1

NARROW BAND LOW NOISE AND MEDIUM POWER AMPLIFIERS

Model No.	Freq (GHz)	Gain (dB) MIN	Noise Figure (dB)	Power-out @ P1-dB	3rd Order ICP	VSWR
CA01-2111	0.4 - 0.5	28	0.6 MAX, 0.4 TYP	+10 MIN	+20 dBm	2.0:1
CA01-2113	0.8 - 1.0	28	0.6 MAX, 0.4 TYP	+10 MIN	+20 dBm	2.0:1
CA12-3117	1.2 - 1.6	25	0.6 MAX, 0.4 TYP	+10 MIN	+20 dBm	2.0:1
CA23-3111	2.2 - 2.4	30	0.6 MAX, 0.45 TYP	+10 MIN	+20 dBm	2.0:1
CA23-3116	2.7 - 2.9	29	0.7 MAX, 0.5 TYP	+10 MIN	+20 dBm	2.0:1
CA34-2110	3.7 - 4.2	28	1.0 MAX, 0.5 TYP	+10 MIN	+20 dBm	2.0:1
CA56-3110	5.4 - 5.9	40	1.0 MAX, 0.5 TYP	+10 MIN	+20 dBm	2.0:1
CA78-4110	7.25 - 7.75	32	1.2 MAX, 1.0 TYP	+10 MIN	+20 dBm	2.0:1
CA910-3110	9.0 - 10.6	25	1.4 MAX, 1.2 TYP	+10 MIN	+20 dBm	2.0:1
CA1315-3110	13.75 - 15.4	25	1.6 MAX, 1.4 TYP	+10 MIN	+20 dBm	2.0:1
CA12-3114	1.35 - 1.85	30	4.0 MAX, 3.0 TYP	+33 MIN	+41 dBm	2.0:1
CA34-6116	3.1 - 3.5	40	4.5 MAX, 3.5 TYP	+35 MIN	+43 dBm	2.0:1
CA56-5114	5.9 - 6.4	30	5.0 MAX, 4.0 TYP	+30 MIN	+40 dBm	2.0:1
CA812-6115	8.0 - 12.0	30	4.5 MAX, 3.5 TYP	+30 MIN	+40 dBm	2.0:1
CA812-6116	8.0 - 12.0	30	5.0 MAX, 4.0 TYP	+33 MIN	+41 dBm	2.0:1
CA1213-7110	12.2 - 13.25	28	6.0 MAX, 5.5 TYP	+33 MIN	+42 dBm	2.0:1
CA1415-7110	14.0 - 15.0	30	5.0 MAX, 4.0 TYP	+30 MIN	+40 dBm	2.0:1
CA1722-4110	17.0 - 22.0	25	3.5 MAX, 2.8 TYP	+21 MIN	+31 dBm	2.0:1

ULTRA-BROADBAND & MULTI-OCTAVE BAND AMPLIFIERS

Model No.	Freq (GHz)	Gain (dB) MIN	Noise Figure (dB)	Power-out @ P1-dB	3rd Order ICP	VSWR
CA0102-3111	0.1-2.0	28	1.6 Max, 1.2 TYP	+10 MIN	+20 dBm	2.0:1
CA0106-3111	0.1-6.0	28	1.9 Max, 1.5 TYP	+10 MIN	+20 dBm	2.0:1
CA0108-3110	0.1-8.0	26	2.2 Max, 1.8 TYP	+10 MIN	+20 dBm	2.0:1
CA0108-4112	0.1-8.0	32	3.0 MAX, 1.8 TYP	+22 MIN	+32 dBm	2.0:1
CA02-3112	0.5-2.0	36	4.5 MAX, 2.5 TYP	+30 MIN	+40 dBm	2.0:1
CA26-3110	2.0-6.0	26	2.0 MAX, 1.5 TYP	+10 MIN	+20 dBm	2.0:1
CA26-4114	2.0-6.0	22	5.0 MAX, 3.5 TYP	+30 MIN	+40 dBm	2.0:1
CA618-4112	6.0-18.0	25	5.0 MAX, 3.5 TYP	+23 MIN	+33 dBm	2.0:1
CA618-6114	6.0-18.0	35	5.0 MAX, 3.5 TYP	+30 MIN	+40 dBm	2.0:1
CA218-4116	2.0-18.0	30	3.5 MAX, 2.8 TYP	+10 MIN	+20 dBm	2.0:1
CA218-4110	2.0-18.0	30	5.0 MAX, 3.5 TYP	+20 MIN	+30 dBm	2.0:1
CA218-4112	2.0-18.0	29	5.0 MAX, 3.5 TYP	+24 MIN	+34 dBm	2.0:1

LIMITING AMPLIFIERS

Model No.	Freq (GHz)	Input Dynamic Range	Output Power Range Psat	Power Flatness dB	VSWR
CLA24-4001	2.0 - 4.0	-28 to +10 dBm	+7 to +11 dBm	+/- 1.5 MAX	2.0:1
CLA26-8001	2.0 - 6.0	-50 to +20 dBm	+14 to +18 dBm	+/- 1.5 MAX	2.0:1
CLA712-5001	7.0 - 12.4	-21 to +10 dBm	+14 to +19 dBm	+/- 1.5 MAX	2.0:1
CLA618-1201	6.0 - 18.0	-50 to +20 dBm	+14 to +19 dBm	+/- 1.5 MAX	2.0:1

AMPLIFIERS WITH INTEGRATED GAIN ATTENUATION

Model No.	Freq (GHz)	Gain (dB) MIN	Noise Figure (dB)	Power-out @ P1-dB	Gain Attenuation Range	VSWR
CA001-2511A	0.025-0.150	21	5.0 MAX, 3.5 TYP	+12 MIN	30 dB MIN	2.0:1
CA05-3110A	0.5-5.5	23	2.5 MAX, 1.5 TYP	+18 MIN	20 dB MIN	2.0:1
CA56-3110A	5.85-6.425	28	2.5 MAX, 1.5 TYP	+16 MIN	22 dB MIN	1.8:1
CA612-4110A	6.0-12.0	24	2.5 MAX, 1.5 TYP	+12 MIN	15 dB MIN	1.9:1
CA1315-4110A	13.75-15.4	25	2.2 MAX, 1.6 TYP	+16 MIN	20 dB MIN	1.8:1
CA1518-4110A	15.0-18.0	30	3.0 MAX, 2.0 TYP	+18 MIN	20 dB MIN	1.85:1

LOW FREQUENCY AMPLIFIERS

Model No.	Freq (GHz)	Gain (dB) MIN	Noise Figure dB	Power-out @ P1-dB	3rd Order ICP	VSWR
CA001-2110	0.01-0.10	18	4.0 MAX, 2.2 TYP	+10 MIN	+20 dBm	2.0:1
CA001-2211	0.04-0.15	24	3.5 MAX, 2.2 TYP	+13 MIN	+23 dBm	2.0:1
CA001-2215	0.04-0.15	23	4.0 MAX, 2.2 TYP	+23 MIN	+33 dBm	2.0:1
CA001-3113	0.01-1.0	28	4.0 MAX, 2.8 TYP	+17 MIN	+27 dBm	2.0:1
CA002-3114	0.01-2.0	27	4.0 MAX, 2.8 TYP	+20 MIN	+30 dBm	2.0:1
CA003-3116	0.01-3.0	18	4.0 MAX, 2.8 TYP	+25 MIN	+35 dBm	2.0:1
CA004-3112	0.01-4.0	32	4.0 MAX, 2.8 TYP	+15 MIN	+25 dBm	2.0:1

CIAO Wireless can easily modify any of its standard models to meet your "exact" requirements at the Catalog Pricing.

Visit our web site at **www.ciaowireless.com** for our complete product offering.

Ciao wireless

Ciao Wireless, Inc. 4000 Via Pescador, Camarillo, CA 93012

Tel (805) 389-3224 Fax (805) 389-3629 sales@ciaowireless.com

Raytheon Awarded U.S. Army Contract for Wireless Power Beaming Technology

Raytheon, an RTX business, was awarded a contract from the U.S. Army to work on directed energy wireless power beaming capabilities that will distribute power across the battlefield, simplify logistics and safeguard locations for U.S. troops.

Work is being conducted as part of a larger effort under the Department of Defense's Operational Energy Strategy. Under the contract, Raytheon's Advanced Technology team will develop advanced wireless power transmitter and receiver technologies to enable a long-range demonstration in line with the needs of U.S. Army manned and unmanned system requirements.

Wireless power beaming reduces the need for troops to carry additional fuel and batteries, easing logistics, increasing their operation time and safeguarding their locations. In addition, wireless power enables energy uniformity in the battlespace, allowing ease of capture and delivery of energy to sensor systems without needing potentially vulnerable concentrated fuel depots.

Raytheon has a long history in wireless power transmission dating back to the 1960s with William Brown pioneering the first demonstration that still holds the record for the highest energy transfer and the longest range independently. In recent years, the company has been focused on developing state-of-the-art technologies to enable wireless power across long ranges and incorporate them in systems of the future.

Wireless Power Beaming (Source: RTX)

Verus® Research Awarded DARPA Contract to Continue Efforts in High-Power Microwave Waveforms Project

Verus® Research, a New Mexico-based team of scientists and engineers specializing in advanced research and technology development, has secured a Defense Advanced Research Projects Agency (DARPA) contract to expand on its multi-phase effort. This project is in partnership with the Naval Research Laboratory (NRL).

Verus Research specializes in the research and development of RF communications for high-power microwave (HPM) systems and nuclear engineering, with extensive modeling, simulation, testing and design work.

> Extends the range and effectiveness of HPM systems for back-door attacks.

Under this one-year, $1.8 million contract, Verus Research will partner with NRL to continue its work on the Waveform Agile RF Directed ENergy (WARDEN) project, which began in 2021. The WARDEN program seeks to develop hardware, theory and computational models to extend the range and effectiveness of HPM systems for back-door attacks. HPMs are a class of directed energy weapons that use electromagnetic radiation to disrupt, disable or damage targeted electronic components and circuits.

Skunk Works Demos Airborne Battle Management of AI-Controlled Aircraft

Lockheed Martin Skunk Works®, in partnership with Lockheed Martin's Demonstrations and Prototypes organization and the University of Iowa's Operator Performance Laboratory (OPL), showcased a crewed-uncrewed teaming mission where an airborne battle manager issued real-time commands to AI-controlled aircraft through a touchscreen pilot vehicle interface.

In a series of flight tests, the Skunk Works and OPL teams simulated an offensive counter air mission where an airborne, human "battle manager" aboard an L-39 Albatros assigned targets to two AI-controlled L-29 Delfin jets, which then worked together to defeat two mock enemy jets using simulated mission systems and weapons.

"The work we're doing with the University of Iowa's OPL is foundational for the future of air combat, where a family of crewed and uncrewed systems will work together to execute complex missions," said John Clark, vice president and general manager, Lockheed Martin Skunk Works. "We're excited to leverage our diverse skillsets to advance all elements of this new way of operating."

These flight tests build on previous experiments that demonstrated AI-controlled air-to-ground jamming and geolocation. This year, the tests shifted to AI in air-to-air combat, where AI sends commands directly to the planes' autopilots. This is the third test of this type and the first to include a real-time human battle manager overseeing the AI's actions.

For More Information
Visit mwjournal.com for more defense news.

L3Harris Selected to Develop Autonomous Swarms Prototype

L3Harris was selected by the Defense Innovation Unit (DIU) to prototype a command-and-control system that can simultaneously operate hundreds, or even thousands, of autonomous assets.

Advancing the U.S. Department of Defense's (DOD's) Replicator initiative, the prototype integrates commercial technologies to deliver collaborative autonomy for the U.S. military to operate swarms of uncrewed aircraft, ground vehicles and seacraft.

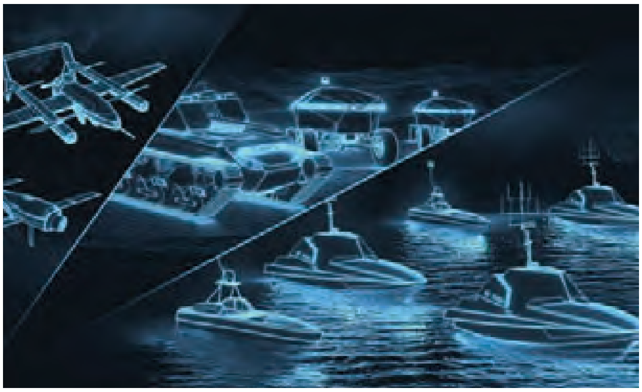

Swarms Prototype (Source: L3Harris Technologies)

"We are delivering a multi-domain and multi-mission autonomous ecosystem that can be trusted to operate in contested environments," said Toby Maggsig, vice president and general manager of Enterprise Autonomous Solutions for L3Harris. "We are focused on the scalability the U.S. military and allied nations need in a mission space that will shape the future of warfighting."

L3Harris was selected to provide a user interface, develop a collaborative autonomy capability and serve as a systems integrator for the autonomy architecture.

The collaborative autonomy project highlights the L3Harris approach to partner with venture capital-backed startups and non-traditional technology firms to foster new defense and commercial technologies.

The DIU is the latest DOD organization to select L3Harris' enterprise autonomy architecture to prototype new mission scenarios. The open architecture system is currently in use for experimentation to create collaborative autonomy at scale. Because it supports rapid integration of algorithms and models from third-party systems, it can evolve quickly depending on the needs of each mission.

PROPRIETARY TECHNOLOGIES

LTCC Filter Innovations

The Industry's Widest Selection

LEARN MORE

Ultra-High Rejection

- Rejection floor down to 100+ dB
- Excellent selectivity
- Built-in shielding
- 1812 package style
- Patent pending

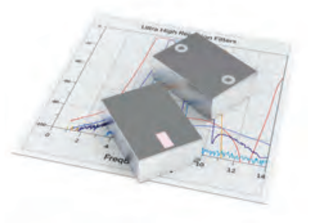

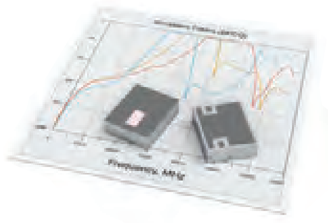

mmWave Passbands

- Passbands to 50+ GHz
- The industry's widest selection of LTCC filters optimized for 5G FR2 bands
- Growing selection of models for Ku- and Ka-band Satcom downlink
- 1812 & 1008 package styles

Substrate Integrated Waveguide

- First commercially available SIW LTCC filter in the industry
- Narrow bandwidth (~5%) and good selectivity
- Internally shielded to prevent detuning
- 1210 package style

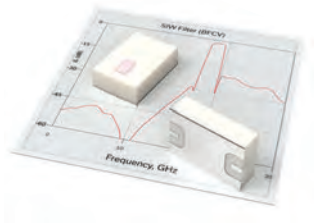

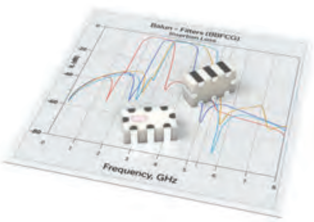

Integrated Balun-Bandpass Filters

- Combine balun transformer and bandpass filter in a single device
- Saves space and simplifies board layouts in ADCs, DACs and other circuits
- 1210, 1008 & 0805 package styles

Mini-Circuits®

CommercialMarket

Cliff Drubin, Associate Technical Editor

Ericsson Mobility Report: Early Movers Pursue Performance-Based Business Models

Communications service providers (CSPs) are expecting 5G Standalone (SA) and 5G Advanced to be key focuses for the remainder of the decade as they deploy new capabilities to create offerings centered on value delivery rather than data volume. The analysis is included among a wealth of statistical network insights in the November 2024 edition of the Ericsson Mobility Report, which extends the forecast period until the end of 2030.

While the rate of mobile network traffic data growth is declining, estimated at 21 percent year-on-year for 2024, it is still expected to grow almost three-fold by the end of 2030 from present-day numbers.

The report highlights how early-mover service providers are already offering value delivery models based on differentiated connectivity, guaranteed uninterrupted high-end connectivity when you need it most, to create new monetization and growth opportunities. Related case studies from T-Mobile in the U.S. and Elisa in Finland are included.

Fredrik Jejdling, executive vice president, head of Business Area Networks, Ericsson, said, "Service differentiation and performance-based opportunities are crucial as our industry evolves. This is highlighted in the November 2024 Ericsson Mobility Report, which includes detailed analysis, statistical insights and customer use cases. The shift towards high performing programmable networks, enabled by openness and cloud, will empower service providers to offer and charge for services based on the value delivered, not merely data volume. This report offers valuable insights into what our industry can achieve and the steps necessary to get there."

The report underlines the global potential for differentiated connectivity development by highlighting that, beyond China, 5G mid-band is currently only deployed at about 30 percent of sites globally.

Almost 60 percent of the 6.3 billion global 5G subscriptions forecast by the end of 2030 are expected to be 5G SA subscriptions. On global mobile data traffic, 5G networks are expected to carry about 80 percent of total mobile data traffic by the end of 2030, compared to 34 percent by the end of 2024.

Fixed Wireless Access (FWA) continues to grow in popularity globally as the second largest 5G use case after enhanced Mobile Broadband (eMBB). Of the 350 million projected global FWA connections by the end of 2030, almost 80 percent are forecast to be over 5G.

The report also addresses how AI, including generative AI applications — already integrated across smartphones, laptops, watches and FWA products — could impact uplink and downlink network traffic, driving potential mobile traffic growth beyond current predictions.

The first 6G deployments are expected in 2030, building on and scaling the capabilities of 5G SA and 5G Advanced.

North American Wi-Fi Sensing CPE Installations to Surge as the Technology's Maturing Unleashes New Business and Service Models

Wi-Fi Sensing uses Wi-Fi RF wave attenuation to detect presence and motion, offering a cost-effective, easily deployable solution. Major Wi-Fi chipset vendors supporting infrastructure markets are backing this technology. It is already being used in the U.S. for remote healthcare, security and smart home automation. The number and diversity of applications are expected to rise rapidly following the final approval of the 802.11bf Wi-Fi Sensing standard, currently scheduled for March 2025. According to ABI Research, the emergence of new Wi-Fi Sensing-based value-added services will result in the install base of Wi-Fi Sensing-compatible customer premises equipment in North America increasing at a 51.6 percent CAGR between 2024 and 2030 to reach 112 million.

> **Already being used in the U.S. for remote healthcare, security and smart home automation.**

In recent years, a rich ecosystem of vendors developing and commercializing Wi-Fi Sensing has emerged, reflecting the industry's confidence in the future of the technology. Key contributors to the IEEE 802.11bf Wi-Fi Sensing Task Group include Huawei, LG Electronics, Ericsson and Meta, where the Wi-Fi Sensing Work Group within the Wireless Broadband Alliance contains members such as CableLabs, Comcast, Cisco and Turk Telekom. Notable companies monetizing Wi-Fi Sensing today include Origin, which has formed commercial partnerships with Airties, Verisure, Verizon and Cognitive, whose sensing solution has been integrated into the HomePass platform of value-added service provider Plume, enabling it with over 100 ISPs globally.

Another significant vendor is Nami, which is currently testing advanced Wi-Fi Sensing for aged care within healthcare facilities in Japan. The industry promises many other exciting future Wi-Fi Sensing applications, ranging from people counting and audio tracking to people identification and breathing monitoring. Yet the feasibility of these applications, and more importantly, consumers' willingness to pay for them, remains unclear.

These findings are from ABI Research's Wi-Fi Sensing Market Opportunities and Challenges report.

For More Information

Visit mwjournal.com for more commercial market news.

Soaring Civil & Commercial Applications Propel Drone Market

The drone economy is set to soar, with unprecedented growth on the horizon. According to ABI Research, civil and commercial applications of small unmanned aerial systems (sUAS), also known as drones, will expand dramatically, rising from just 8 percent to an impressive 32 percent of the total market by 2030. In this timeframe, annual drone shipments will more than double from 1.5 million units in 2024 to 3.32 million, fueling an ecosystem poised to quadruple in value. By the decade's end, the sector will generate U.S.$123 billion in annual revenue, marking a transformative shift in the commercial and civil drone landscape.

The commercial drone market is rapidly expanding, with companies like Gather artificial intelligence (AI) making strides in warehouse automation while Flyability and Percepto enhance inspection efficiency across industries. In agriculture and real estate, service providers such as Sentera and Skywash leverage drone technology to unlock new value. However, the largest growth area for sUAS will be last-mile delivery. ABI Research projects that revenue from this segment will soar from U.S.$800 million to U.S.$12.4 billion by 2030, achieving an impressive 50.2 percent compound annual growth rate (CAGR). Leading the charge in this transformative space are Zipline, Google's Wing and Amazon's Prime Air, each poised to capture significant market share in the delivery vertical.

> Airborne robotics bring appealing value propositions to nearly every industry.

Attachment rates for critical hardware advantages will grow significantly to manage the greater utilization of air space. The use of radar, LiDAR and high-definition cameras will increase. At the same time, the attachment rates of cellular antennas will grow to cater to remote deployments and provide the private network capabilities of telecommunication companies, including Ericsson and Nokia, which aim to deploy to expand drone usage. Attach rates for AI chipsets (GPU and ASIC) will grow to encompass 79 percent of all drones by 2030, a CAGR of 50 percent. Incorporating AI chipsets in sUAS enables performance-enhancing value adds such as simultaneous localization and mapping, machine vision and semi-autonomous flight.

Airborne robotics bring appealing value propositions to nearly every industry, promising to transform current business models while unlocking new robotics use cases and applications.

These findings are from ABI Research's "The Small Unmanned Aerial System Ecosystem" market data report.

Around the **Circuit**

Barbara Walsh, Multimedia Staff Editor

MERGERS & ACQUISITIONS

Teledyne Technologies Inc. announced that it has entered into an agreement to acquire select aerospace and defense electronics businesses from **Excelitas Technologies Corp.** for $710 million in cash. The acquisition includes the Optical Systems (OS) business known under the Qioptiq® brand based in Northern Wales, U.K., as well as the U.S.-based advanced electronic systems (AES) business. The U.K.-based OS business provides advanced optics for heads-up and helmet-mounted displays, dismounted tactical night vision systems and proprietary glass used in space and satellite applications. In the U.S., the AES business provides custom energetics, including electronic safe and arm devices, high voltage semiconductor switches and rubidium frequency standards for defense and space applications.

Molex announced the signing of an agreement to purchase **AirBorn Inc.**, an employee-owned company headquartered in Georgetown, Texas, specializing in the design and manufacturing of rugged connectors and electronic components for global original equipment manufacturers serving the aerospace and defense, commercial air, space exploration, medical and industrial markets. For more than 60 years, AirBorn products have been trusted to perform in extreme conditions where mission-critical reliability is vital to success.

COLLABORATIONS

Infineon Technologies AG and **Quantinuum** announced a strategic partnership to develop the future generation of ion traps. This partnership will drive the acceleration of quantum computing and enable progress in fields such as generative chemistry, material science and artificial intelligence. Infineon innovates with a dedicated team to make their trapped-ion QPUs the heart of the leading quantum computers. The company has invested in this field since 2017, applying its expertise in high volume processing technologies and developing technologies, like integrated photonics and control electronics, to enable their partners to scale the qubit count of their machines.

NEW STARTS

Smiths Interconnect offers RF Solution Services for unique filter product designs and extremely challenging requirements. With decades of experience and multitudes of proven RF filter solutions, many customers can identify Smiths Interconnect commercial-off-the-shelf products or products needing only minor variation to meet their needs. However, in some situations, customers need unique products and/or products to meet extremely challenging requirements. These opportunities will be addressed by Smiths Interconnect's RF Solution Services. The new service has been developed to support filter design and manufacturing for critical applications involving satellites, space flight, radars, unmanned vehicles, military programs and other areas that require unusual or demanding solutions.

Gapwaves announced the opening of its pilot line production facility in Gothenburg, which serves as a production and industrialization hub. This strategic investment is a key step in Gapwaves' journey to become a certified supplier of waveguide antennas to the automotive market while expanding production capacity to meet the demands of customers in other market segments. The pilot line includes the assembly and testing of injection-molded waveguide and multi-layer waveguide antennas, developed by Gapwaves for its partners and customers. Beyond its production capabilities, the facility functions as an industrialization hub, where scalable production processes are developed and validated before being transferred to Gapwaves' qualified high volume production partners worldwide.

ACHIEVEMENTS

Anritsu Corporation announced full support for 5G and LTE Next Generation eCall (NGeCall) validated test cases on its 5G NR Mobile Device Test Platform ME7834NR, enabling GCF certification. eCall is a European initiative designed to provide rapid assistance to motorists involved in accidents. It uses an in-vehicle system equipped with sensors that, when triggered (e.g., by airbag deployment), automatically place an emergency call to the pan-European Emergency Number 112. Along with the voice call, essential data such as location, passenger count and vehicle direction is sent to the PSAP.

CONTRACTS

L3Harris Technologies has received an indefinite delivery, indefinite quantity award from the **U.S. Navy**, worth up to $999 million, to provide U.S. and coalition forces with resilient communications technology. Over the next five years, L3Harris will deliver its Multifunctional Information Distribution System Joint Tactical Radio System Terminals (MIDS JTRS). L3Harris is one of two providers of the MIDS JTRS solution, which is a critical, software-defined Link 16 resilient communication radio for a variety of air, ground and maritime platforms.

BAE Systems was awarded a follow-on contract from the **U.S. Army** to further develop its Multi-Class Soft Kill System (MCSKS) countermeasures to protect ground combat vehicles against guided missiles and adjacent threats, improving vehicle survivability and mission success. Under the MCSKS contract, BAE Systems will further develop its laser-based Stormcrow™ and TERRA RAVEN™ countermeasure systems, advancing the Army's electronic warfare (EW)-based Active Protection System work. The advanced systems effectively counter threats and allow crews to conserve kinetic countermeasures.

Raytheon, an RTX business, has been awarded a contract from the **U.S. Army** to work on directed energy

For More Information For up-to-date news briefs, visit mwjournal.com

wireless power beaming capabilities that will distribute power across the battlefield, simplify logistics and safeguard locations for U.S. troops. The work is being conducted as part of a larger effort under the Department of Defense's Operational Energy Strategy. Under the contract, Raytheon's Advanced Technology team will develop advanced wireless power transmitter and receiver technologies to enable a long-range demonstration in line with the needs of U.S. Army manned and unmanned system requirements.

PEOPLE

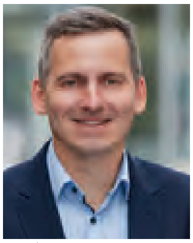

▲ *Markus Fischer*

Markus Fischer, previously executive vice president of operations, has been appointed to the **Rohde & Schwarz Executive Board**. As chief operating officer, he will collaborate with CEO Christian Leicher and CTO Andreas Pauly to continue to keep the company on course for growth in these challenging times. With Fischer, Rohde & Schwarz has once again bolstered its top management team from within the company's own ranks. He joined the technology group in 2011 as head of Corporate Material Sourcing at the Munich headquarters. After another management role at Rohde & Schwarz Messgerätebau GmbH in Memmingen, he assumed overall responsibility for the group's supply chain in 2017. In July 2020, he was appointed executive vice president of operations, becoming a member of corporate management.

REP APPOINTMENTS

PEI-Genesis announced its new distribution agreement with **XMA Corporation**. As an authorized global distributor for XMA, PEI-Genesis enhances its ability to meet the growing demand for advanced RF solutions across industries such as telecommunications, aerospace, defense and cryogenics. XMA Corporation, an Amphenol company, is an industry leader in microwave and mmWave RF technology, primarily focusing on interconnect RF products for the space, aerospace and defense, quantum computing/cryogenics, telecommunications (5G) and test and measurement industries. This strategic partnership brings RF attenuators, RF terminations, power dividers/combiners, couplers, equalizers and DC blocks to PEI-Genesis' portfolio.

Quantic PMI (Planar Monolithics Inc.), a business of **Quantic® Electronics** and designer and manufacturer of RF and microwave components, integrated modules and subsystems, announced a global distribution agreement with **Richardson RFPD**, a specialized electronic component distributor. Through this agreement, Quantic PMI will provide customers with expanded global access to in-stock and commercial-off-the-shelf products. This agreement enables immediate access to select products from the Richardson RFPD storefront and expands global reach for Quantic PMI's modified-off-the-shelf products and custom solutions.

INVITED PAPER

Metamaterial Innovations: From Xerox PARC to Leading Companies

Pat Hindle and Eric Higham
Microwave Journal, Norwood, Mass.

Metamaterials are emerging as a transformative technology in the RF and microwave markets. Taken in the abstract, a metamaterial is a composite material that is used to affect electromagnetic waves. While practical models and methods, along with artificial metamaterials, are new developments within the past three decades or so, explorations of using artificial dielectrics to influence electromagnetic waves were reported at the end of the 19th century.[1]

One of the biggest drivers of fundamental research into and implementation of metamaterials has been the Xerox Palo Alto Research Center (PARC). Metamaterial technology originating from this research at Xerox PARC has enabled breakthroughs in fields ranging from telecommunications and radar to security screening. This article discusses metamaterial fundamentals, along with the evolution of this technology at Xerox PARC from inception to commercialization. As is often the case with new technologies at research centers, the efforts have incubated several companies. The article also addresses companies like Kymeta, Echodyne, Pivotal Commware and Evolv Technology that have spun out of activities at Xerox PARC. Each company is harnessing metamaterials in unique and innovative ways to enable new and exciting possibilities in a broad range of industries and applications. These activities are also sparking tremendous interest in the future and potential of this technology. ***Figure 1*** shows the entrance to the Xerox PARC facility in Palo Alto, Calif.

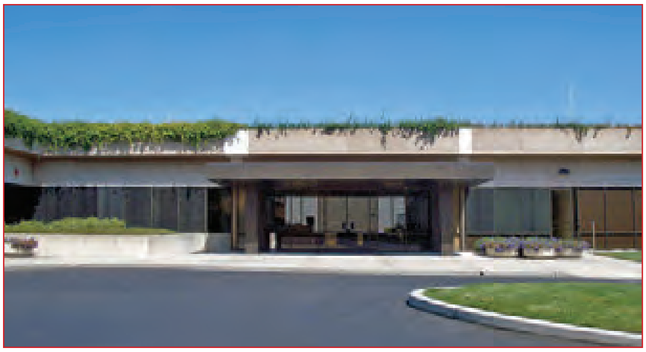

Fig. 1 Xerox PARC in Palo Alto. *Source:* en.wikipedia.org/w/index.php?title=File:Parcentrance.jpg

UNDERSTANDING METAMATERIALS

Metamaterials are typically composed of structured arrays of elements at sub-wave-

length sizes. These elements interact with the electromagnetic waves. The structured design allows researchers and designers to control the wave propagation properties by manipulating how these materials interact with light, sound or even thermal energy. A notable property of metamaterials is their ability to achieve a negative refractive index, which causes light to bend in the opposite direction when passing through the material. This phenomenon can be applied to create what are called "superlenses." This phenomenon in these lenses enables resolution beyond the diffraction limit, the smallest detail that a lens can resolve, of conventional lenses. By extending this limit, metamaterial lenses can have much better resolution than traditional lenses. In addition, the negative refractive index can be used for stealth technologies that could render objects effectively invisible by bending light around them.

The properties of metamaterials are determined by their internal structure rather than their composition alone. These properties and the dependence on internal structure open many exciting avenues for customization. By altering the size, shape or arrangement of these internal elements, the metamaterial can be tailored to exhibit specific properties. This ability to customize can have far-reaching implications for telecommunications applications, where metamaterials can improve the performance of antennas, filters and waveguides by optimizing signal propagation and reducing interference. ***Figure 2*** shows a negative-index metamaterial array of split-ring resonators realized in an array measuring 10 × 100 × 100 mm. In this example, the array consists of 3 × 20 × 20 unit cells.

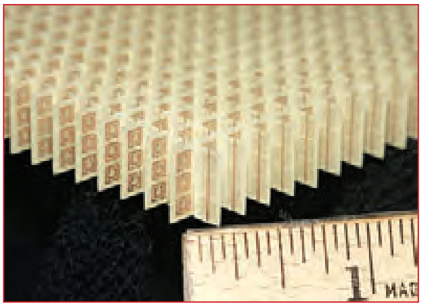

Fig. 2 Split-ring resonators. *Source:* en.wikipedia.org/wiki/Metamaterial

METAMATERIAL FOUNDATIONS: THE XEROX PARC ERA

At Xerox PARC, the exploration of metamaterials focuses on three primary areas: telecommunications, optics and energy. For telecommunications applications, metamaterials are used to enhance signal transmission and reception. There are a variety of telecommunications applications for metamaterials, including reconfigurable intelligent surfaces (RIS), that can be used in antennas for beamforming, polarization control, signal redirection and signal strength enhancement. These developments will be significant in efforts to improve wireless network coverage and capacity, along with enabling the development of IoT. PARC researchers have shown that metamaterial structures enhance the efficiency and range of wireless communication systems, making them more resilient to interference and capable of operating at higher frequencies.

In optics, Xerox PARC's metamaterials research aims to develop advanced lenses and imaging systems. Traditional lenses rely on the curvature and refractive index of glass or plastic to focus light. Metamaterial lenses use their structural properties to achieve similar effects but with greater control and the ability to manipulate the light waves. The expectation is that this research and these developments will lead to ultra-thin, lightweight lenses with applications in cameras, microscopes and even virtual and augmented reality devices that are important to the emerging 6G vision.

Xerox PARC's exploration of metamaterials also extends to the energy sector, where these materials can be used to enhance the efficiency of photovoltaic cells, along with solar energy and energy storage solutions. Research is showing that the thermal or electromagnetic properties of metamaterials can be tailored to enable solar cells to capture a broader spectrum of sunlight or concentrate solar energy more effectively. Additionally, metamaterials can be designed to store thermal energy or to control heat transfer, which has applications in energy-efficient buildings and thermal management systems in electronics.

Xerox PARC has long been known for innovative research in computing and materials science. The company has played a pivotal role in metamaterial development. Since metamaterials are engineered composite materials, the Xerox PARC researchers are focusing on developing intricate structures that enable metamaterials to manipulate light, sound and radio waves beyond the limitations of natural materials. Key advancements from Xerox PARC include the development of metamaterial lenses, enabling compact and high-resolution imaging systems and other breakthroughs that continue to lay the groundwork for practical applications in telecommunications, sensing and other applications. In late April of 2023, Xerox announced the donation of the lab to SRI International, a non-profit research institute with the hopes of further building, expanding and scaling capabilities among a diverse set of technology and scientific areas.

XEROX PARC AS AN INCUBATOR

As mentioned, some of these developments have grown beyond Xerox PARC and spawned the formation of new companies. The rest of this article will look at some of the companies that have grown out of activities at Xerox PARC with some insight into the activities at these companies.

Kymeta Corporation: Metamaterials Revolutionizing Satellite Communications

Founded in 2012, Kymeta Corporation emerged from Xerox PARC's metamaterial research with a mission to improve satellite communications. Kymeta's core technology revolves around metamaterial-based electronically steerable antennas (ESAs). Traditional satellite antennas, such as parabolic dishes, are bulky and mechanically cumbersome, limiting their application in mobile and remote environments. Kymeta's ESAs use metamaterials to electronically steer beams

without moving parts, offering significant advantages in terms of size, weight and adaptability. These antennas enable high speed, mobile satellite connectivity, bridging the digital divide in remote areas and enhancing communication capabilities for maritime, aviation and military sectors.

Technical Capabilities of Kymeta's Products:

- **Metamaterial Antennas:** Kymeta's ESAs use metamaterials to steer beams across the satellite spectrum electronically. These antennas provide connectivity in mobile environments where deploying traditional antennas would present challenges.
- **Compact Form Factor:** By eliminating the need for mechanical components, Kymeta's antennas are much smaller and lighter than conventional satellite dishes, making them well-suited for integration into vehicles, aircraft and portable communication systems
- **Adaptability and Efficiency:** Metamaterial-based design enables Kymeta's antennas to adjust beam direction and shape dynamically. These features optimize signal strength and minimize interference to enhance communication efficiency.

Kymeta's solutions are being widely adopted, establishing the company as a leader in metamaterial applications for satellite communications.

Echodyne Corporation: Metamaterials Redefining Radar Systems

Echodyne Corporation, founded in 2014, specializes in metamaterial-based radar systems that improve detection and imaging performance. Traditional radar systems rely on large, mechanically scanned arrays to achieve high-resolution and accuracy. Echodyne's metamaterial ESAs are a compact, solid-state alternative that provides rapid beam steering and high-resolution imaging.

Technical Capabilities of Echodyne's Products:

- **Metamaterial ESAs:** Echodyne's radar systems leverage metamaterials to electronically steer beams with precision, enabling rapid scanning and better resolution than conventional radars
- **Enhanced Imaging:** The use of metamaterials allows Echodyne's radars to achieve finer resolution and improved signal clarity, essential for applications such as autonomous vehicles, perimeter security and drone detection
- **Compact and Lightweight:** By eliminating bulky mechanical parts, Echodyne's metamaterial-based radars are more portable and easier to integrate into various platforms without compromising performance.

Echodyne's radar solutions have advanced situational awareness across industries, demonstrating the potential of metamaterial technologies.

Pivotal Commware: Metamaterials Enabling 5G Communications

Pivotal Commware, established in 2016, focuses on using metamaterials to enhance wireless communications, particularly for 5G networks. The transition to 5G introduces challenges such as signal propagation at higher mmWave frequencies and the need for precise beamforming. Beamforming is a technique that focuses a wireless signal toward a specific direction rather than broadcasting it in all directions. This technique reduces interference and allows signals to overcome obstacles more easily. Pivotal Commware's antennas use metamaterials to implement holographic beamforming, dynamically shaping and steering radio waves for optimal coverage and performance.

Technical Capabilities of Pivotal Commware's Products:

- **Holographic Beamforming Antennas:** Pivotal Commware's antennas use metamaterials to im-

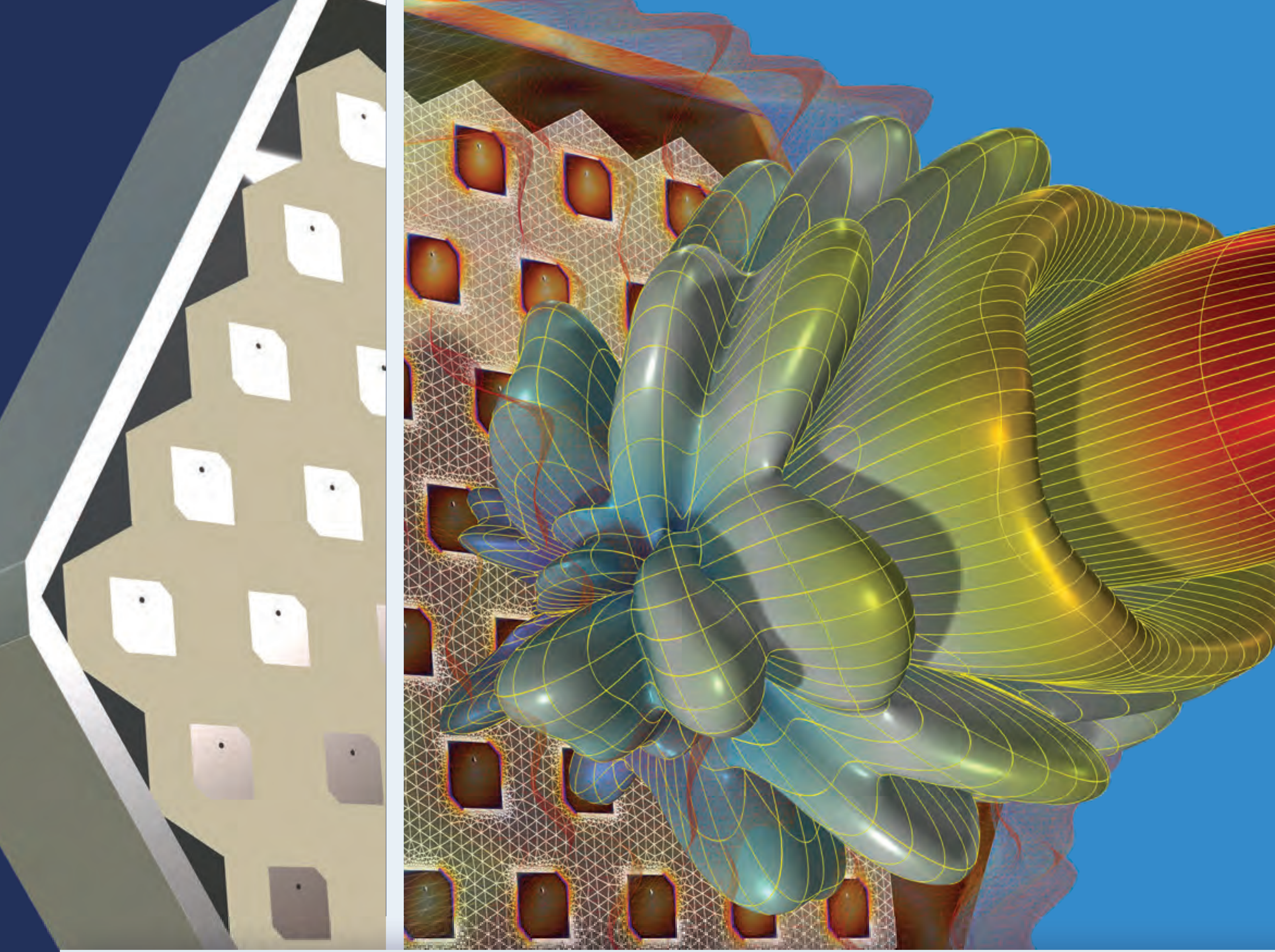

Take the Lead in RF Design

with COMSOL Multiphysics®

Multiphysics simulation is expanding the scope of RF analysis to higher frequencies and data rates. Accurate models of microwave, mmWave, and photonic designs are obtained by accounting for coupled physics effects, material property variation, and geometry deformation. Ultimately, this helps you more quickly see how a design will perform in the real world.

» *comsol.com/feature/rf-innovation*

COMSOL

plement holographic beamforming, dynamically shaping and steering radio waves for optimal coverage and performance
- **mmWave Optimization:** Metamaterial-based antennas improve the efficiency and range of mmWave transmissions, facilitating the deployment of 5G networks in urban environments and beyond
- **Adaptive Beam Steering:** By adjusting the beam direction in real-time, Pivotal Commware's antennas mitigate signal blockage and interference, ensuring consistent and reliable connectivity for 5G applications.

Pivotal Commware's metamaterial solutions are accelerating the deployment of 5G infrastructure worldwide, addressing challenges in next-generation wireless communications.

Evolv Technology: Metamaterials Enhancing Security Screening

Evolv Technology, founded in 2013, applies metamaterials to advance security screening systems, transforming how threats are detected and mitigated in public venues.

Technical Capabilities of Evolv Technology's Products:

- **Metamaterial Sensors:** Evolv Technology's security screening systems employ metamaterial sensors capable of detecting a wide range of threats, including metallic and non-metallic items, with high accuracy and minimal false alarms
- **High Throughput Screening:** The integration of metamaterial technology enables Evolv's systems to process large volumes of individuals efficiently, enhancing throughput rates at security checkpoints
- **Non-Intrusive Screening:** Unlike traditional methods that require physical contact or removal of belongings, Evolv's metamaterial-based sensors allow for discreet and non-intrusive screening, improving the overall passenger experience.

Evolv Technology's innovative use of metamaterials is helping to redefine and improve security screening standards, offering scalable solutions that prioritize safety and efficiency in public spaces.

FUTURE DIRECTIONS AND IMPLICATIONS

The evolution of metamaterials from theoretical concepts to practical implementation starts with companies like Xerox PARC. It is evolving with companies that have spun out of Xerox PARC, like Kymeta, Echodyne, Pivotal Commware and Evolv Technology, to commercialize the technology. The number of companies working with metamaterials underscores the potential of the technology across many industries and applications. As research and development activities in metamaterials continue to evolve, more opportunities for metamaterial innovation and integration into new applications will emerge.

Metamaterials, born from research at Xerox PARC, are catalyzing a wave of innovation and spawning companies that will continue to lead the charge in satellite communications, radar systems, 5G technology and security screening. Each company, Kymeta, Echodyne, Pivotal Commware and Evolv Technology, highlights the promise of metamaterials in pushing technological boundaries and addressing complex challenges. As these companies continue to innovate and expand their applications, metamaterials are poised to shape the future trajectory of technology, unlocking new possibilities for connectivity, security and beyond. ■

Reference

1. J. Ramsay, "Microondas antena de guía de ondas y técnicas antes de 1900," *Proceedings of the IRE* (Abstracto), 46 (2): 405, 1958. doi: 10.1109/JRPROC.1958.286869. ISSN: 0096-8390. S2CID 51663713.

INVITED PAPER

Microwave SSPAs in EW and Radar Systems: The Current Situation and Trends

Terry Edwards
Engalco-Research, Bridlington, U.K.

For several decades, the microwave electronics industry has exhibited strong market growth, especially for solid-state components, including solid-state power amplifiers (SSPAs).[1] This article focuses on these types of amplifier products in various electronic warfare (EW) and radar system applications. It provides background information together with some forecast data indicating the expected progress for the markets to the year 2030.

Complete microwave systems require substantial signal processing between the inputs and the antennas. In this article, the focus will be on communications systems, EW (including jamming) and radars. Immediately "behind" the antenna, on the transmission side, there is always the need for a microwave power amplifier (PA). Today, solid-state semiconductor technologies are almost universally implemented in PAs.

Fig. 1 Jamming pod. *Source:* L3Harris Corporation.

OVERVIEW OF MICROWAVE SSPA TECHNOLOGY OPTIONS

This article focuses on microwave module-based SSPAs. For radar applications, excluding active electronically scanned arrays (AESAs), the focus is on those systems that incorporate SSPA modules or related MMICs. Low- to medium-power MMIC-based SSPAs are often supplied in QFN packages. Higher power SSPAs are packaged in metal casings and cooling is necessary. Until quite recently, traveling wave tube (TWT) devices often fulfilled the requirement for microwave PAs, but semiconductors are now dominating. Occasionally, a combination of an SSPA and a TWT is used in a traveling wave tube amplifier (TWTA). In these cases, the TWT is driven by an SSPA. However, the focus of this article is entirely on microwave SSPAs used in EW, mainly for jamming applications and military radar applications. A typical jamming pod, the Next Generation Jammer, used in EW applications is shown in ***Figure 1***. These types of systems are installed immediately beneath the metal skin of the aircraft. An example of Northrop Grumman's AN/SPQ-9B multimode X-Band pulsed Doppler radar is shown in ***Figure 2***.

Fig. 2 Northrop Grumman's AN/SPQ-9B radar. *Source:* Northrop Grumman Corporation.

According to Northrop Grumman, their AN/SPQ-9B can detect

TABLE 1
MICROWAVE SSPA CATEGORIES

	MPA	HPA	VHPA
Power Output (W)	Up to a few	Up to several hundred	Up to several thousand
Typical Size (cm)	A few in each dimension	10 x 15 x 5	12 x 18 x 6

all known and projected sea-skimming missiles. In this application, the microwave SSPAs are packaged in aluminum boxes with SMA connectors.

Several parameters characterize an SSPA, but the RF output power is almost always the primary consideration. This output power can range from a few watts (30 to 40 dBm) to several kilowatts. The RF power output can be continuous wave (CW) for EW or pulsed with a typical 10:1 duty cycle for radar systems. In this article, SSPAs are characterized as medium-power amplifiers (MPAs), high-power amplifiers (HPAs) and very high-power amplifiers (VHPAs). ***Table 1*** shows a categorization of these classifications.

These amplifier designations can generally be described with the following characteristics:

MPAs (CW): Most often, GaAs-based MMICs in QFN packages with DC supply voltages typically around 12 V.

HPAs (CW): GaN-based MMICs for tens to hundreds of watts. Hybrid circuits are used for the higher power levels and LDMOS is used at lower frequencies. The DC supply voltage is typically 40 V. Multiple transistors or pallets are often used and the balanced circuit configuration is frequently adopted.[1] The minimum requirement is two transistors or MMICs, per balanced circuit. This means there may be 20 transistors or MMICs used for 10 parallel circuits in a pallet.

VHPAs: Circuits use LDMOS or GaN discrete transistors. They are pulsed for radar applications with several kW peak power not uncommon. DC supply voltages are typically around 100 V or more. Multiple blocks, in parallel, are often used and the balanced circuit configuration is often adopted, like HPAs.

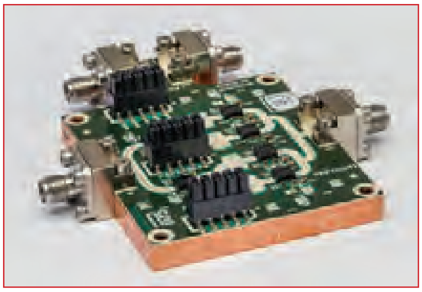

▲ **Fig. 3** **CMX90A705A6 Ka-Band MMIC-based SSPA. *Source:* CML Micro Compound Semiconductor Design team.**

GaN HEMT devices, typically using GaN-on-SiC technology, are already significant and growing in importance in this industry. MMICs are used wherever possible, but discrete transistors within a hybrid circuit may be the best solution for higher microwave power levels. CW systems are required for most EW system applications, whereas pulsed amplifiers are common for most non-AESA radar systems. These systems generally operate in L-Band (0.3 to 2 GHz), S-Band (2 to 4 GHz), C-Band (4 to 8 GHz), X-Band (8 to 12 GHz), Ku-Band (12.4 to 18 GHz) and Ka-Band (26.5 to 40 GHz). In some instances, ITU band designations of UHF (0.3 to 3 GHz) and SHF (3 to 30 GHz) may be used.[2,3]

As a practical example, ***Figure 3*** shows a MMIC-based Ka-Band SSPA developed by CML Micro Compound Semiconductor Design team. This SSPA uses six GaN-based MMICs designed by PRFI. Two of the MMICs are close to the input side with the remaining four located near the output. The device operates with a 10 percent duty cycle and provides an average output power of 5.5 W from 27.5 to 31 GHz.

MICROWAVE SSPA MANUFACTURERS (OEMS)

A wide range of companies, most of whom are headquartered in the U.S., supply various types of microwave SSPAs. Leading OEMs include overall market leader Stellant Systems, Kratos Defense, MACOM, CPI, Mercury Systems,

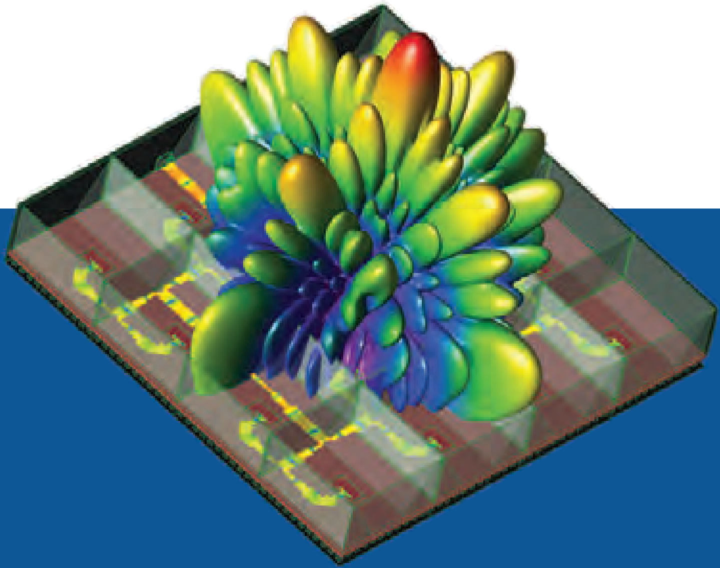

MtronPTI, Qorvo, RFHIC, CAES (recently acquired by Honeywell) and Nanowave Technology. Stellant, Kratos, MACOM and CPI lead the pack, in that order.[2,3]

There are 56 OEMs captured in the cited references and approximately three-quarters of all the OEMs employ between 1 and 300 people, so these are not large conglomerates. Many of these companies either specialize in the manufacturing of microwave SSPAs or those products form a significant part of their overall portfolios. The OEM distribution by the number of employees is shown in ***Figure 4***. This chart uses typical numbers rather than the actual data.[3]

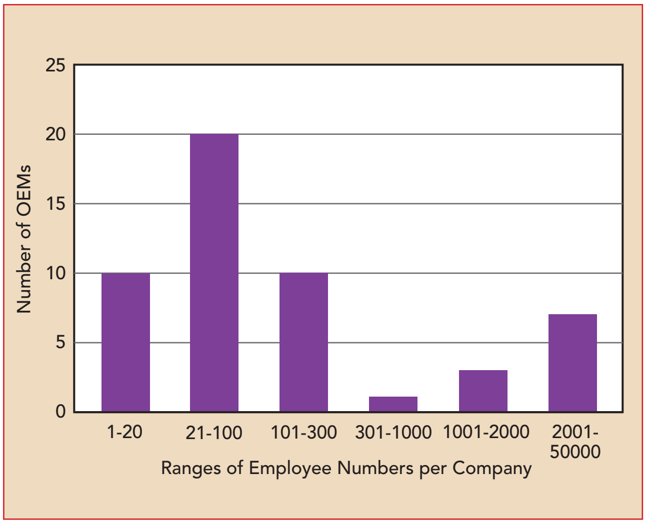

Fig. 4 **OEM count as a function of the representative number of employees.**

The distribution exhibited in Figure 4 is typical in that it tends to apply to almost any electronic assembly. The distribution indicates that most OEMs are SMEs employing no more than 300 people. The number of companies peaks in the 21 to 100 employee range before a dip follows this initial peaking trend. After this dip, a moderate increase is seen that applies to large and very large companies. For this class of companies that employ upwards of 1000 people, microwave SSPAs have always represented a relatively small part of their overall product portfolios.

In terms of location, the U.S. is home to the largest number of companies. There are 34 companies, 61 percent of the overall total, headquartered and having primary operations in the U.S. The majority of these companies, 18, are located in California. The U.K. occupies second place with five OEMs, although most are very small operations. South Korea takes third place with four OEMs headquartered in this country. The Gyeonggi-do high-tech defense-related cluster is particularly important in this regard.

In terms of the total available market, revenue from the MMIC or chipset will always be substantially lower than the value of the complete microwave SSPA and the system. The SSPA requires additional digital, processing and RF functions. It will be in a housing of some type with electrical and RF connections to the remainder of the system that contains an antenna, which is often the most expensive component. In addition, some cooling may be required, particularly for HPAs and VHPAs. This is likely to involve forced air cooling, but in some cases, like airborne jamming pods used in EW applications, natural air flow provides substantial in-flight cooling.

EW AND RADAR SYSTEM MARKET SHARE

Advances and developments at system suppliers are the primary driving features for module and subsystem manufacturers. Therefore, the dynamics associated with those systems have already been accounted for in the forecast data. The forecast reports rely heavily on primary and secondary research into the industry, the players and the technologies.

For each product category in the microwave SSPA family, the forecast lists total addressable market (TAM) data for the 2023 to 2030 forecast period. In this case, TAM addresses the merchant market, which is the portion of the market that is broadly addressed by distributors, agents,

MI-WAVE

Millimeter Wave Products Inc.

NEW!

COMPACT ULTRA WIDEBAND OMNI-DIRECTIONAL ANTENNAS

Available from 5.0-70 GHz

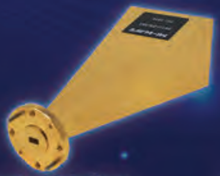

Standard Gain Horns

Available from 8.2 to 750 GHz

Trihedral Corner Reflector Antenna

Standard sizes from 1 to 8 inch configurations

Conical Horn Antennas

Available from 8.2 to 325 GHz

Cassegrain Reflector Antennas

Available from 5.0-110 GHz

Diameters from 10 to 48 Inches

Prime Focus Antennas

Available from 5.0-110 GHz

Diameters from 10 to 48 Inches

Linear to Circular Polarizers

Available from 8.5 – 220 GHz

RF Orthomode Transducers OMT

Available from 8.5 – 220 GHz

NEW!

Frequency Agile Radar Signal Generation Synthesizers

APPLICATIONS

- Automated Test Equipment (ATE)
- Frequency Agile Radar Signal Generation
- Local Oscillators & System Clock Source
- Telecommunications/Satellite Communications
- Embedded Systems
- Secure Communications & Electronic Warfare
- Beamforming & MIMO R&D
- Spectroscopy

MI-WAVE SYNTHESIZER CONTROL INTERFACE

FEATURES

- ***Output Power +20 dBm Typical, Higher Output Power Available***
- ***Digital Phase Shifter*** with 0.0002° resolution and Full 360° range
- ***Remote RF Control:*** Seamlessly operate RF signals via an intuitive GUI over Wi-Fi or Ethernet.
- ***Four Operating Modes:*** CW, Frequency Sweep, Frequency Hop, and External Trigger.
- ***Modulation:*** Supports external configuration for FSK modulation.
- ***CW Mode Filter:*** Customizable internal filter for precise and clean signal output.
- ***High Resolution:*** Achieve fine frequency adjustments with 0.01 Hz resolution.
- ***Ultra-Fast Switching:*** Less than 10 µs for rapid frequency transitions.
- ***Integrated Attenuators:*** Up to 70 dB attenuation for enhanced signal management.
- ***Low Phase Noise:*** Ensures outstanding signal clarity and quality.
- ***Reference Switching:*** Easily switch between internal and external references, including an integrated 10 MHz or 100 MHz option.
- ***Reference Compatibility:*** Supports a wide range of reference frequencies, from 10 MHz to 250 MHz.
- ***Temperature Monitoring:*** Built-in sensor for stable and consistent performance.
- ***Single Supply Operation:*** Efficiently runs on 8VDC to 15VDC power.

958 SERIES

GUI CONTROLLED WIDEBAND SYNTHESIZERS

0.1-8 GHz
0.1-16 GHz
0.1-32 GHz
0.1-67 GHz
V-Band (WR-15)
E-Band (WR-12)
W-Band (WR-10)

2007 Gandy Blvd N Suite 1310
St. Petersburg, FL 33702

Tel: (727) 563-0034
Email: sales@miwv.com

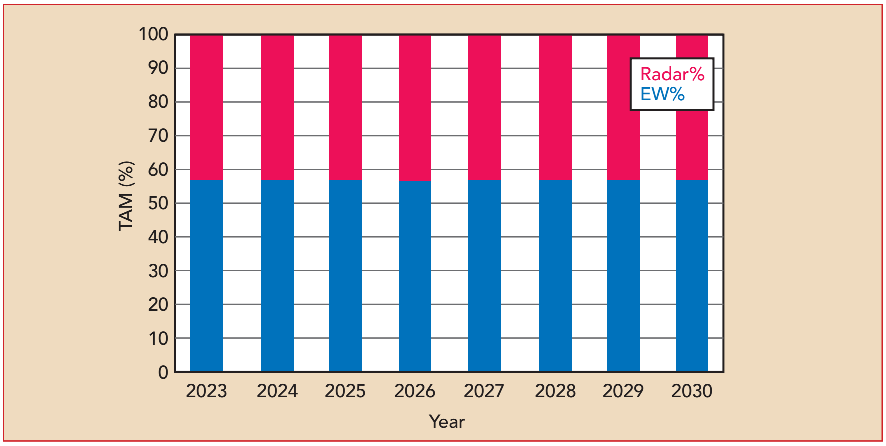

Fig. 5 EW and radar systems TAM.

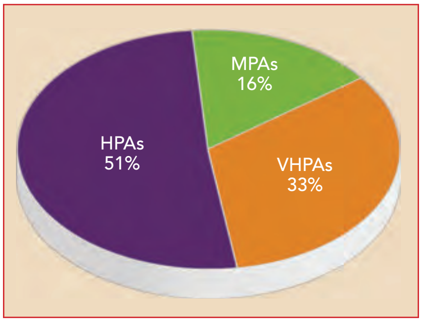

Fig. 6 Microwave SSPA product categories by 2024 revenue.[3]

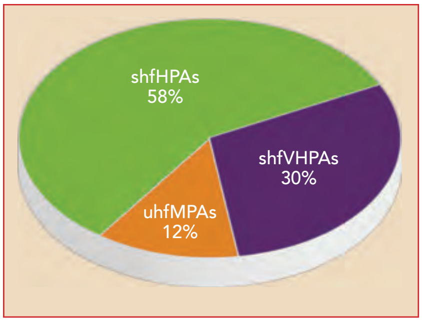

Fig. 7 2024 TAM share by frequency band for microwave SSPAs.

sales subsidiaries or directly from the OEM. The total market also includes the captive portion of the market, where system OEMs use internally manufactured devices. Estimating captive revenue is not feasible because it entails a knowledge of the internal transfer considerations at each company in the forecast. The simple relationship is: TAM = (total market) - (captive market).

The captive market can be significant, especially in the defense segment. For a number of technology, security and commercial reasons, defense contractors may prefer to retain control over electronics design, IP and manufacturing capabilities. Engalco-Research's latest forecast for microwave SSPA TAM and the distribution between EW and radar applications is shown in ***Figure 5***. It is important to note that China trails only the U.S. in terms of defense spending. However, the methodology of primary and secondary research, coupled with the current geopolitical situation, does not allow for a reliable and accurate estimation of activity in China.

Figure 5 shows that microwave SSPA revenue for EW applications consistently exceeds the revenue for radar applications. Over the forecast period, the EW market share will see a slow but steady increase. The global TAM is expected to surpass $1 billion in 2026. We expect revenue in this market will experience year-over-year growth rates from 5 percent to just over 6 percent over the forecast period. A slight reduction in the growth rates is anticipated during the later years of the forecast.

Regionally, North America, mainly the U.S., always leads the markets. It is home to Tier 1 corporations like L3Harris, Northrop Grumman and Raytheon. Europe is the second-largest region with Tier 1 companies that include BAE Systems, Leonardo and Thales. Israel, because of geopolitical challenges, occupies the third spot in the forecast with suppliers like Elbit Systems, Israel Aerospace Industries and Rafael Advanced Defense Systems. Southeast Asia, driven mainly by Australia, India, Japan and Korea occupies fourth place over the forecast period.


SM435B
SM435B
PN400

MARKET SHARE BY PRODUCT CATEGORY AND FREQUENCY BAND

Figure 6 shows the 2024 market share data for the three categories of microwave SSPAs defined earlier.[3] From Figure 6, the importance of HPAs is evident. These PAs find applications in X-Band, (most notably) and Ku-Band systems for both EW and radar applications. The revenue from VHPAs is also substantial, mainly because of the relatively high unit prices of these amplifiers. It is important to observe the market shares given in Figure 6 are in terms of revenue, not units. The selling price of amplifiers tends to increase as the required output power increases. The average unit prices of the MPA category of PAs tend to be the lowest of all three categories. This contributes to this category having the smallest revenue in 2024, with a market share of 16 percent.

Segmentation by frequency band also shows some interesting results. ***Figure 7*** shows the anticipated 2024 composite radar and EW revenue for the three microwave SSPA categories over two different frequency bands. Again, the HPA segment accounts for more than half of the total revenue. The SHF HPAs are mainly used in EW applications. The next largest segment is VHPAs in the SHF frequency range. These PAs are used in both radar and EW applications, with the radar share edging the EW share by a small margin. The UHF MPAs, once again, account for the smallest share. This opportunity is satisfied mainly by MMICs in QFN packages for EW applications. Since Figure 7 uses the broader SHF and UHF frequency designations, it is instructive to note that X-Band applications dominate within the SHF frequency range. In practice, these X-Band SSPAs may operate across a frequency band such as 8 to 10 GHz as opposed to the full 8 to 12 GHz band.

Figure 8 shows the microwave SSPA market share in terms of units. This data paints a much different picture. From a unit standpoint, the MPA category is the largest, with an estimated 2024 market share of

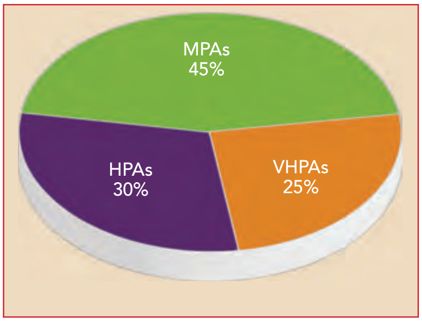

Fig. 8 2024 microwave SSPA shipments power level.

45 percent. This is in sharp contrast to the revenue market share profile from Figure 6 and it reflects the low price and high volume nature of these products that are often realized as MMICs. The HPA category is next from a volume standpoint, with an estimated 30 percent market share in 2024.

CONCLUSION

Microwave SSPA usage in military applications is well-established and these devices are vital to system performance. These products are steadily displacing TWTAs at higher power levels and we believe this trend will continue. The general trend toward systems operating at ever-decreasing RF power levels will also continue to favor solid-state amplifiers. With the well-established presence of several powerful and effective OEMs, it will be very difficult for any newcomers to penetrate these markets seriously. Newcomers will have to demonstrate a strong and highly competitive product or products to be able to make their presence felt in the highly demanding EW and military radar markets. Corporate expansion will be largely by acquisition rather than through organic growth. ■

References

1. T. Edwards, "Technologies for RF Systems," *Artech House*, Boston, Mass., 2018.
2. T. Edwards, "Microwave SSPAs: Technologies & Industry" (an industrial monograph), *Engalco-Research*, August 2024.
3. "Microwave Solid State Power Amplifiers (SSPAs) into Free-World EW and Radar Markets. Industry Structure & Market Forecasts to 2030," *Engalco-Research*, September 2024.

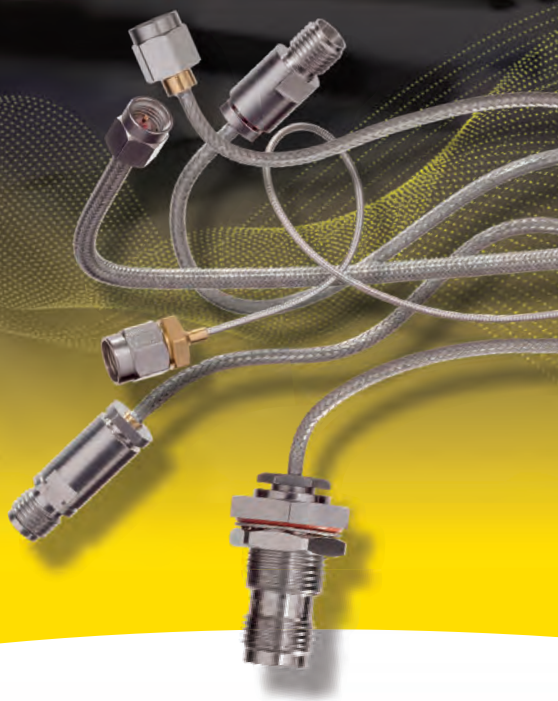

INVITED PAPER

Using AI for Antenna Design, Analysis and Optimization

Sudarshan Sivaramakrishnan, Vishwanath Iyer, Tina Gao and Giorgia Zucchelli
MathWorks, Natick, Mass.

AI is significantly impacting almost all engineering fields, but its potential is especially promising for antenna analysis and optimization to minimize the need for repeated full-wave electromagnetic simulations. Although AI models have proven effective in characterizing and optimizing various antennas, the field lacks a comprehensive framework for both standard and custom antenna solutions. To address this gap, AI techniques are applied to create scalable and generalizable models for antenna design and analysis, enabling adoption by engineers without expertise in electromagnetic theory or AI.

To support the design and optimization of a comprehensive AI-driven workflow with minimal specialized knowledge in machine learning (ML) and electromagnetics, engineers can rely on pre-trained ML, AutoML and optimization algorithms. The AI-driven approach, coupled with the pre-trained algorithms, accelerates the antenna design process. It also democratizes access to advanced design tools, allowing for faster and more flexible customization and performance enhancement.

RAPID ANTENNA ANALYSIS WITH PRE-TRAINED MODELS

For engineers, it begins with developing pre-trained AI models for antenna analysis while addressing the lack of commercially available design software with built-in AI capabilities. The approach consists of the following steps:

1. **Catalog Standard Antennas:** Begin with a set of standard antennas with parameterized geometries suitable for full-wave electromagnetic simulation.
2. **Prototype Design Development:** For each antenna, derive an initial design prototype using a combination of design variables (e.g., geometric parameters) to ensure resonance at a specified frequency.
3. **Tunable Design Variables:** Identify a subset of design variables that can be adjusted within specified tolerances (e.g., ±15 percent) to explore variations around the initial design point. Simulate how these adjustments affect key performance metrics.
4. **Intelligent Sampling:** Use intelligent sampling to create a dataset of simulations that represent the antenna's design space.

5. **ML Model Training:** Train ML models to predict performance across wide parameter ranges with high accuracy and minimal computation time.
6. **Frequency Scaling Generalization:** Extend each prototype's ML model to other initial design frequencies using frequency scaling principles.

This strategy enables workflows for early-stage design exploration and interactive visual examination that were previously impractical. For instance, if an engineer needs a planar inverted-F antenna (PIFA) to resonate at 1 GHz, they can quickly generate a design blueprint. Using a pre-trained ML model to predict resonant frequency, engineers can efficiently explore and optimize dimensions such as length, width, height and short pin width to maintain the 1 GHz resonance. Once an optimal design is identified, full-wave electromagnetic simulations can verify AI predictions and guide further refinement. ***Table 1*** shows a comparison of an ML model and full-wave simulation method of moments (MoM) results for a PIFA with dimensions adjusted by -9 percent in length, +12 percent in width, +5 percent in height and -4 percent in short pin width from the 1 GHz prototype. Full-wave simulations use a frequency sweep from 700 MHz to 1.3 GHz with 1 MHz resolution for resonant frequency and bandwidth analysis. As shown in Table 1, ML models provide results much faster than electromagnetic simulations. Parameter sweeps of a 1 GHz PIFA using the pre-trained regression ML model to predict resonant frequencies based on varying geometric properties are shown in ***Figure 1***. These results illustrate that resonant frequencies for 2500 configurations can be predicted in seconds, facilitating rapid iteration during early-stage design without costly simulations.

AI-accelerated parameter sweeps also help narrow the design space. In ***Figure 2***, a pre-trained ML model classifies 2500 PIFA configurations based on 50 Ω matching. The impedance matching scenarios were determined for a PIFA antenna designed at 300 MHz. Each configu-

TABLE 1

COMPARISON OF MACHINE LEARNING MODEL AND FULL-WAVE SIMULATION RESULTS FOR A PIFA

	Initial Design		*Modified Design*	
	fR (GHz)	BW (MHz)	fR (GHz)	BW (MHz)
ML	1.0038	61.705	1.0079	80.048
MoM	1.0040	61.756	1.0072	79.085
Percent Error	-0.0270%	-0.0820%	0.0712%	1.2180%
Computation time (seconds)	ML: 0.1865 MoM: 46.4830		ML: 0.1216 MoM: 46.6629	

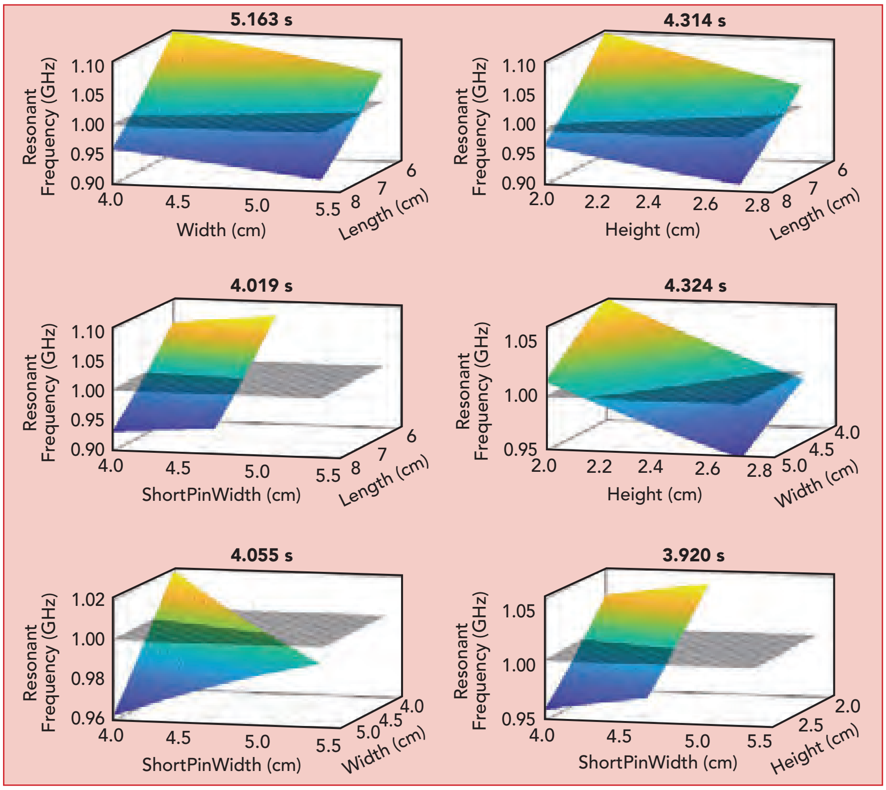

Fig. 1 1 GHz PIFA parameter sweeps using the pre-trained regression machine learning model.

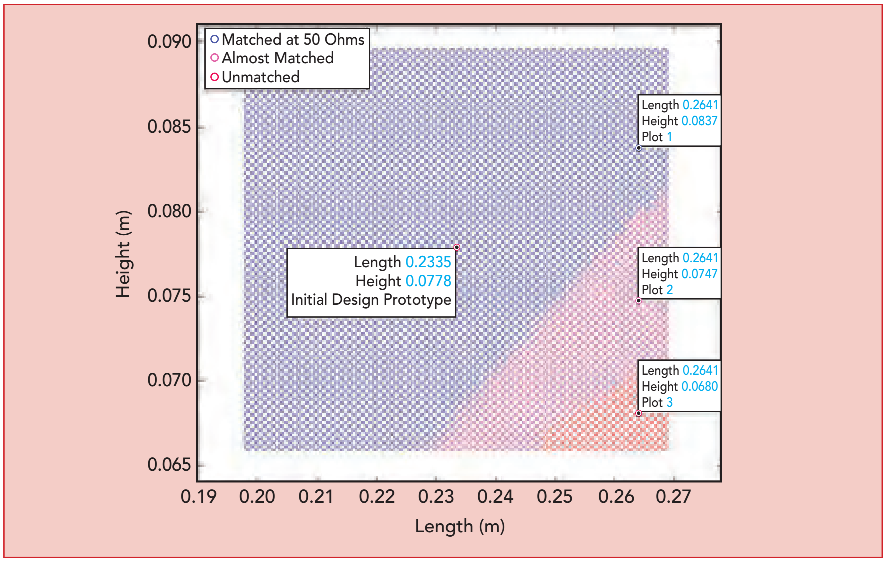

Fig. 2 Impedance matching scenarios for a PIFA antenna designed at 300 MHz.

ration varies in length and height around a PIFA designed for 300 MHz resonance. The results were predicted in under 10 seconds when using the pre-trained classification ML model.

Figure 3 shows the full-wave electromagnetic verification of bandwidth and impedance matching conditions for the points shown in Figure 2. It verifies the classification of three designs against full-wave simulation, focusing on the "Plot 1," "Plot 2" and "Plot 3" regions referenced in Figure 2. Although classification alone does not finalize the design, it indicates that a length-to-height ratio below 3.5 is necessary for matching. This refines the optimization space and improves efficiency for subsequent methods.

The scalability of this approach is demonstrated by the "AIAntenna" object in Antenna Toolbox, which provides access to pre-trained ML models for various catalog antennas, including PIFA and other patch antennas. This capability allows for rapid AI-accelerated parameter sweeps of standard antennas. This, in turn, enables quick analysis and categorization of design spaces, identification of optimal dimensions for specific performance goals and insights into the design space's response surface.[1]

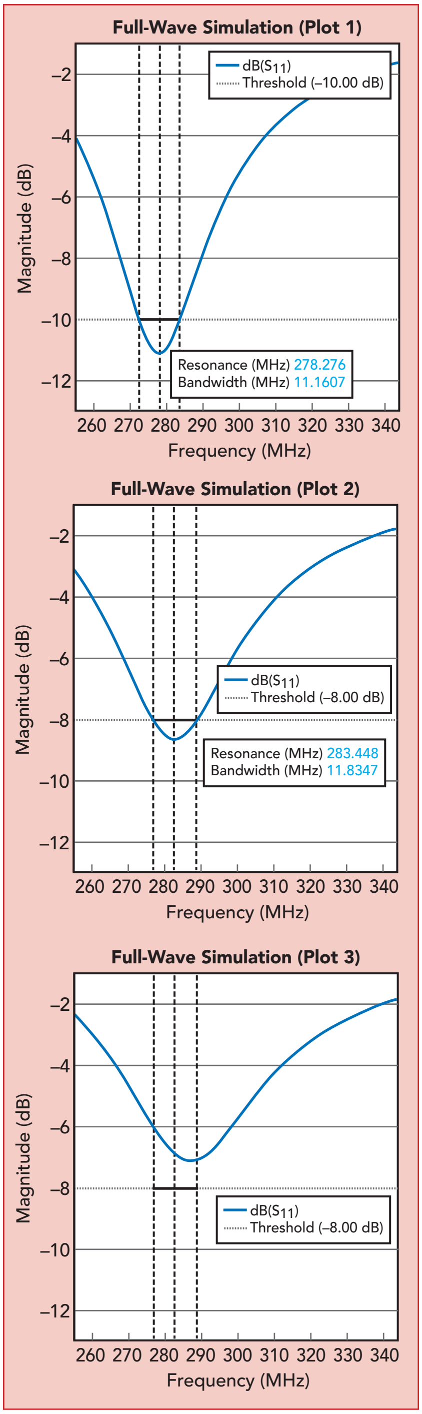

Fig. 3 Full-wave electromagnetic verification of bandwidth and impedance matching conditions.

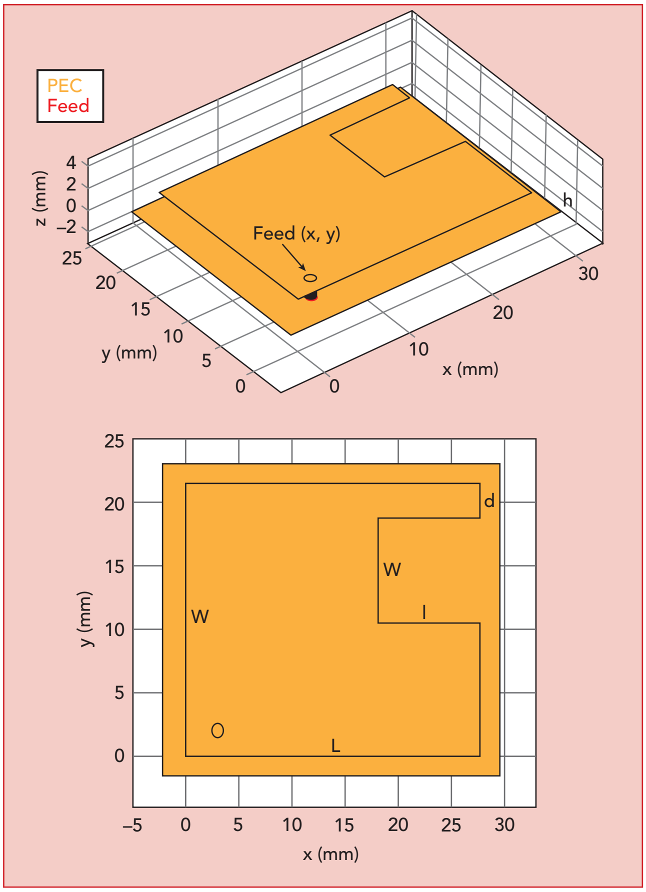

Fig. 4 C-shaped microstrip patch antenna.

AUTOML TRAINING CUSTOM ANTENNAS AI MODELS

AI models can extend their utility beyond standard antenna types (e.g., dipoles, patches and horns) to custom antenna structures. However, developing these models typically requires expertise across disciplines. Knowledge of antenna design and electromagnetic analysis is crucial for problem formulation, setting up measurement systems, identifying key parameters and interpreting results. Simultaneously, a background in statistics, design of experiments (DOE) theory and ML is necessary for implementing the training framework, sampling data, designing AI models and validating their performance with reliable metrics. This cross-disciplinary requirement can hinder the application of AI techniques for antenna design and analysis. Therefore, automation frameworks and low-code tools are essential. The general ML workflow involves:

1. Modeling and parameterizing the antenna for simulation
2. Defining design variables as predictors and metrics as responses
3. Conducting a DOE for sampling the design variables
4. Performing electromagnetic simulations to generate response data
5. Preprocessing and exploring data in preparation for training
6. Iteratively training and tuning ML models for optimal performance
7. Evaluating the ML model against simulation results for accuracy on new data.

This workflow is demonstrated by training an ML model to characterize a probe-fed C-shaped microstrip patch antenna[2] and predict its resonant frequency based on its dimensions. Stochastic DOE meth-

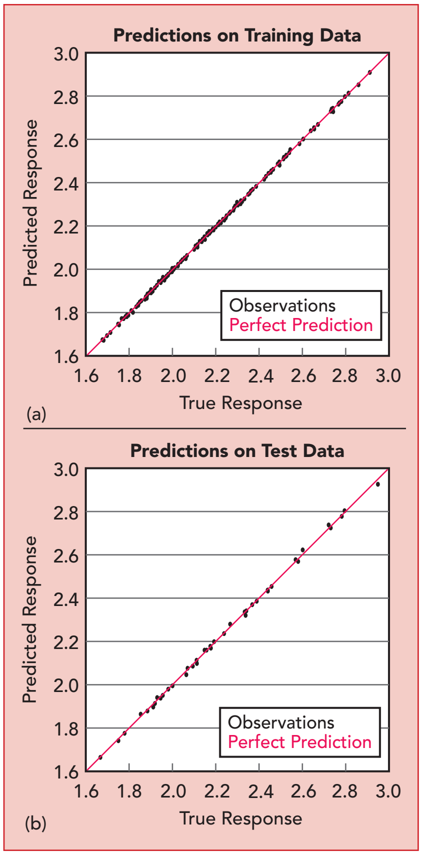

▲ **Fig. 5** **Model performance on training (a) and test (b) datasets.**

odologies and low-code AutoML for model selection, training and tuning are used for creating an antenna model. This is different from what was reported in other works. ***Figure 4*** shows the parameterization of the C-shaped microstrip patch antenna with the nominal values for the design variables being: L = 24 mm, W = 20 mm, l = 10 mm, w = 7.2 mm, d = 2.4 mm and h = 1.6 mm.

The antenna is modeled with an air substrate, but the approach can be applied to dielectric structures. Design variables are varied within a ±25 percent range around nominal values, resulting in 200 data points. Each configuration is simulated from 1 to 4 GHz using a full-wave MoM solver to find the resonant frequency. The data is split 80 percent into training and 20 percent into test sets, covering steps 1 to 5.

AutoML automates step 6 of the ML workflow using the "fitrauto" function from the Statistics and Machine Learning Toolbox. This function performs regression model selection and hyperparameter tuning. It employs Bayesian optimization to evaluate ML models like Gaussian process regressors (GPRs), support vector machines and artificial neural networks, selecting a model with minimized generalization error.

This results in a low-code solution. Step 6 is executed with a single line of code, producing a tuned GPR model with less than 1 percent prediction error on both training and test data. The model's accuracy is detailed in ***Table 2*** and visualized in ***Figure 5***, providing both quantitative and qualitative assessments as per step 7 of the ML workflow.

TABLE 2

MODEL PERFORMANCE ON TRAINING AND TEST DATASETS

Dataset	Percent Absolute Error (%)				
	Minimum	Maximum	Mean	Median	Std. Dev.
Training	0.00096	0.5808	0.1457	0.1170	0.1264
Test	0.0223	0.9037	0.3134	0.2361	0.2538

EVOLVING THE ANTENNA SHAPE WITH SURROGATE OPTIMIZATION

Pre-trained AI models for standard and custom antenna structures provide valuable insights. However, surrogate optimization offers an alternative by learning subsets of the design space during optimization. As the surrogate model is developed and updated during the optimization, this technique can be applied to evolving antenna shapes where pre-trained models provide insufficient insights.

Traditional antenna optimization relies on full-wave electromagnetic analysis, which is resource-intensive in terms of time and memory. Strategies to mitigate solver complexity include higher-order basis functions, iterative methods like the fast multi-

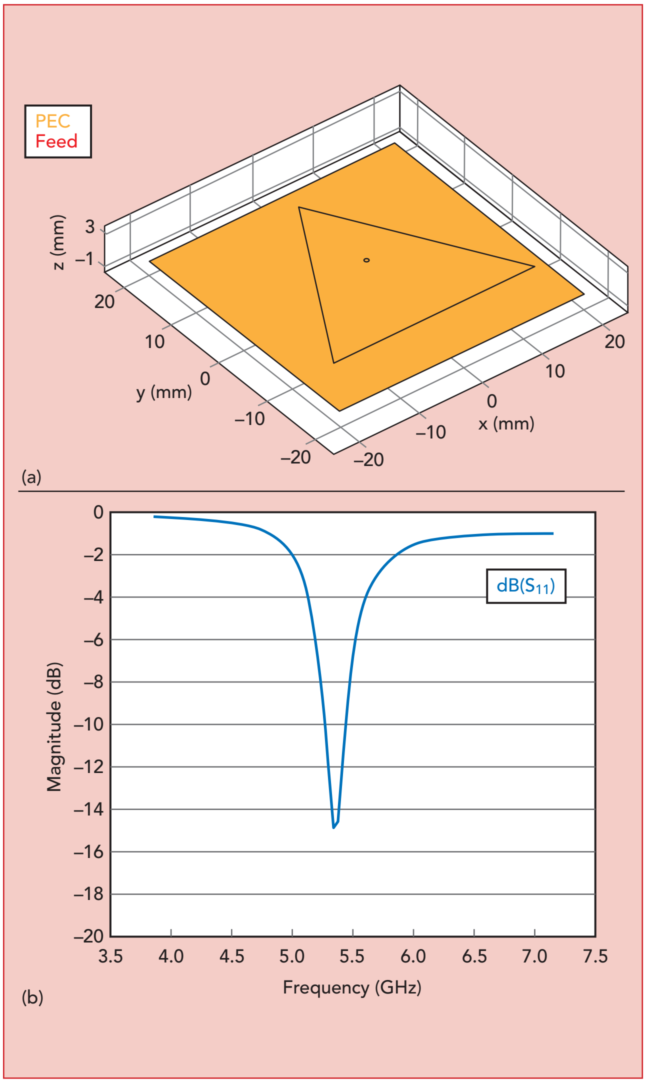

Fig. 6 Probe-fed equilateral patch antenna (a) and simulated S_{11} (b).

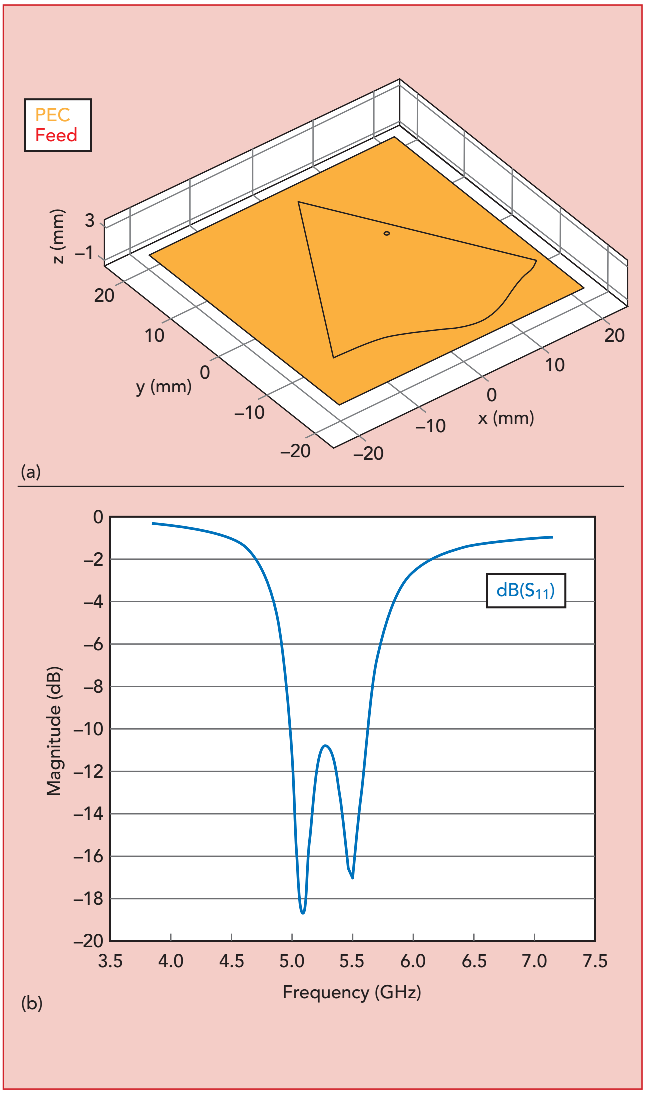

Fig. 7 Evolved probe-fed patch antenna shape (a) and simulated S_{11} (b).

pole method, GPU acceleration and hybrid full-wave/asymptotic methods. Despite these, a single parameter set requires significant computational resources and exploring multiple design variables adds a combinatorial challenge. The search space often contains multiple extrema, typically framed as minimization problems. This necessitates either defining bounds to ensure a unique local minimum or employing global optimization techniques to explore the true solution space. Surrogate-based optimizers[3] fall into the global optimization category but differ by reducing expensive electromagnetic solver calls. They build a surrogate model that initially learns the search space characteristics using the electromagnetic solver and then drives the optimization. To maintain accuracy, the surrogate's outputs are occasionally verified against the electromagnetic solver. Any deviations in the outputs prompt updates with new true solution points, continuing the optimization while minimizing electromagnetic solver calls.

The use of surrogate optimization is demonstrated starting with a standard triangular microstrip patch antenna and evolving its shape to achieve a target performance objective. This surrogate-based approach is applied to enhance the bandwidth of a single-feed, probe-fed triangular patch antenna on an air substrate by evolving the side shapes.[4] Initially, a standard probe-fed equilateral patch antenna is designed for the lower half of the 5 GHz band, with a -10 dB bandwidth of about 3 percent, as shown in ***Figure 6***.

The surrogate optimizer aims to improve bandwidth to cover 5.0 to 5.6 GHz by adjusting the shapes of the three sides while leaving the corners and ground plane unchanged. Three Gaussian functions, defined in ***Equation 1***, represent each side's shape, introducing three optimization variables per side: mean (μ), standard deviation (σ) and scaling term (w).

$$f(p) = \frac{w}{\sigma\sqrt{2\pi}} e^{-0.5\left(\frac{p-\mu}{\sigma}\right)^2} \quad (1)$$

These three variables adjust the curve's amplitude relative to the original edge, with p as the position along the side. The feed coordinates (x, y) add two more degrees of freedom, totaling 11 independent variables for the shape optimization.

The surrogate optimization uses the structure, objective function, constraints and bounds to evolve the patch shape. The final shape and its simulated reflection coefficient are depicted in ***Figure 7***. Comparing Figures 6 and 7, the shape evolution increases bandwidth from 3 to 12 percent through double resonance. Although not shown, the far-field pattern remains stable over this band. This approach uses fewer degrees of freedom but achieves comparable bandwidth enhancement.

AI-DRIVEN ENGINEERING FOR SCALABLE, EFFICIENT AND AGILE SOLUTIONS

These AI-based design, analysis and optimization capabilities lay the groundwork for a transformative ap-


QORVO
QPA0017
QORVO
QPA0812
QORVO
QPA0001

proach to antenna engineering. By leveraging AI, engineers can create a scalable, extensible and automatable suite of tools that significantly enhance the efficiency and effectiveness of antenna design processes. These tools enable rapid "what-if" analyses, enabling engineers to quickly assess the impact of design changes on performance metrics without the need for exhaustive simulations. This capability is particularly valuable in the early stages of design, where flexibility and speed are crucial.

Moreover, the efficient exploration of the design space facilitated by AI models reduces the computational burden traditionally associated with antenna optimization. By narrowing down the most promising design parameters early in the process, engineers can focus their resources on refining these designs, leading to faster development cycles and reduced time-to-market.

The integration of AI also accelerates design optimization, allowing for the fine-tuning of both standard and custom antenna geometries. This adaptability is essential in today's rapidly evolving technological landscape, where custom solutions are often required to meet specific performance criteria or to integrate seamlessly with other components in complex systems.

Beyond the immediate benefits of design and optimization, the AI-driven framework supports continuous improvement and learning. As more data is gathered and models are refined, the system becomes increasingly accurate and predictive, further enhancing its value to engineers.

Overall, this AI-driven framework not only addresses current challenges in antenna engineering but also positions the field to tackle future demands with greater agility and precision. By embracing AI, engineers unlock new possibilities for innovation and efficiency, setting the stage for advancements that could redefine the boundaries of what is achievable in antenna design and performance. To help engineers get started, several examples are identified in the references. All EM simulations use MoM solvers in MATLAB and Antenna Toolbox. ■

References

1. "Artificial Intelligence (AI) for Rapid Analysis and Design of Patch Antenna," *MathWorks, Inc.*, Web: mathworks.com/help/antenna/ug/ai-for-rapid-analysis-and-design-of-microstrip-patch.html.
2. "Train Machine Learning Model for Analysis of Custom Antenna," *MathWorks, Inc.*, Web: mathworks.com/help/antenna/ug/train-mlmodel-for-analysis-of-custom-antenna.html.
3. B. Liu, H. Aliakbarian, Z. Ma, G. A. E. Vandenbosch, G. Gielen and P. Excell, "An Efficient Method for Antenna Design Optimization Based on Evolutionary Computation and Machine Learning Techniques," *IEEE Transactions on Antennas and Propagation*, Vol. 62, No. 1, Jan. 2014, pp. 7–18.
4. V. Iyer, S. Sivaramakrishnan, T. Gao and G. Zucchelli, "Bandwidth Enhancement of a Probe-fed Patch Antenna through Shape Modification Using a Gaussian Function," *2024 IEEE International Symposium on Antennas and Propagation and ITNC-USNC-URSI Radio Science Meeting*, Florence, Italy, 2024.

MiCable

New

0.5~6.2GHz

Drop-in/Surface Mount

High Power Bi-Directional Coupler

- High Power Handling
- Low VSWR & Insertion Loss, High Directivity
- Excellent Coupling & Flatness
- Small Case Style
  High Performance & Cost-Effective

Drop-in Bi-Directional Coupler

Freq. Range (GHz)	P/N	CW Power Max.(W)	Nominal Coupling (dB)	Directivity Min.(dB)	Main Line VSWR Max.(:1)	Coupling VSWR Max.(:1)	Insertion Loss* Max.(dB)	Coupling Max.(dB)	Flatness Max.(dB)	Dimension (mm)
0.5~3	D2004T050300	200	20	17	1.30	1.30	0.40	20±1.0	±0.75	43.2 x 25.4 x 4.0
	D3004T050300	200	30	17	1.30	1.30	0.35	30±1.3	±0.75	43.2 x 25.4 x 4.0

Surface Mount Bi-Directional Coupler

Freq. Range (GHz)	P/N	CW Power Max.(W)	Nominal Coupling (dB)	Directivity Min.(dB)	Main Line VSWR Max.(:1)	Coupling VSWR Max.(:1)	Insertion Loss* Max.(dB)	Coupling Max.(dB)	Flatness Max.(dB)	Dimension (mm)
0.7~1.23	D3002M070123	100	30	20	1.25	1.25	0.25	30±1.5	±1.0	14.22 x 8.89 x 1.97
0.9~1.6	D1504M090160	200	15	20	1.25	1.25	0.20	15±1.0	±0.6	16.51 x 12.19 x 2.30
1~2	D1501M100200	50	15	16	1.25	1.25	0.25	15±1.0	±1.0	6.30 x 5.80 x 2.00
	D2004M100200	200	20	20	1.28	1.28	0.20	20±1.0	±1.2	14.22 x 8.89 x 2.26
1.9~2.2	D3001M190220	50	30	15	1.25	1.25	0.20	30±1.5	±1.0	6.35 x 5.08 x 1.97
2~2.7	D0501M200270	50	5	16	1.20	1.20	0.30	5±0.6	±0.4	6.35 x 5.08 x 1.60
2.2~3	D2001M220300	50	20	18	1.20	1.20	0.25	20±1.0	±0.6	6.35 x 5.08 x 1.72
2.6~6.2	D2002M260620	100	20	15	1.30	1.30	0.25	20±1.0	±1.2	14.22 x 8.89 x 1.58

*Power loss at coupled port excluded

More Information-
Scan the QR Code

MIcable Inc.

www.micable.cn sales@micable.cn +86-591-87382856

INVITED PAPER

Examining RF Architectures for Software-Defined Radios

Brandon Malatest
Per Vices, Toronto, Canada

Software-defined radios (SDRs) enable an increasing number of mission-critical systems across radar, electronic warfare, signals intelligence, communications and other defense applications. The essential requirements of these systems are performance, reliability and price. SDRs are typically designed to include an analog RF front-end (RFE), digital-to-analog converters (DACs) for the transmit path, analog-to-digital converters (ADCs) for the receive path and a digital processor. This article focuses on the analog RFE. It compares the three most common architectures with a deep dive into the architecture that is typically the best approach for mission-critical applications.

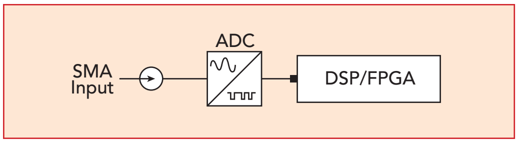

Fig. 1 Direct sampling architecture block diagram.

ARCHITECTURES

Various RF architectures can be utilized in SDRs, but the most prevalent are direct sampling, direct conversion (zero-IF) and superheterodyne.

Direct Sampling Architecture

Direct sampling, or direct RF sampling, involves digitizing the RF signal directly using an ADC without any prior frequency conversion. A representative block diagram of this architecture is shown in ***Figure 1***. This approach is simple in design and offers wideband operation, limited only by the ADC. While this design enables simultaneous processing of a wide range of frequencies, this architecture usually sacrifices RF performance, especially dynamic range, which is essential in many mission-critical applications. This issue is further complicated by high power consumption and the prices of the high speed converters required for these architectures.

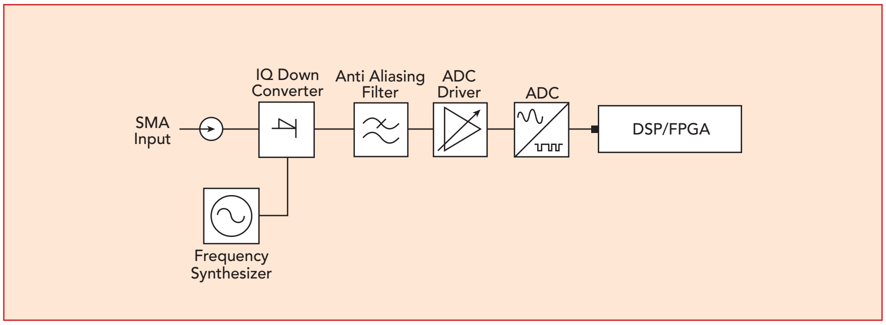

Fig. 2 Direct conversion architecture block diagram.

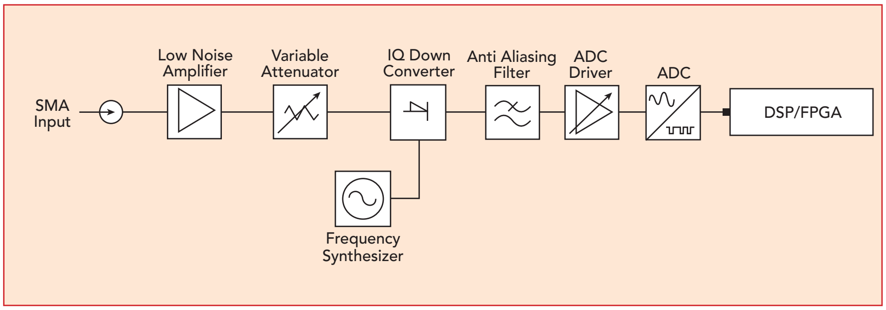

Fig. 3 Superheterodyne architecture block diagram.

Direct Conversion (Zero-IF) Architecture

Another architecture to consider is direct conversion or zero-IF. In this architecture, the signal is down-converted directly to a DC baseband signal in one step using mixers. A representative block diagram of this architecture is shown in ***Figure 2***. Although slightly more complicated than the direct sampling architecture, this approach simplifies the filter design since it requires only lowpass filters as needed. The RF performance is mid-range in this architecture as it offers efficient spectrum usage because the absence of intermediate frequencies reduces the risk of images. Despite reducing image signals, this architecture does introduce DC offsets and I/Q imbalances that can cause distortion. This architecture is also susceptible to low frequency noise, so it is classified as having mid-range RF performance.

Superheterodyne Architecture

The superheterodyne architecture is more complex. This approach involves converting the RF signal to an intermediate frequency (IF) before digitization and while this is a well-established RF architecture, it can be challenging to implement. The representative block diagram for this architecture is shown in ***Figure 3***. SDRs that implement this design provide the benefits of high selectivity, sensitivity and dynamic range. By offering excellent filtering characteristics and the ability to amplify only the desired signals, these SDRs provide superior performance when operating in congested or contested RF environments. With the ability to handle a broad range of signal strengths effectively, SDRs with this superheterodyne architecture become the clear choice for many mission-critical applications.

These systems have some drawbacks, but many are abstracted from the end user and the burden falls to the RF designer and SDR manufacturer. The design of this architecture adds stages within the RF chain and more components are often needed to achieve optimal performance. This means these designs are usually complex and can increase the overall size and cost of the SDR. There is also the possibility of image frequency interference being present, which is often addressed through added filtering and image-rejection mixers. This can lead to higher power consumption and costs.

COMPONENT SELECTION FOR THE SUPERHETERODYNE ARCHITECTURE

The rest of this article focuses on the components included in most superheterodyne architectures and the essential characteristics associated with component selection. The superheterodyne architecture is an excellent choice for mission-critical systems. Its structure includes several stages. Each stage requires specific components, which are discussed in the following section. The critical characteristics to consider when selecting these components are highlighted.

The first stage of the superheterodyne architecture has the RF connector, filter and low noise amplifier (LNA). The RF connector selection may appear trivial, but there are important elements to consider for the first component within the architecture. It is essential to consider the following:

Frequency Range: The connector must be rated for the system's frequency range. Otherwise, the RF performance may be degraded immediately as signal integrity issues and losses can occur if the connector is not rated to the correct frequency range.

Insertion Loss: High insertion loss can reduce receiver sensitivity and lead to poor performance. Low insertion loss connectors are essential to ensure the best overall performance.

Power Handling Capacity: The connector must work at the maximum specified system power. Exceeding the connector's power handling capacity can result in signal integrity issues, failed connections and overheating.

Price and Availability: It is critical to ensure that the connector selection supports the production schedule and that the price does not negatively impact the overall system price for the target applications.

The RF filter is the next element to consider in the design. The filter removes out-of-band signals to prevent them from reaching the later stages. These filters can be designed from discrete components or as an integrated chip to meet the performance and design requirements. The key parameters that must be evaluated when selecting the proper RF filter are bandwidth and selectivity. The filter must work at the maximum signal power without distortion while offering aggressive filtering to ensure unwanted signals are effectively removed before entering the remaining sections of the radio chain.

The last element within the first RF stage is typically the LNA. The LNA amplifies weak signals while limiting the noise added to the incoming signal. LNAs are designed for better overall RF performance, unlike traditional amplifiers that can produce extra noise. The key characteristics to consider for this component are noise figure, gain and linearity. The noise figure refers to the amount of added noise from the amplifier. The gain of the amplifier relates to how much the weak signals will be increased, ideally without added distortion. Linearity is critical to minimize intermodulation distortion, which can degrade signal quality.

The next stage in the superheterodyne architecture contains the system's mixing elements, which change the signal frequency. These elements are the mixer and local oscillator (LO). A mixer is a nonlinear three-terminal device. The LO signal drives the mixer diodes and the mixer produces output frequency signals based on the sum and difference of the RF and LO signal frequencies. If the incoming RF signal is being down-converted, the intermediate frequency (IF) from the mixer will be the difference between the RF and LO frequencies. When selecting the appropriate mixer within a system, looking for high conversion gain, low noise figure and good isolation between ports is important.

High conversion gain is an important feature. It contributes to a better signal-to-noise ratio (SNR), reducing the need for more amplification within the system. It also increases sensitivity and improves the receiver's ability to detect weaker signals. This improves the overall dynamic range of the system, enabling a wider range of signal strengths without exceeding allowable distortion levels, which enhances performance in weak signal conditions.

Good isolation between ports is also an essential selection criterion for the mixer. High port-to-port isolation helps to minimize signal and LO leakage, avoid IF feedthrough, reduce intermodulation products and improve receiver sensitivity and dynamic range. Because the superheterodyne architecture relies heavily on this set of characteristics for good performance, mixer selection is crucial.

As mentioned, the mixer relies on the LO signal to drive the nonlinear mixing elements to the proper levels and at the right frequency. The LO generates a stable frequency signal with a value selected to mix with the RF signal and produce the proper IF frequency. LO choice is also critical for the superheterodyne architecture and the key characteristics to evaluate include frequency stability, phase noise and tuning range. A stable LO ensures a consistent conversion frequency, while the low phase noise minimizes signal degradation. The wide tuning range is important as it allows the flexibility to generate different IFs for various applications, which is the key element for wideband operation.

Next in line is the IF stage. This section contains the IF filter and IF amplifiers. An IF filter is designed to pass the desired IF signal and reject others. This provides the selectivity that enables better performance. The key specifications of the IF filter are center frequency, bandwidth and shape factor. A narrow bandwidth improves selectivity, while a good shape factor ensures efficient signal separation with minimal adjacent channel interference. The filter should also have low insertion loss to preserve signal strength and low SNR for better sensitivity.

The IF amplifier, as the name suggests, amplifies the filtered IF signal to a level suitable for demodulation. The key parameters for this component are gain, bandwidth and linearity. The gain and bandwidth are important to ensure that the IF signal has the appropriate signal strength to drive the demodulator across the entire signal bandwidth. Linearity is an important parameter because it affects signal integrity and distortion before it reaches the demodulation stage. Other parameters influencing the optimal IF amplifier selection are noise and dynamic range. The noise added to the signal should be low and the dynamic range should be high to ensure varying signal strengths do not create distortion.

The demodulator is the fourth stage. This single component is vital as it extracts the original information from the modulated IF signal. The critical selection criteria for this stage relate to the demodulator type or modulation scheme and signal processing capability. Performance metrics include sensitivity, selectivity and noise immunity. The demodulator should accurately recover the signal with minimal distortion and offer the necessary signal processing capabilities based on the application. Ensuring compatibility with the modulation type and sufficient processing power for real-time signal processing is essential. Other available features in the advanced demodulator selection process include error correction and signal enhancement features.

The final stage is baseband processing. The components for this stage are the ADC and digital signal processor (DSP). The ADC converts the analog demodulated signal to a digital format. Several processes occur within this chip and there are many different characteristics to consider, with some directly impacting the platform's utility for specific applications. The four key elements are the number of channels, resolution (number of bits), sampling rate and dynamic range. The number of channels relates to the number of RFEs the DSP must support and the architecture being implemented. The resolution is another key element, as higher resolution can help improve signal fidelity, SNR and overall data quality. For example, in test and measurement applications, the number of bits directly correlates to the accuracy and measurement reliability. In this case, higher reso-

lution is better. The sampling rate directly limits the receiver's bandwidth and affects signal fidelity. It can also help reduce aliasing, which will occur when the sample rate is too low and may cause a false lower frequency signal component to appear in the sampled data. The sampling rate will directly contribute to post-processing flexibility. The power consumption of the ADC is always an important consideration to ensure it operates properly within the intended system performance and environmental constraints.

The DSP stage can come in many forms. It can be a field programmable gate array (FPGA) or another dedicated DSP chip. Regardless of the component choice, the digital signal is processed for further operations like decoding, filtering and error correction at this stage. The processing speed, amount of logic resources, programmability and power consumption are critical considerations for this element. It is important to consider how much data will be processed and, if application-specific, what specific DSP operations are required. For greater flexibility, ensuring that the chipset is fast with a large number of logic resources will enable real-time processing and advanced operations. The programmability of the DSP directly influences the flexibility to change functionality along with allowing updates and modifications that are often necessary to adapt to different signal types and conditions.

In many instances and for many applications, it is beneficial for the data processed within the DSP block to be transferred to another device for storage or additional processing. For these situations, the interface with the equipment becomes very important. Many options are available, including Ethernet, PCIe, serial interfaces, FPGA mezzanine card and optical interfaces, with each interface type offering benefits. When determining the best interface for the platform, it is crucial to consider the rate at which the data needs to be transferred, the interfacing equipment and the overall application.

CONCLUSION

Overall, there are many different architectures to consider in the design of an SDR. Each architecture offers benefits, but component selection is critical regardless of the chosen architecture. It is essential to ensure the components designed into the system meet the overall system frequency range, bandwidth and RF performance, such as noise figure, linearity, etc. It is also necessary to consider power consumption, size, weight and environmental factors associated with the intended application to ensure the best product performance for the specific use case.■

Broadband 8 × 8 Butler Matrix with High Phase Accuracy

MIcable Inc.
Fuzhou, China

A Butler matrix is a passive beamforming network used to feed a phased array of antenna elements. Compared to an active beamforming network, a Butler matrix has several advantages. It can have higher performance stability, repeatability, more reliable accuracy, a simpler configuration, smaller size and lower cost. However, there are also disadvantages. Limitations in component performance and manufacturing technology have historically made obtaining the required accuracy and frequency bandwidth a difficult challenge. MIcable is solving these challenges with cutting-edge design and advanced manufacturing to improve the accuracy and bandwidth of Butler matrices to new levels of performance. As an example, the SA-7-8B006073, a 0.6 to 7.25 GHz 8 × 8 Butler matrix, will be used to highlight these accuracy and bandwidth improvements.

8 × 8 BUTLER MATRIX FUNCTIONALITY

Figure 1 shows the SA-7-B006073 8 × 8 Butler matrix configuration, highlighting the layout and connections of the matrix. The diagram shows a reciprocal signal transfer between any of the eight input ports and any of the eight output ports. This enables simultaneous operation of the Butler matrix in both the transmit and receive path. This means that a signal on any A port will appear as outputs on the B1 to B8 ports simultaneously. These signals will have eight different phase values and this allows the system to enable as many as eight different sub-beams if the Butler matrix is connected to eight antennas. The Butler matrix is reciprocal, so a signal on any B port will appear as simultaneous outputs on ports A1 to A8. An SP8T switch can be used to select which of the A ports, from A1 to A8, will be the input or which of these ports will be supplying the output signal if the B ports are used as inputs.

The diagram of Figure 1 shows fixed phase shift stages in the Butler matrix configuration. These are used to change the relative phase of the signals. ***Table 1*** shows the resulting phase relations among the eight output ports. The data in Table 1

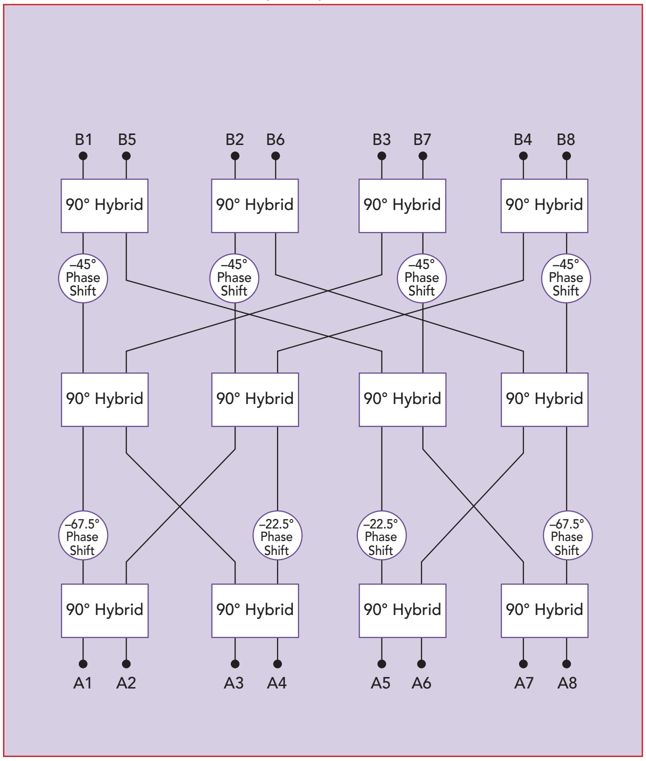

Fig. 1 **SA-7-8B006073 8 x 8 Butler matrix configuration.**

TABLE 1

SA-7-8B006073 8 X 8 BUTLER MATRIX PHASE RELATIONSHIPS

Input / Output	A1	A2	A3	A4	A5	A6	A7	A8
B1	-112.5	-202.5	-135	-225	-112.5	-202.5	-180	-270
B2	-135	-45	-247.5	-157.5	-180	-90	-337.5	-247.5
B3	-157.5	-247.5	0	-90	-247.5	-337.5	-135	-225
B4	-180	-90	-112.5	-22.5	-315	-225	-292.5	-202.5
B5	-202.5	-292.5	-225	-315	-22.5	-112.5	-90	-180
B6	-225	-135	-337.5	-247.5	-90	0	-247.5	-157.5
B7	-247.5	-337.5	-90	-180	-157.5	-247.5	-45	-135
B8	-270	-180	-202.5	-112.5	-225	-135	-202.5	-112.5

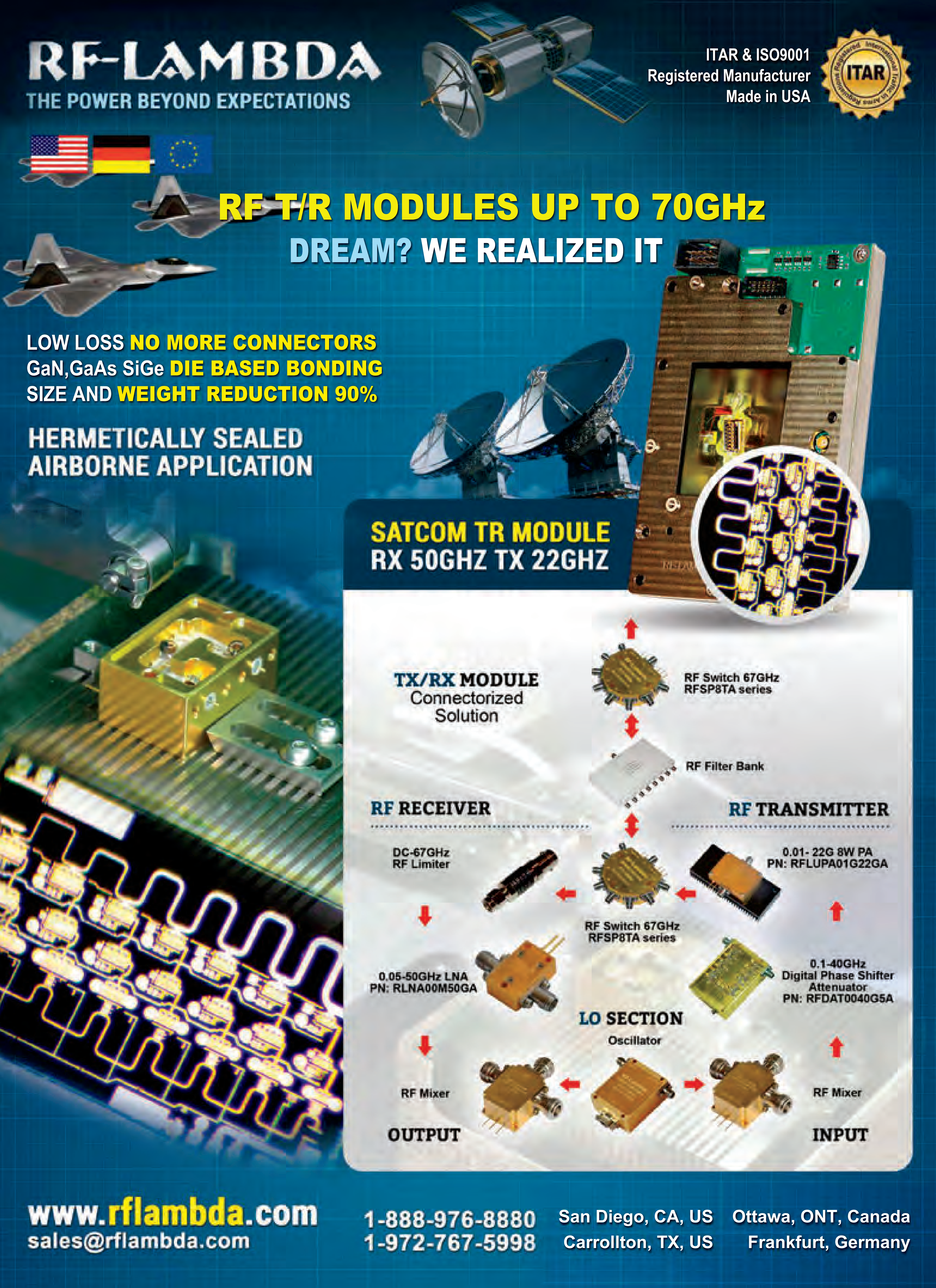

RF-LAMBDA
THE POWER BEYOND EXPECTATIONS
ITAR & ISO9001
Registered Manufacturer
Made in USA
ITAR
RF T/R MODULES UP TO 70GHz
DREAM? WE REALIZED IT
LOW LOSS NO MORE CONNECTORS
GaN,GaAs SiGe DIE BASED BONDING
SIZE AND WEIGHT REDUCTION 90%
HERMETICALLY SEALED
AIRBORNE APPLICATION
SATCOM TR MODULE
RX 50GHZ TX 22GHZ
TX/RX MODULE
Connectorized
Solution
RF Switch 67GHz
RFSP8TA series
RF Filter Bank
RF RECEIVER
RF TRANSMITTER
DC-67GHz
RF Limiter
0.01- 22G 8W PA
PN: RFLUPA01G22GA
RF Switch 67GHz
RFSP8TA series
0.05-50GHz LNA
PN: RLNA00M50GA
0.1-40GHz
Digital Phase Shifter
Attenuator
PN: RFDAT0040G5A
LO SECTION
Oscillator
RF Mixer
RF Mixer
OUTPUT
INPUT
www.rflambda.com
sales@rflambda.com
1-888-976-8880
1-972-767-5998
San Diego, CA, US
Carrollton, TX, US
Ottawa, ONT, Canada
Frankfurt, Germany

shows how the Butler matrix architecture facilitates reciprocal signal transfer between any of the eight input ports and any of the eight output ports, enabling simultaneous operation as both a transmission and receiving system.

SPECIFICATIONS

Table 2 shows the RF performance specifications for the SA-7-8B006073 8 × 8 Butler matrix across four different frequency bands. These bands have been selected for their importance in 5G New Radio (NR) frequency range 1 (FR1) and Wi-Fi 6E/7E applications. ***Figure 2*** shows representative amplitude balance and phase accuracy plots for port A1 as the input across the entire operating band of the device.

Some additional characteristics of the Butler matrix:

Input Power (max.): 5 W CW (20 W CW available), 500 W peak
Connector: SMA female
Dimensions: 316 × 172.7 × 68.6 mm (L × W × H)
Weight (max.): 5700 g
Temperature: -40°C to +70°C (operating), -55°C to +85°C (storage)
Environmental: Per MIL-STD-202F, Method 204D. Method 213B optional (contact supplier for detailed information).

The advantage of the SA-7-8B006073 8 × 8 Butler matrix is that it operates remarkably well over the entire 600 MHz to 7.25 GHz frequency range. As mentioned, Table 2 shows performance specifications over specific frequency ranges, emphasizing bands attractive to 5G NR FR1 and Wi-Fi 6E/7E applications. Measurements in the actual frequency bands yield much better performance. In 5G NR FR1 and Wi-Fi 6E/7E applications, the SA-7-8B006073 has the following typical performance:

Phase Accuracy: ≤ ±6 degrees
Amplitude Balance: ≤ ±1 dB
Insertion Loss: 2 to 5.6 dB (above the 9 dB theoretical loss)
VSWR: ≤ 1.3:1
Isolation: ≥ 20 dB.

POTENTIAL APPLICATIONS

This performance, especially the phase accuracy and amplitude balance over such a broadband frequency range, differentiates the SA-7-8B006073 from competitive products and solutions. Compared to active phased array beamforming networks, the passive Butler matrix architecture boasts a straightforward across-matrix configuration that achieves the required phase shift in a smaller footprint. The passive architecture also helps ensure accurate and stable performance, higher power handling for each path and cost-effectiveness. The device is reciprocal, so the signals can be input from one port or multiple ports at the same time and used in a transmit or receive path. Operating frequencies from 600 MHz to 7.25 GHz, along with the performance characteristics, will enable beamforming and beam steering in a wide range of applications that include 5G, Wi-Fi, IoT, cellular phone/base station test, automotive electronics, communication, phased arrays and object detection.

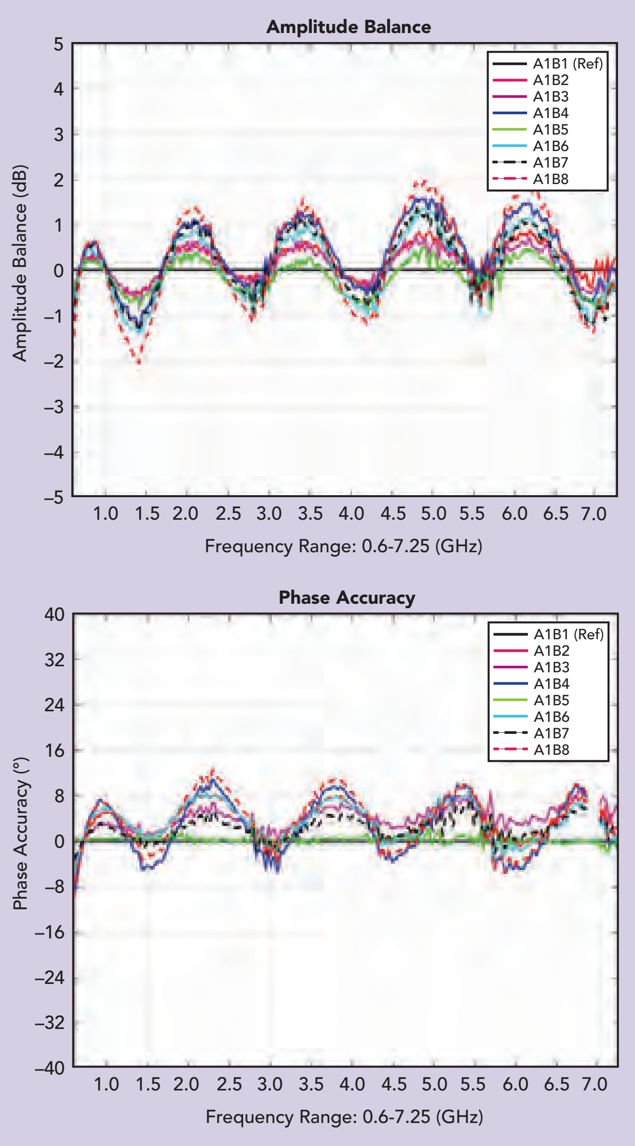

Fig. 2 Amplitude balance and phase accuracy.

TABLE 2

SA-7-8B006073 8 X 8 BUTLER MATRIX PHASE SPECIFICATIONS

Parameter	Frequency Range (GHz) 0.617 to 0.960	1.427 to 2.690	3.3 to 5.0	5.15 to 7.25
VSWR for all RF ports (max.)	1.4:1	1.5:1	1.5:1	1.6:1
Insertion Loss* (dB max.)	12.0	13.2	14.6	15.9
Amplitude Balance (dB max.)	±1.5	±1.4	±1.4	±1.5
Amplitude Flatness (dB max.)	±1.4	±1.6	±1.6	±1.7
Phase Accuracy (Degrees max.)	±13	±12	±14	±14
Isolation dB (min.)	17	14	14	13

** Theoretical 9 dB included*

MiCable

NEW

SUPERBEND®

High Performance Millimeter Wave Cable Assemblies

Really tight bend radius to save installation space & eliminate the need for costly right angle connectors without performance degradation

67GHz 67GHz 67GHz

- **Low Loss** <5.7dB/m@67GHz
- **Low VSWR** <1.35:1@67GHz
- **High Shielding Efficiency** <-90dB
- Shielded with stainless steel braids with high mechnical strength & flexure durability

Test Report for 0.2M Cable Assemblies

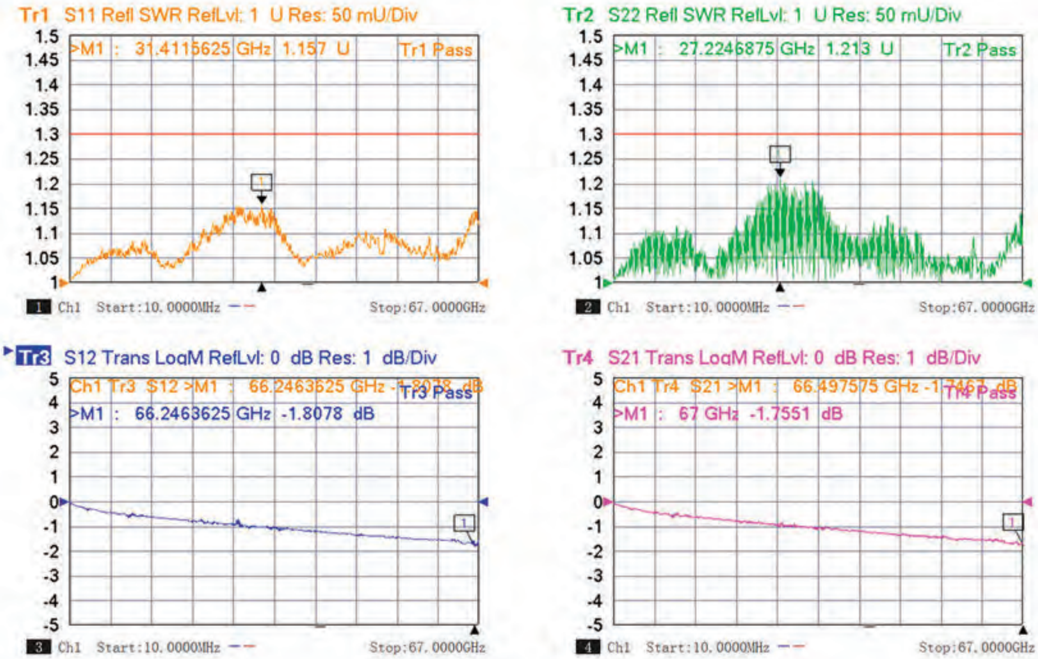

More Information-
Scan the QR Code

MIcable Inc.

www.micable.cn sales@micable.cn +86-591-87382856

Versatile Integrated Phase Noise and VCO Tester Streamlines Workflows

Signal Hound
Battle Ground, Wash.

Stable signal sources are essential for many high-precision electronic systems, such as wireless communications, RF testing and radar equipment. A key parameter of a stable signal is low phase noise. Phase noise is a characteristic of any fixed or tunable frequency source, from reference oscillators to frequency synthesizers. This phase modulation noise consists of short-term fluctuations in the frequency or phase of a source's output signal. At the system level, additional components, including cables connected to a signal source, can also contribute residual phase noise. Excessive phase noise can limit the sensitivity and performance of various types of receivers used across many fields, making phase noise testing critical throughout a broad range of industries.

TRADITIONAL PHASE NOISE TESTING METHODS

The direct spectrum method uses a spectrum analyzer to directly analyze the frequency spectrum of the signal. This is a quick method of testing and quite simple in comparison with other methods. However, the sensitivity and measurement accuracy can be limited by the spectrum analyzer's own noise floor.

Time domain analysis generally requires a high-end oscilloscope or time interval analyzer. This method is well-suited for broadband noise and analyzing wideband signals and applications where time stability is important. Time domain analysis can lack sensitivity for low phase level measurements and has limited offset resolution which is often required for RF and microwave applications. Additionally, high-end oscilloscopes are usually quite costly.

The cross-correlation method employs two identical measurement setups in parallel, usually requiring low noise reference oscillators, phase detectors, spectrum analyzers and cross-correlation software. This method excels at ultra-low phase noise measurement and is ideal for applications that

Fig. 1 **PN400 Phase Noise and VCO Tester.**

require precise phase noise measurement. This method has been notoriously complex, time-consuming and expensive.

Some labs and production facilities use specialized or integrated phase noise analyzers. These analyzers combine reference sources, phase detectors, PLLs and cross-correlation functionality into a single box. These analyzers can simplify the testing process through automation, ease of use and flexibility, but are often cost-prohibitive.

ALL-IN-ONE PHASE NOISE AND VCO TEST SOLUTION

Signal Hound has introduced a revolutionary phase noise and VCO test solution. The PN400 all-in-one test solution uses cross-correlation methodology and feature-rich software to provide a level of performance and sensitivity beyond the capabilities of one spectrum analyzer. The PN400 system offers enterprise-grade accuracy and innovative features that can compete with dedicated and costly phase noise testers for applications such as phase noise testing and characterization, VCO testing and characterization, production and manufacturing testing, source characterization, system-level debug and SDR characterization. The PN400 all-in-one test solution is shown in ***Figure 1***.

This unique and innovative phase noise test solution incorporates the PN400 hardware with an Advanced Phase Noise Test Tool Kit and requires two Signal Hound SM-series spectrum analyzers for operation. Combining the PN400 with two SM200 or SM435 spectrum analyzers enables cross-correlated phase noise measurements and VCO characterization via low noise tuning and supply voltage. It also offers all the power and flexibility of Signal Hound's spectrum analysis capabilities.

Introduction of the Advanced Phase Noise Test Tool Kit via Signal Hound's powerful Spike™ spectrum analysis software brings a comprehensive suite of tools to this new test solution. Combined with the PN400 hardware, the new VCO characterization mode in Spike's licensed phase noise test tool kit enables automatic sweeps across a configurable VCO tuning range. It allows accurate and low noise voltage sources to be combined with easy-to-use software supporting efficient characterization for R&D and manufacturing lines. However, the features go even further. Configurable automation, measurement of phase noise and amplitude noise or a combination of both, along with automatic signal detection, are just a few of the valuable capabilities included in the tool kit. ***Figure 2*** shows an example of the output of the Spike spectrum analysis software.

Fig. 2 **Representative Spike spectrum analysis software output.**

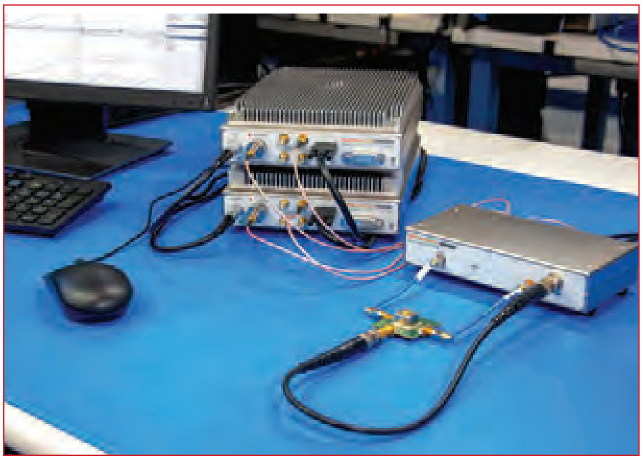

Fig. 3 **PN400 system using SM435B spectrum analyzers.**

The PN400 Phase Noise and VCO Tester operates at an input frequency range of 100 kHz up to 43.5 GHz, depending on the pairing of the SM-series spectrum analyzers. The utilization of two Signal Hound high frequency spectrum analyzers to perform cross-correlation measurements allows the system to achieve phase noise floors 20 to 30 dB lower than the capabilities of a single SM-series spectrum analyzer (-160 dBc/Hz at 40 GHz). This advanced hardware pairing creates an ideal system for applications that require precision phase noise measurement. The PN400 system, using two identical SM435B 43.5 GHz real-time spectrum analyzers for cross-correlated phase noise measurements and VCO characterization, is shown in ***Figure 3***.

The PN400 test system has a standard operating temperature range of -40°F to 185°F (-40°C to +85°C) and can be seamlessly integrated into a wide range of test environments. The phase noise test solution is also compact enough to fit easily on a benchtop. Traditional methods for precise phase noise measurement have been complex, time-consuming and expensive. Due to its ease of use, flexibility and affordability, the PN400 tester is poised to streamline workflows for a broad segment of users.

Signal Hound
Battle Ground, Wash.
signalhound.com

Miniaturized High Performance E-Band Filters

TERASi
Stockholm, Sweden

In recent years, the demand for high capacity wireless links has driven the development of technologies operating in the mmWave frequency spectrum. Among these, E-Band (60 to 90 GHz) has gained significant attention. This is primarily due to its potential to support a wide range of applications, including high capacity backhaul links for cellular networks, satellite communication networks and high-resolution radar systems.

E-Band microwave technology supports high data throughput, minimizes latency and enables small RF front-ends, making it an ideal band for space-constrained installations. As the demand for these systems grows, the development of small microwave bandpass filters is crucial for maintaining system performance at E-Band. Traditional filter designs often fall short of the cost, size, weight and performance needs. Meeting these needs has led to the development and adoption of advanced fabrication techniques, such as TERASi's Aircore™ waveguide technology.

TABLE 1
FILTER CHARACTERISTICS

E-Band Bandpass Filters				
Model	**Passband (GHz)**	**Insertion Loss max at f_c (dB)**	**Return Loss (min. dB)**	**Rejection (min. dB)**
TSiBPF101	71 to 76	0.4	20	75 at 81 to 86 GHz
TSiBPF103	73.65 to 76	0.7	20	25 at 73.35 GHz
TSiBPF211	81 to 86	0.4	20	75 at 71-76 GHz

TERASi's Aircore technology offers significant advantages for E-Band applications. It enables compact and precise components with micrometer-scale features. This reduction in filter size, in turn, allows the creation of compact and high performance RF devices crucial for modern wireless systems.

TERASi's Aircore filters are created by forming 3D structures in planar silicon substrates using a variety of etching techniques. Smooth interior surfaces and high conductivity coatings provide low signal loss and high Q-factor. In addition, the high thermal conductivity and low coefficient of thermal expansion of silicon offer high thermal stability and heat dissipation, ensuring reliable operation in varying environmental conditions.

TERASi has recently developed a patented system-in-package (SiP) solution to enable the integration of MMICs with the company's best-in-class passive components. This will enable TERASi to offer complete module solutions with industry-lead-

Fig. 1 Comparison of CNC-milled waveguide filter and TERASi Aircore filter.

ing size, weight and performance. TERASi's products are manufactured in Stockholm, Sweden, using batch fabrication to ensure high reproducibility and cost-effective manufacturing.

TERASi's product catalog includes several innovative and compact E-Band waveguide bandpass filters that offer significantly smaller footprints and lower weight than standard waveguide filters without compromising performance. Typical specifications of three such filters are given in ***Table 1***. The filters are designed around standard waveguide flange interfaces to ensure compatibility with conventional waveguide systems and do not require any additional fixtures or fittings.

The filters listed in Table 1 operate using the TE10 mode. They are engineered to achieve minimal insertion loss in the passband while ensuring high attenuation in the reject bands to enhance signal clarity and reduce interference. Elliptical RF filter design topologies are used to achieve a steep roll-off and improved selectivity by incorporating transmission zeros within their frequency response. These transmission zeros are strategically placed to provide significant attenuation at specific frequencies to enhance the filter's rejection and passband edge sharpness performance. An example of the TERASi Aircore filter versus a conventional waveguide filter is shown in ***Figure 1***. With thicknesses below 5 mm and weighing less than 5 g, these filters are significantly more compact and lightweight than existing offerings. These benefits open the door to a range of new use cases for E-Band, such as high data rate links between unmanned aerial vehicles, IoT devices or compact SmallSats.

TERASi's off-the-shelf filters are offered with passband frequencies of 71 to 76 GHz and 81 to 86 GHz. Their Q of approximately 1900 enables an insertion loss of less than 0.4 dB at the center frequency, with more than 75 dB of rejection at 81 GHz for the 71 to 76 GHz filter and at 76 GHz for the 81 to 86 GHz filter. The S-parameter performance of the 81 to 86 GHz filter is shown in ***Figure 2***. Additionally, rejection levels of at least 40 dB are maintained up to 105 GHz for the 71 to 76 GHz filter and up to 120 GHz for the 81 to 86 GHz filter.

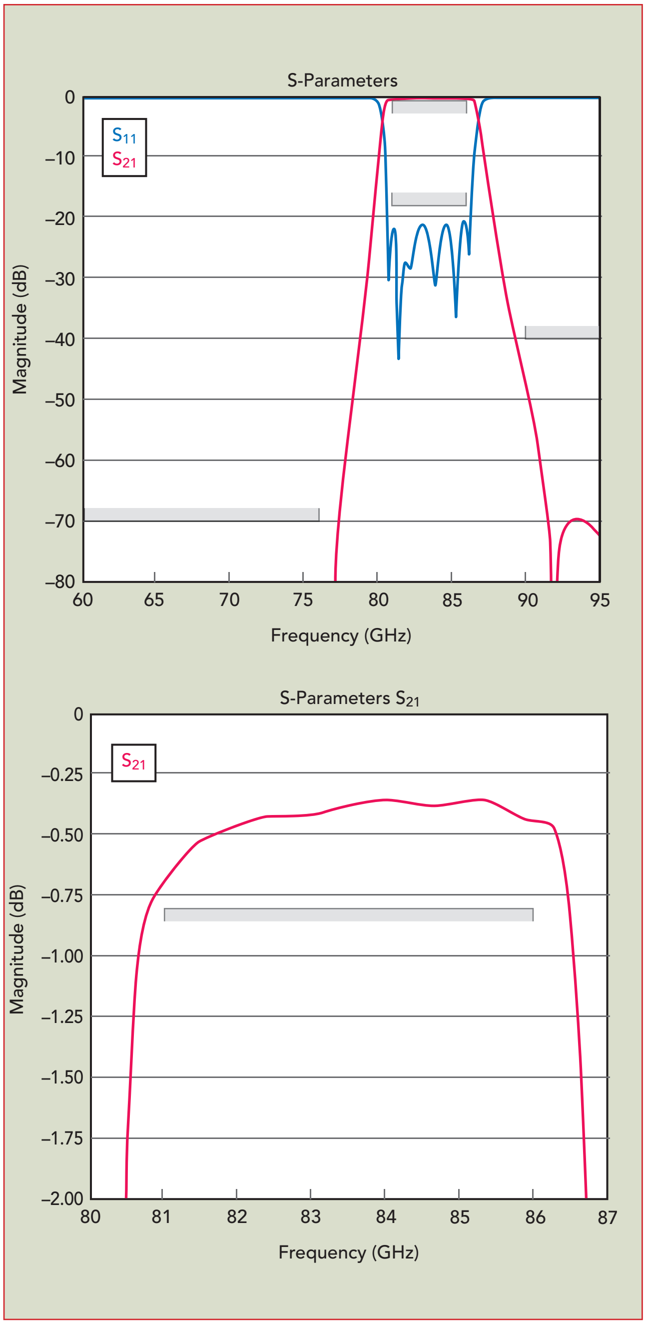

Fig. 2 S-parameters of 81 to 86 GHz bandpass filter.

Channel filters are also available with narrower pass bands and steeper roll-offs. As an example, TSiBPF103 features a passband from 73.65 to 76 GHz and high rejection at the lower stopband region. The insertion loss at the center frequency is lower than 0.7 dB with a rejection of 28 dB at 73.35 GHz. Moreover, the filter provides a minimum rejection of 60 dB at the upper stop band, from 80 to 110 GHz.

The filters are offered in packaged versions designed for use with UG-387 and IEEE P1785 flanges with a 20 mm × 20 mm footprint. Custom interfaces are also available to meet specific needs, including surface-mount device configurations for direct integration with printed circuit boards. The filters are available for purchase directly from TERASi and selected partners. Volume orders and custom design needs can be met upon request.

TERASi
Stockholm, Sweden
terasi.io/products/
sales@terasi.io

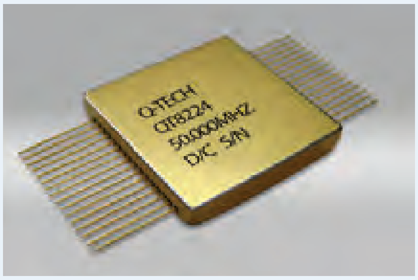

Full Space-Qualified Quad-Output TCXOs

Q-Tech's QT8220 Series is the industry's first quad-output temperature-controlled crystal oscillator (TCXO) series qualified for full space applications. The QT8220 Series CMOS TCXO, with its multiple CMOS outputs, offers significant size, weight and power advantages compared to the traditional design approach of using multiple single-output TCXOs. These new Q-Tech multi-output CMOS TCXOs enable designers to clock multiple inputs, such as multiple field-programmable gate arrays, with just a single component, rather than needing multiple oscillators for the same functionality.

The QT8220 Series TCXOs are available with two to four CMOS outputs, packaged in a hermetically sealed 32-pin flatpack with either 3.3 V or 5.0 V supply voltages and a frequency range from 20 to 100 MHz. Designed for full space applications requiring stability in the range of ±0.5 to 4.0 ppm over a temperature range of -40°C to +85°C, QT8220 TCXOs exhibit a radiation tolerance of greater than 100kRad(Si) TID and greater than 85MeV-cm²/mg SEL, along with low phase noise and jitter. All QT8220 devices are screened and inspected for quality conformance to MIL-PRF-55310, Level S.

Q-Tech was founded in 1972 to provide state-of-the-art crystal clock oscillators and frequency control solutions. The company is built on a philosophy of building products with leading-edge oscillator technology, along with a dedication to quality, on-time delivery and customer service. Q-Tech is a leading U.S. manufacturer of MIL-PRF-55310-qualified products, as well as other ultra-high reliability standards. The company is registered to AS9100 Rev D with ISO9001:2015 quality management systems. Q-Tech is renowned for its innovative design and manufacturing capabilities for the military, aerospace, down-hole and deep space industries.

Q-Tech Corporation
www.q-tech.com
sales@q-tech.com

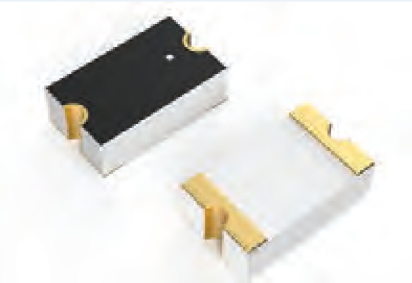

Ultra-Low Profile UWB Antenna

Leankon, a technology-driven global antenna solution provider, specializes in simplifying antenna solutions for global customers, guiding them seamlessly from design to mass production. The company introduces the LK1820201. This latest innovation is an ultra-low profile, ultra-wideband (UWB) antenna designed with the smallest form factor to support UWB Channels 5, 6, 7, 8 and 9 simultaneously.

The LK1820201 is a state-of-the-art surface-mount device UWB antenna, measuring 3.2 x 1.6 x 0.5 mm. With a minimal clearance requirement of 5 mm x 4 mm on your PCB, this antenna maximizes space efficiency, making it ideal for today's compact devices. Its design enhances isolation performance, making it perfect for applications that require multiple UWB antennas.

As IoT devices trend toward smaller and thinner designs, antenna challenges become more complex. The LK1820201 is engineered to overcome these challenges, ensuring stable wireless connections in increasingly compact devices. Key features and benefits include:

Wide Bandwidth: Excellent omnidirectional performance ensures robust connectivity.

Compact Size: This antenna is the smallest in its class, fitting seamlessly into designs.

Ultra-Slim Profile: The height allows for easy integration into thin devices, making the antenna particularly suitable for wearable technology and healthcare applications.

The goal at Leankon is to be the foremost provider of innovative antenna solutions across wireless technologies such as 5G, 4G LTE, Wi-Fi, Bluetooth, UWB, mmWave, ISM, NFC, GPS/GNSS, satellite and others, driving the evolution of IoT connectivity. Leankon invites you to explore the possibilities with their LK1820201 antenna. To facilitate your development, they offer free samples and evaluation boards. Partner with Leankon to elevate your antenna solutions and stay ahead in these rapidly evolving applications.

Leankon
Shanghai, China
www.leankon.com

6G Development: Learning From the Lessons of 5G

Anritsu's blog explores 5G roadblocks, how 6G will address them and factors for engineers to consider.

Anritsu
bit.ly/48Gkshy

What Is A RF Amplifier, And What Are They Used For?

Discover the essentials of RF amplifiers in this blog post.

Pasternack
https://blog.pasternack.com/

Unlocking Precision: How UWB and BLE Channel Sounding Are Redefining Positioning Technologies

In this blog post, learn about the indoor location services market, and how it is having no trouble locating growth.

Qorvo
bit.ly/4iiLzTW

Custom Magnetic Builder

The Quantic ECI Custom Magnetic Builder enables you to create your ideal custom inductor or transformer with ease. This intuitive builder guides you through the design process, allowing you to input your specific requirements, such as frequencies, power levels, topology and more.

Quantic ECI
www.quanticeci.com/custom-magnetic-builder

Ferrite-Based RF & Microwave Solutions

Quantic M-Wave's new website features their latest isolator, circulator, adapter and termination solutions for aerospace, defense, phased array radar and quantum computing applications.

Quantic M-Wave
www.quanticmwave.com

AntennaXpert by Taoglas

Taoglas introduces AntennaXpert, a suite of user-friendly, digital tools to streamline, simplify and customize antenna design and integration. Available on the Taoglas website, the toolset includes Taoglas Antenna Integrator, Antenna Builder and Cable Builder.

Taoglas
www.taoglas.com

NEW PRODUCTS

FOR MORE NEW PRODUCTS, VISIT WWW.MWJOURNAL.COM/BUYERSGUIDE
FEATURING VENDORVIEW STOREFRONTS

DEVICES/ COMPONENTS/MODULES

IMU Family

VENDORVIEW

ADI expands its IMU portfolio with the ADIS1657x IMU family. This small but powerful product offers tactical grade stability and vibration rejection in a rugged 22.4 × 24.5 × 14 mm package. The performance density of ADIS1657x is highlighted by an in-run bias stability of 2.0 degree/hr (gyro) and 2.9 μg (accelerometer) with 0.2 degree/$\sqrt{}$hr angular random walk; making this family of products ideal for a wide range of applications from precision instrumentation to avionics and more.

Analog Devices
www.analog.com

100 W Surface-Mount 90-Degree Hybrid

VENDORVIEW

Mlcable released the new 1.2 to 2.2 GHz high-power surface-mount 90-degree hybrid. It has low insertion loss (0.25 dB maximum), excellent VSWR (1.25:1 maximum), extremely good amplitude unbalance (±0.5 dB maximum) and phase unbalance (±3 degrees maximum), high isolation (20 dB minimum) and 100 W power handling capability with excellent stability and heat dissipation ability in a small package. It is suitable for power amplifier, power combining network, antenna feed network, modulator and phase shifter applications.

Mlcable
www.micable.cn

Ka-Band TSAB Transceiver

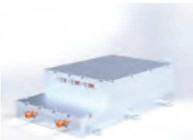

The NSR-SDR-K/Ka-HDR-NEM delivers up to 500 Mbps data rates for K-Band waveforms. Fully complaint with DVB-S2 standards and CCSDS ranging, it features NSA TSAB encryption, supporting top secret and below. The NSR-SDR-K/Ka-HDR-NEM has the unique ability to remain unclassified during production, reducing costs and simplifying logistics, before being keyed up to top secret use at launch. This turnkey solution integrates a low noise amplifier, power amplifier and RF channel filtering, all tested end-to-end, ensuring seamless integration into spacecraft systems and alleviating design and testing challenges and costs.

Vulcan Wireless
www.vulcanwireless.com

RF Switch Modules

WithWave's RF switch modules have absorptive and reflective type such as SP4T, SP8T, SP10T and SP12T and 4-port matrix according to types of switches, frequency range and switching applications. They deliver high isolation, low insertion loss and fast switching time, making these devices ideal for RF signal routing in wireless infrastructure and applications up to maximum frequency range. External connectors included 2.92 mm vertical launch connectors for all RF port. They are powered and controlled through a USB type-C connector.

withwave co., ltd
www.with-wave.com

Baluns

VENDORVIEW

Würth Elektronik has expanded its WE-BAL series of baluns. The components for coupling symmetrical and asymmetrical transmission lines feature improved materials and manufacturing processes, and now cover wider frequency ranges from 673 MHz to 5900 MHz. In numerous applications, such as antenna systems, audio and video devices, wireless communication systems, power-over-ethernet systems and measuring instruments, it is necessary to couple symmetrical and asymmetrical transmission lines in such a way that prevents signal loss.

Würth Elektronik
www.we-online.com

SPDT Switch

Z-Communications Inc. announced the RFSW30 general-purpose single-pole, double throw (SPDT) switch. The RFSW30 features low insertion loss of -3 dB over the entire frequency range of 9 kHz to 30 GHz, and high input linearity of 1 dB power compression (P1dB) of 28 dBm. The RFWS30 is part of Z-COMM's new product line of connectorized modules for lab bench and prototyping applications, varying from test and measurement, radar, ECMs, VSAT and potential OEM partnerships.

Z-Communications Inc.
www.zcomm.com

CABLES & CONNECTORS

Mini-FAKRA Cable Assemblies

Amphenol RF expanded their AUTOMATE Type A mini-FAKRA portfolio with additional pre-configured breakout cable options designed on industry-standard cable types. These assemblies are available in two new configurations: quad-port mini-FAKRA straight jack to four straight FAKRA plugs on TFC 302LL and dual-port mini-FAKRA straight jack to two FAKRA straight jacks on RG-174 cable. Both versions provide reliable RF performance up to 6 GHz with ruggedized construction ideal for autonomous applications such as new automotive designs and industrial automation technologies.

Amphenol RF
www.amphenolrf.com

Spring-Loaded Adapters for SMP, SMPM and SMPS Connectors

VENDORVIEW

Fairview Microwave launched its new spring-loaded adapters for the SMP, SMPM and SMPS connector series. Available in a variety of lengths, the adapters are designed to meet the needs of high frequency applications where reliability and precision are critical. The new adapters offer enhanced performance for RF connectivity, making them essential for industries such as telecommunications, aerospace and defense.

Fairview Microwave
www.fairviewmicrowave.com

Connectors

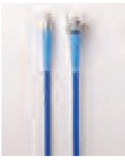

Junkosha announced the launch of its own branded connectors, which will be integrated into Junkosha microwave/mmWave coaxial cable assemblies in February 2025. This initiative is a direct response to escalating demands within the microwave and mmWave markets, driven by 5G, AI and data center growth — all of which require advanced interconnect solutions capable of supporting high speed and data-heavy workloads. Leveraging its expertise in fluoropolymer processing and high performance cable manufacturing, Junkosha is expanding its design and development capabilities to provide fully-integrated cable and connector solutions.

Junkosha
www.Junkosha.com

New**Products**

Low Loss and Low PIM Cable Assemblies

Pasternack launched new options for low loss and low PIM cable assemblies. The new offerings feature a variety of LMR cable assemblies and low PIM configurations designed to meet the growing demand for superior signal transmission and minimal interference. The expanded line includes LMR cable assembly options available in PVC, fire-rated, ultra-flexible and lightweight variations, offering a broad selection of cable types for a wide range of uses.

Pasternack
www.pasternack.com

Microwave Assemblies

Samtec, Inc. announced full production quantity availability of its LL043 Series Nitrowave™ high performance microwave cable assembly. Nitrowave™ is Samtec's new flexible, low loss microwave coaxial cable product line that demonstrates outstanding amplitude and phase stability in test and measurement, as well as 5G datacom, defense, aerospace and computer/semiconductor applications. Nitrowave™ is easily recognizable by its distinctive orange color and is backed by Samtec Sudden Service® which includes part availability, quick delivery and access to people and tools that help streamline a design process.

Samtec
www.samtec.com

AMPLIFIERS

2.0–8.0 GHz, 500 W CW & Pulse

Exodus AMP2085P-LC, dual-mode (CW and pulse) excellent TWT replacement, ideal for automotive pulse/radar EMC-testing and commercial applications. Pulse widths to CW, duty cycle to CW, 57 dB gain with outstanding pulse fidelity. Monitoring parameters for forward/reflected power in watts and dBm, VSWR, voltage, current and temperature, with unprecedented reliability and ruggedness in a compact 7U chassis of 12.25 (H) × 19 (W) × 29 (D) in. nominally 90 lbs.

Exodus Advanced Communications
www.exoduscomm.com

Low Noise Amplifier

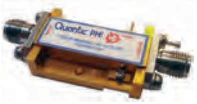

Quantic PMI Model PE2-16-300M20G-1R7-15-12-SFF is a low noise amplifier (LNA) that works from 0.3 to 20 GHz. This amplifier has an extremely low noise figure over this broad frequency range. This LNA provides 16 dB of small signal gain while requiring only a single supply of +12 V. The P1dB output power of 15 dBm allows this LNA to function as a lo driver for balanced, I/Q or image reject. Supplied in Quantic's standard PE2 housing, 1.08 × 0.71 × 0.29 in., which can be used as an SMA connectorized or a surface-mount component.

Quantic PMI
www.quanticpmi.com

Surface-Mount Positive Gain Slope Driver Amplifier

The Marki Microwave AMM-9619PSM is a surface-mount amplifier suitable for use as a single tone driver or general-purpose gain block from 2 to 26 GHz. This amplifier has exceptionally low input and output reflections, and a low 1.6 dB typical noise figure from 8 to 18 GHz. It exhibits a positive gain slope to equalize frequency dependent losses and comes in a 4 mm QFN for surface-mount integration onto printed circuit boards.

RFMW
www.rfmw.com

SEMICONDUCTORS

Lancang-USRR Chip

Calterah's Lancang-USRR chip is a 60 GHz mmWave radar system-on-chip (SoC) special-

New**Products**

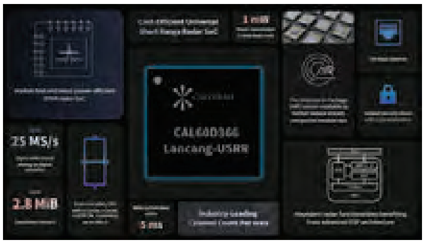

ly optimized and tailored for in-cabin sensing applications like child presence detection. With six transmitters and six receivers, this radar SoC offers powerful angular detection and provides a flexible radar signal processor. It can operate in a low-power deep sleep mode and wake up very quickly. Additionally, leveraging Calterah's antenna-in-package technology, this SoC enables more compact radar modules to fit various challenging installation scenarios.

Calterah
www.calterah.com

SOURCES

Signal Generator

VENDOR**VIEW**

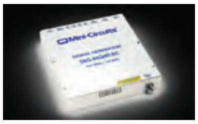

Mini-Circuits' modelSSG-44GHP-RC is a compact signal generator with frequency range of 0.1 to 44.0 GHz and 1 Hz tuning resolution. Well-suited for 5G frequency range 1 and 2 band testing, the 50 Ω source generates continuous-wave (CW) as well as pulsed signals with minimum pulse width of 0.5 μs and 0.65 ms settling time. It offers +23 dBm output power to 22 GHz and +17 dBm to 44.0 GHz with -30 dBc typical harmonics and includes USB and Ethernet interface.

Mini-Circuits
www.minicircuits.com

ANTENNAS

Dual-Ridged Horn Antenna

VENDOR**VIEW**

Featuring a 1 mm female coaxial feed port, model SAV-1431141129-1F-S1 provides frequency coverage from 14 to 110 GHz with gain spanning 5 to 16 dBi. Return loss is 10 dB or better across the operating bandwidth. The beam width varies from 100 degrees at 14 GHz to 20 degrees at 110 GHz.

Eravant
www.eravant.com

MIMO Antennas

Raltron Electronics announced the release of its new RDM Series of MIMO antennas. Designed for a wide range of applications including industrial IoT, transportation and communication systems, these antennas meet the increasing demand for multi-frequency solutions that offer enhanced performance, efficiency and durability in challenging environments. The RDM Series MIMO antennas support a wide range of frequencies from 690 MHz to 5.85 GHz, including LTE, Wi-Fi, GPS, GNSS, LoRa and more.

Raltron Electronics
www.raltron.com

TEST & MEASUREMENT

High Performance Oscilloscope

Pico Technology has significantly enhanced its PicoScope 9400 Series by launching the PicoScope 9404A-25, a high performance oscilloscope offering an impressive 25 GHz bandwidth on four channels. This latest addition builds on the existing PicoScope 9400 Series, which features models with 5 GHz and 16 GHz bandwidths, expanding the reach and capabilities of this advanced family of oscilloscopes. Pico Technology's unique Sampler-Extended Real-Time Oscilloscope technology combines the advantages of traditional real-time acquisition with sampling oscilloscope capabilities, offering engineers the best of both worlds.

Pico Technology
www.picotech.com

High-Resolution Oscilloscopes

RIGOL's new DHO/MHO5000 Series oscilloscopes offer high-resolution, high performance, more channels and lower price. Combining 12-bit resolution with 500 MHz or 1 GHz bandwidth, four, six or eight analog channels, mixed-signal configurations and optional integrated function generator, the DHO/MHO5000 Series high-resolution oscilloscopes have a lot to offer designers, engineers, researchers and educators alike.

RIGOL
www.RIGOLna.com

Phase Noise & VCO Tester

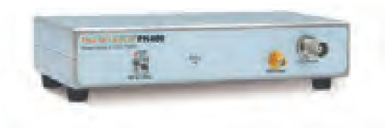

Signal Hound announced the addition of the PN400 phase noise and VCO tester to its expanding range of products. This powerful, all-in-one, phase noise test solution unlocks enterprise-grade accuracy and cutting-edge features in your test and measurement environment. Utilizing cross-correlation methodology and feature-rich software, the system provides a level of performance and sensitivity beyond the capabilities of a single spectrum analyzer.

Signal Hound
www.signalhound.com

Reviewed by: Katerina Galitskaya

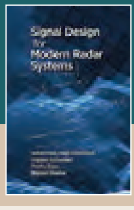

Bookend

Signal Design for Modern Radar Systems

By: Mohammad Alaee-Kerahroodi, Mojtaba Soltanalian, Prabhu Babu and Bhavani Shankar

Authors of "Signal Design for Modern Radar Systems" present a thorough and highly technical exploration into the world of radar signal processing. Written with a clear focus on the most cutting-edge developments in adaptive, cognitive radar systems, this book is a valuable resource for engineers, mathematicians and system designers looking to deepen their understanding of radar signal design. What sets this book apart is its attention to optimization techniques used for designing radar waveforms that adapt in real-time to dynamic environments. In the past, radars often relied on fixed waveforms that could not adjust to changes in the environment or counter electronic threats. Today, however, with improvements in computing power, radar systems can adapt their waveforms in real-time, adjusting to different conditions. The authors explain how this shift has transformed radar performance, especially in areas like defense, automotive and space exploration. One of the highlights of this book is the structured journey through both convex and non-convex optimization techniques. From traditional convex methods to more advanced non-convex approaches, the authors give readers a rich toolkit for solving the signal design challenges that arise in modern radar systems. Particularly insightful are the discussions on local optimization algorithms, such as power method iterations and majorization-minimization techniques. The chapters on emerging applications are especially valuable for those interested in cutting-edge technology. The book explores 4D imaging for automotive MIMO radar, waveform design for spectrum sharing and advanced Doppler-tolerant waveforms, to name just a few areas. These sections are not only theoretically rich but also demonstrate real-world relevance, particularly as automotive radar and other commercial uses grow. In summary, this book is ideal for professionals and advanced students with a background in radar or signal processing. It is highly technical but also practical, offering both theoretical foundations and real-world applications. If you are looking to understand the latest methods in radar waveform design and optimization, this book is an excellent guide.

ISBN: 9781630818920
Pages: 392
To order this book, contact:
Artech House (2022)
us.artechhouse.com

Advertising**Index**

Sales Representatives

Eastern and Central Time Zones
Carl Sheffres
Group Director
(New England, New York, Eastern Canada)
Tel: (781) 619-1949
csheffres@mwjournal.com

Michael Hallman
Associate Publisher
(NJ, Mid-Atlantic, Southeast, Midwest, TX)
Tel: (301) 371-8830
Cell: (781) 363-0338
mhallman@mwjournal.com

Pacific and Mountain Time Zones
Brian Landy
Western Reg. Sales Mgr.
(CA, AZ, OR, WA, ID, NV, UT, NM, CO, WY, MT, ND, SD, NE & Western Canada)
Tel: (831) 426-4143
Cell: (831) 713-9085
blandy@mwjournal.com

International Sales
Carl Sheffres
Tel: (781) 619-1949
csheffres@mwjournal.com

Germany, Austria, and Switzerland (German-speaking)
Victoria and Norbert Hufmann
victoria@hufmann.info
norbert@hufmann.info

France
Gaston Traboulsi
Tel: +44 207 596 8742
gtraboulsi@horizonhouse.com

Korea
Jaeho Chinn
JES MEDIA, INC.
Tel: +82 2 481-3411
corres1@jesmedia.com

China
Shanghai
Linda Li
ACT International
Tel: +86 136 7154 0807
lindal@actintl.com.hk

Wuhan
Phoebe Yin
ACT International
Tel: +86 134 7707 0600
phoebey@actintl.com.hk

Shenzhen
Annie Liu
ACT International
Tel: +135 9024 6961
anniel@actintl.com.hk

Beijing
Cecily Bian
ACT International
Tel: +86 135 5262 1310
cecilyb@actintl.com.hk

Hong Kong
Floyd Chun
ACT International
Tel: +852 28386298
floydc@actintl.com.hk

Taiwan, Singapore
Simon Lee
ACT International
Tel: +852 2838 6298
simonlee@actintl.com.hk

Japan
Katsuhiro Ishii
Ace Media Service Inc.
Tel: +81 3 5691 3335
amskatsu@dream.com

Submitting ad material?
Visit: www.adshuttle.com/mwj
(866) 774-5784
outside the U.S. call
+1-414-566-6940

Ed Kiessling
(781) 619-1963
ekiessling@mwjournal.com

Corporate Headquarters: 685 Canton Street, Norwood, MA 02062 • Tel: (781) 769-9750

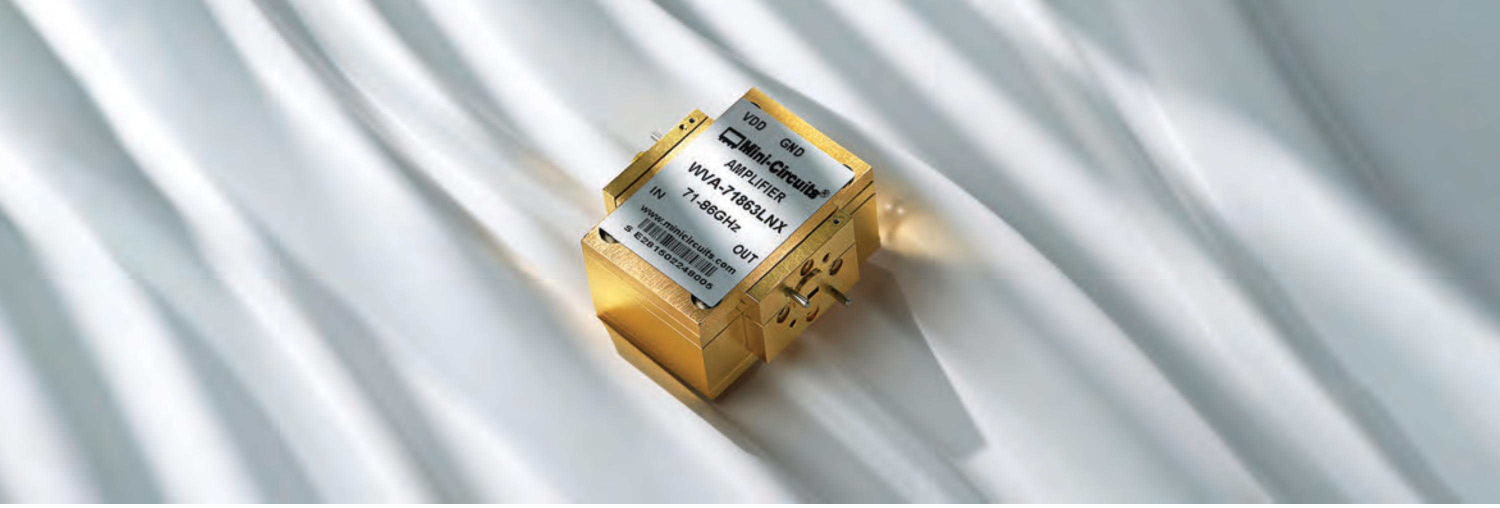

UP TO 110 GHz

High-Frequency Solutions

Amplifiers & Modules for mmWave Applications

WAVEGUIDE AMPLIFIERS

- Bandwidths from 40 to 110 GHz
- Low noise, high gain & medium power options
- WR10, WR12, WR15 & WR15 interfaces
- Ideal for TRP & TIS over-the-air testing

CONNECTORIZED AMPLIFIERS

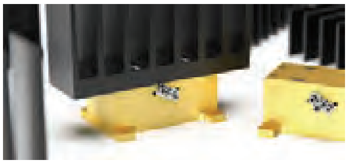

- Bandwidths from 50 kHz to 95 GHz
- 2.92, 2.4, 1.85 & 1.0mm connector options
- Gain up to 45 dB
- NF as low as 1.7 dB
- Power up to 1W

VARIABLE GAIN AMPLIFIERS

- Bandwidths from 18 to 54 GHz
- Gain up to 50 dB
- Calibrated 17 dB attenuation with analog or TTL control
- PSAT up to +1W
- Interactive GUI with telemetry

Mini-Circuits®

FABS and LABS

Werlatone: Underpromise and Overdeliver

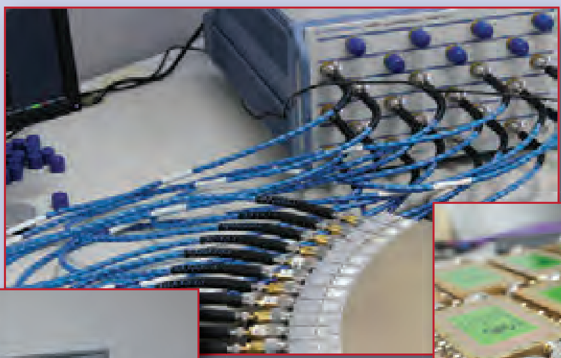

Since its founding in 1965, Werlatone has been one of the leading manufacturers of high-power passive RF components. Located in a large manufacturing and development facility in Patterson, N.Y., the name “Werlatone” has become synonymous with high quality and advancement in the RF industry. Werlatone combines an experienced and knowledgeable engineering and development team with a highly skilled manufacturing department to create fully custom and standard parts to meet customer needs.

Over nearly six decades, Werlatone has evolved from couplers to become a recognized leader in high-power RF and microwave components. While the company is known mainly for its power dividers, combiners, couplers and hybrids, Werlatone’s product portfolio has expanded to include beamforming networks, wideband impedance networks, broadband rectifier circuits, absorptive filters and digital power meters. While many of their products are now standard catalog products, the company prides itself on its ability to produce custom solutions to meet demanding customer needs.

Werlatone’s products are distinguished by their robustness and efficiency, particularly in high-power applications. Along with these impressive operating powers, many of the Werlatone solutions are Mismatch Tolerant®, operating continuously at rated power into high VSWR conditions. To support high-power requirements, Werlatone maintains an extensive solid-state high-power test lab to evaluate prototypes and verify new designs.

With 30 active patents and several pending, Werlatone builds on 265 years of combined engineering experience to continuously innovate and take a leadership role in high-power passive solutions. Their newly patented high-power combiner is based on an E-plane combiner structure where the peak and CW power-handling capabilities are limited only by the waveguide size. The result is a substantial improvement in power handling for N-way combiners. Werlatone is also incorporating ferrite technology along with their passive component expertise to extend the power handling and bandwidth capabilities for beamforming networks, baluns and impedance transformers.

In addition to the high-power capability of their products, Werlatone designs products to operate over wide frequency ranges. Products routinely operate over multi-octave bandwidths, with some reaching a 1000:1 bandwidth. Frequency specific designs operate from DC to Ka-Band.

With a focus on power and performance, it is not surprising that the company is heavily involved with defense markets. The company reports that 70 percent of its customers are engaged in military communications, EW and government testing applications. The balance of their product line serves commercial communications, ISM, semiconductors, medical and university applications.

In addition to performance innovations, Werlatone remains committed to quality and manufacturing improvements. The company’s products can be designed or tested to MIL-STD-810 specifications. Werlatone is ISO 9001:2015- and AS 9100D-certified and adheres to MIL-I-45208 A inspection system requirements.

For nearly 60 years, Werlatone has built a business based on underpromising and overdelivering on standard and custom high-power passive components and fully integrated subsystem architectures.

www.werlatone.com

eXclusive Digital Content >>>

INVITED PAPER

Enhancing Bandwidth and Gain of a Broadband Circularly Polarized Antenna Realized with a Nonuniform Metasurface

Shaoliang Yuan
Fujian Polytechnic Normal University, Fuzhou, China

A new circularly polarized (CP) antenna design incorporates a nonuniform metasurface (MS). The central driven element is a corner-cut and slotted patch connected to the ground plane using a metal via. To achieve CP, additional corner-cut patches are strategically placed around it to form a nonuniform MS. It achieves an impedance bandwidth (IBW) of 2.2 GHz, from 4.4 to 6.6 GHz, with a 3 dB axial ratio bandwidth (ARBW) of 1 GHz from 4.7 to 5.7 GHz. The antenna with its surrounding MS excites two orthogonal modes, resulting in CP radiation and the emergence of an additional axial ratio (AR) minimum. This contributes to a wider bandwidth. Excellent radiation performance makes it well-suited for various applications, including military and civilian communication, as well as point-to-point links.

CP antennas are essential for wireless communication systems and point-to-point links due to their ability to mitigate multipath effects and polarization mismatch. The growing demand for CP antennas that offer high gain, broadband coverage and a wider 3 dB axial ratio angle has prompted the exploration of different design techniques. One such technique is the use of a metasurface, which has proven to be highly effective in generating and enhancing CP radiation. Consequently, several antennas based on metasurfaces have been developed and have demonstrated broadband CP properties.[1,2]

Gao et al.[3] employed a nonuniform MS in a 2 × 2 CP antenna array. The design incorporated a Wilkinson power divider feed network. It demonstrated broad bandwidth capabilities, specifically a 3 dB ARBW of 33.13 percent from 7 to 9.78 GHz and an IBW of 49.6 percent from 6.05 to 10.04 GHz. This work highlighted the potential of using nonuniform MS configurations to enhance the radiation properties of CP antennas.

This study's findings have significant implications for advancing the development of high-performance antennas in wireless communication applications. Nonuniform MS antenna designs can support wider frequency ranges and improved polarization properties, leading to enhanced performance in wireless communication systems. It should be noted that previous works did not consider gain and 3 dB AR beamwidth. Moreover, the bandwidths of MS-based antennas were found to be limited. This article describes a nonuniform MS design used to precisely control the distribution of the electromagnetic field and enable enhanced radiation properties. It achieves high gain and wide bandwidth with a corner-cut slotted patch radiator element surrounded by a nonuniform MS of corner-cut patches. Extensive simulations and measurements validate its effectiveness.

ANTENNA DESIGN

To enhance the axial ratio within the desired frequency range, several adjustments to the dimensions and positioning of the central element (Element A) components are considered. This is shown in ***Figure 1***. This includes modifying the patch and ground plane dimensions, as well as the shape and placement of the off-centered metal via to achieve left-hand circular polarization (LHCP). Additionally, potential losses in the antenna system, such as radiation losses, dielectric losses and conductor losses, are evaluated and minimized. Despite improvements made through iterative simulation, the desired AR of less than -3 dB is not achievable within the frequency range of interest using this structure alone.

A novel approach to achieve CP over the band of interest employs the corner-cut central patch (Element A) encircled by a 3 × 3 array of MS cells; each cell is denoted as Element B, as shown in ***Figure 2***.

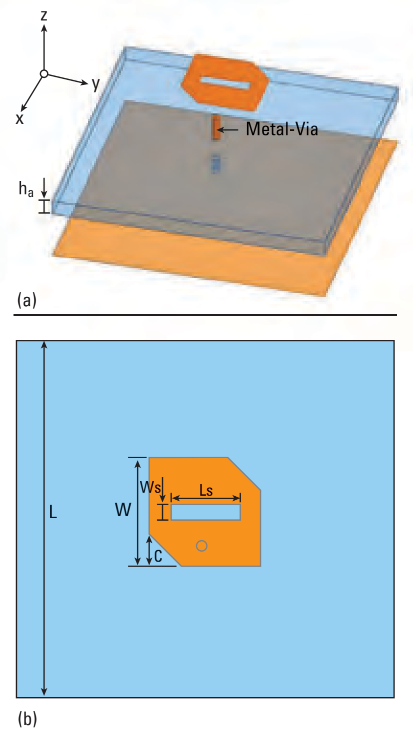

▲ Fig. 1 Initial configuration of antenna Element A: perspective view in 3D (a) and plane view (b).

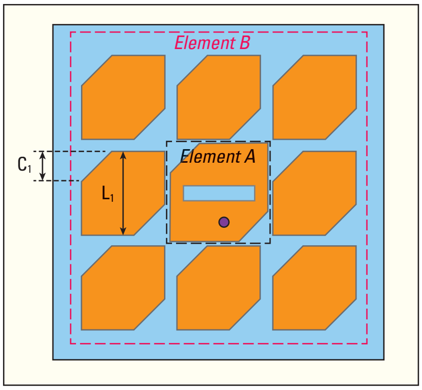

▲ Fig. 2 Nonuniform MS antenna configuration.

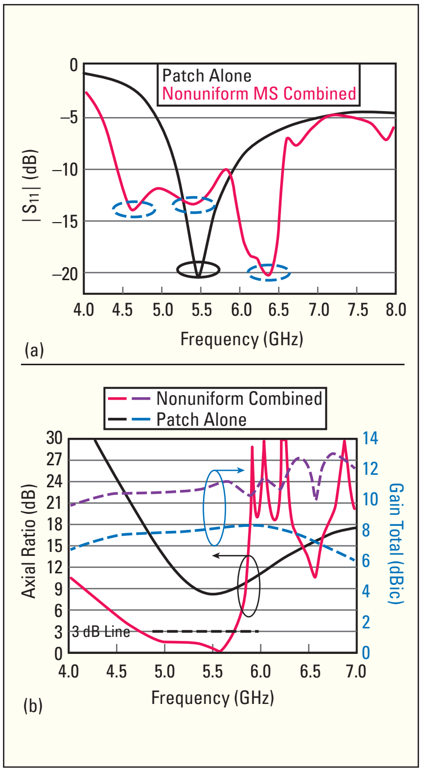

▲ Fig. 3 (a) Simulated $|S_{11}|$ performance. (b) Simulated AR and gain performance.

TABLE 1

UPPER-FREQUENCY HALF-WAVELENGTH SPACING FOR SOME COMMON BANDS

Dimension	Size (mm)	Dimension	Size (mm)
h_a	3.175	L	55
W_s	2	C	5.3
L_s	12	W	16.25
g	2	L_1	13.75
C_1	5		

The resulting configuration forms a nonuniform MS comprising eight corner-cut patches (Element B) surrounding the corner-cut slotted patch (Element A). Both elements are fabricated on a single substrate measuring 55 mm × 55 mm. The dielectric material has a relative permittivity of ε_r = 2.2 and a loss tangent of tan δ = 0.0014.

A coaxial feed simultaneously excites the two CP modes. Simulation using Ansys HFSS is conducted to optimize the distance to the off-centered metal via and adjust geometric parameters of the nonuniform MS to enhance radiation characteristics. The optimized dimensions are shown in ***Table 1***.

Figure 3a shows the simulated $|S_{11}|$ performance results for Element A alone and the complete nonuniform MS antenna. ***Figure 3b*** shows the simulated AR and gain performance results. $|S_{11}|$ for the nonuniform MS array remains below -10 dB over the frequency range of 4.4 to 6.6 GHz. Resonant frequencies are observed at 4.6, 5.3 and 6.4 GHz. In contrast, Element A, alone, exhibits only a single resonant frequency at 5.5 GHz with a narrow impedance bandwidth of 5.3 to 5.6 GHz.

The integration of the MS results in a wider bandwidth and a more compact size. Additionally, it shifts the resonant frequency lower and introduces two new resonant frequencies. This is credited to the seamless integration of the nonuniform MS into the antenna structure. The combined antenna is not only more streamlined in size but also achieves a broader bandwidth.

In contrast, Element A, alone, exhibits no AR values below 3 dB, as shown in Figure 3b, indicating a lack of CP radiation. The nonuniform MS array antenna achieves an AR bandwidth from 4.7 to 5.7 GHz and at 5.5 GHz, it is a near-zero minimum. Additionally, it surpassed Element A, alone, in gain performance, with an average gain that is 2.5 dB higher and a maximum gain of 11 dBic within the AR bandwidth.

Normalized radiation patterns in the far field at 4.6 GHz display a minimal cross-polarization response and negligible back lobes in both the *xoz*- and *yoz*-planes. This is evident for the main lobe gain in the *xoz*-plane in ***Figure 4a*** and the main lobe gain in the yoz-plane in ***Figure 4b***. Cross-polarization levels are -28

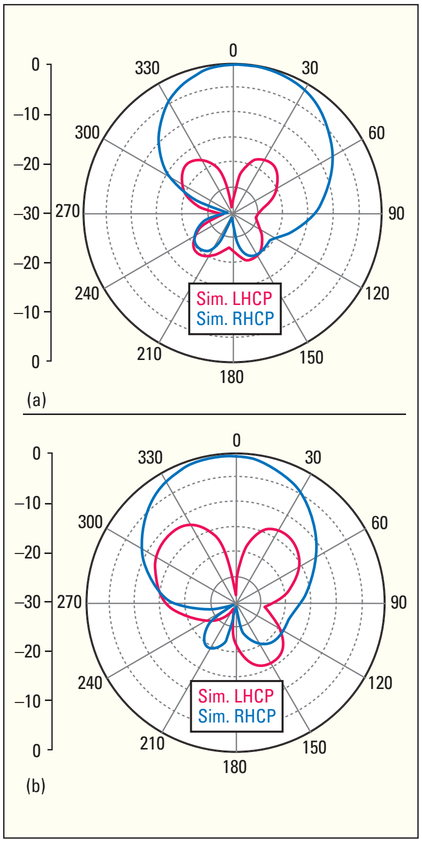

▲ Fig. 4 (a) Simulated main lobe gain in the xoz-plane. (b) Simulated main lobe gain in yoz-plane.

dB and -29 dB in the *xoz*- and *yoz*-planes, respectively, at boresight.

SIMULATION AND MEASUREMENT

To validate antenna array performance, simulations conducted in HFSS are compared with measurements made in an anechoic chamber using a vector network analyzer. ***Figure 5a*** shows the simulated and measured $|S_{11}|$ response of the nonuniform MS antenna array. ***Figure 5b*** shows the simulated and measured response for AR and gain. Figure 5a shows a 10 dB impedance bandwidth of 40 percent, from 4.4 to 6.6 GHz. The measured AR bandwidth of 19 percent from 4.7 to 5.7 GHz shown in Figure 5b closely aligns with the simulation. AR values remain at a consistently low level of approximately 0.25 dB throughout the band. Furthermore, the peak gain is 11 dBic at 5.5 GHz, within the 3 dB AR band.

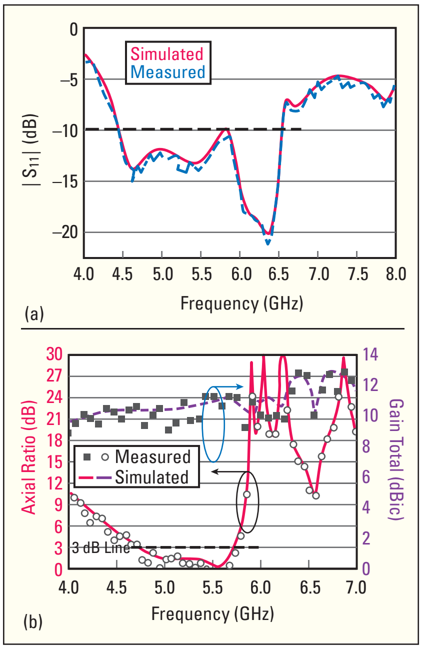

Fig. 5 (a) $|S_{11}|$ response of the nonuniform MS antenna array. (b) AR and gain response of the nonuniform MS antenna array.

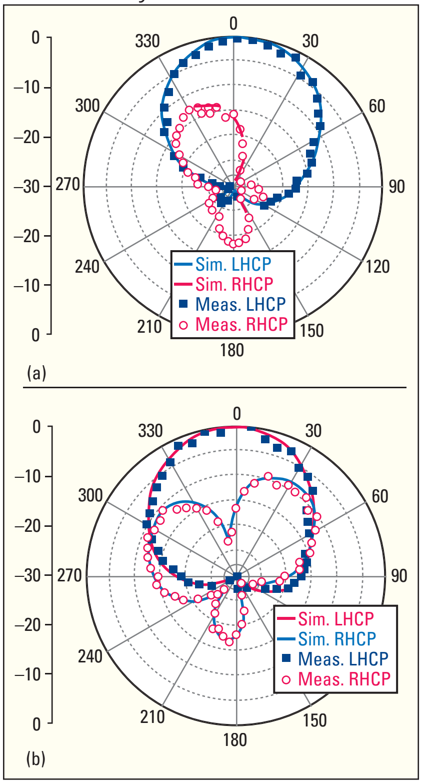

Fig. 6 (a) 5.6 GHz radiation patterns in the **xoz**-plane. (b) 5.6 GHz radiation patterns in the yoz-plane.

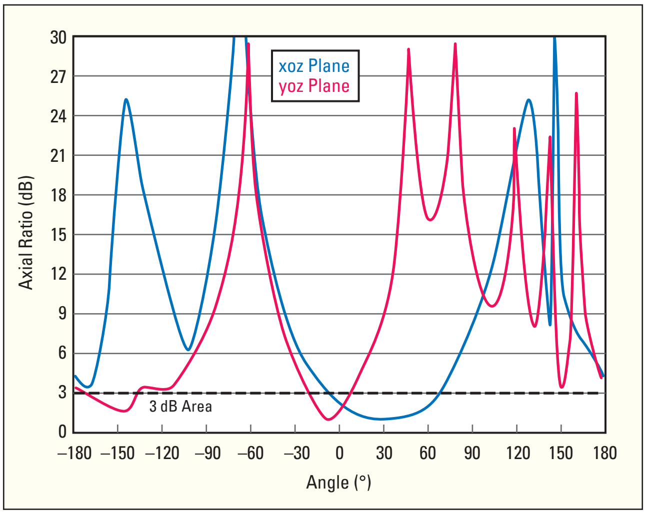

Fig. 7 Simulated AR versus angle in the xoz- and yoz-planes at 5 GHz.

Figure 6a shows

TABLE 2

COMPARISON WITH OTHER WORK

Reference	Size (λ_0^3)	3 dB AR BW (GHz)	Peak Gain (DBic)	3 dB AR Angular Range (Degrees)	Operating Bandwidth (GHz)
This Work	**1 × 1 × 0.05**	**4.4 to 6.6**	**11**	**-28 to 75**	**4.4 to 5.7**
3	2 × 2 × 0.08	7 to 9.78	13.17	–	6.05 to 10.04
4	0.67 × 0.67 × 0.06	1.3 to 2.1	8.7	–	1.4 to 2.1
5	2.6 × 2.63 × 0.36	9.8 to 10.2	13.4	-10 to 10	9.86 to 10.14
6	2.0 × 2.0 × 0.6	7.3 to 7.6	15.1	–	7.3 to 7.6
7	2.0 × 2.0 × 0.88	4.12 to 6.39	14.5	–	3.82 to 6.01
8	3 × 3 × 0.19	9.7 to 10.3	17.8	-15 to 15	9.8 to 10.2

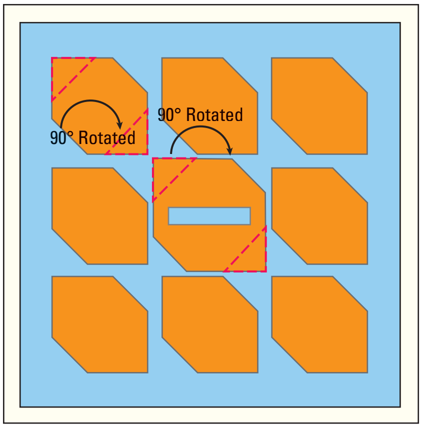

Fig. 8 Configuration of the RHCP antenna.

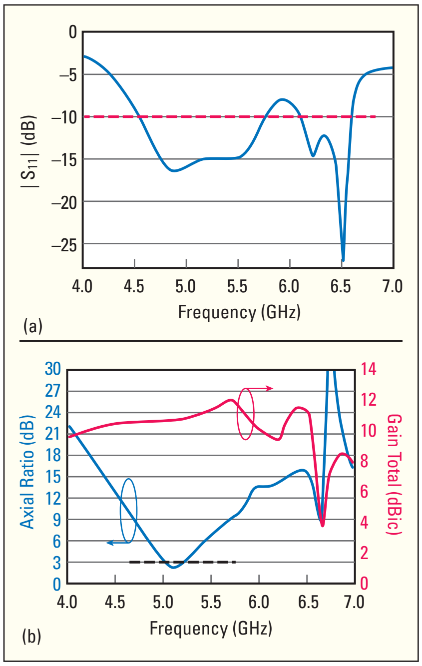

Fig. 9 (a) Simulated $|S_{11}|$ of the RHCP antenna. (b) Simulated AR and gain of the RHCP antenna.

the 5.6 GHz radiation patterns in the xoz-plane and ***Figure 6b*** shows the 5.6 GHz radiation pattern in the *yoz*-plane. These patterns demonstrate a low cross-polarization level of less than -25 dB in both the *xoz*- and *yoz*-planes at boresight. ***Figure 7*** shows the simulated AR versus angle at 5 GHz. In the *xoz*-plane, the AR is less than 3 dB over a range of -28 °C to +75°C. The performance in the *yoz*-plane is narrower but still satisfactory.

Table 2 compares this antenna with other recently proposed MS-based antennas, showing that it outperforms its counterparts in terms of radiation properties. This performance is achieved within a volume of 1.86 × 1.86 × 0.08 $\lambda 0^3$.

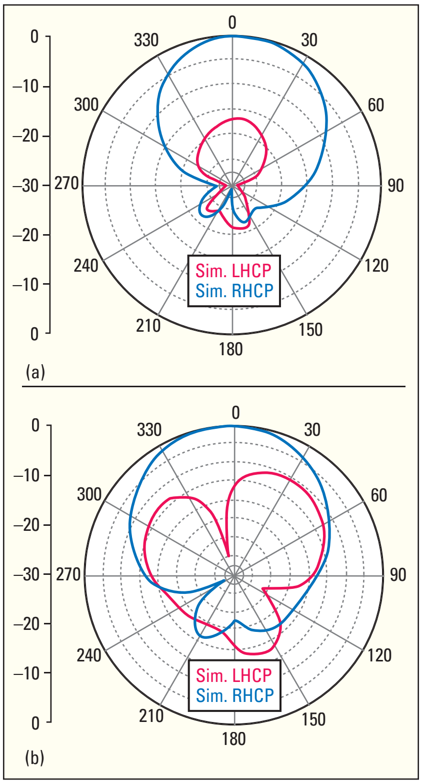

Fig. 10 (a) Simulated RHCP and LHCP radiation patterns in the **xoz**-plane. (b) Simulated RHCP and LHCP radiation patterns in the **yoz**-plane.

ANTENNA MODIFICATION TO ACHIEVE RIGHT-HAND CIRCULAR POLARIZATION (RHCP)

To achieve RHCP, both corner cuts are simply rotated 90 degrees counterclockwise around the center. This is shown in ***Figure 8***. Additionally, a slight adjustment is made to the position of the off-centered coaxial feed point. Using HFSS, the simulated $|S_{11}|$ performance for the RHCP antenna is shown in ***Figure 9a***, and the simulated AR and gain for the RHCP antenna is shown in ***Figure 9b***. From these curves, $|S_{11}|$ is below -10 dB from 4.5 to 6.8 GHz, except for a small region from 5.8 to 6.0 GHz. The 3 dB AR bandwidth is 0.1 GHz, from 5.1 to 5.2 GHz, which can be enhanced with optimization. Gain is relatively flat across the operating band at about 12 dBic. ***Figure 10a*** shows the simulated RHCP and LHCP radiation patterns in the *xoz*-plane and ***Figure 10b*** shows the RHCP and LHCP radiation patterns in the *yoz*-plane.

Note that this same design can be used to construct a 2 × 2 array, which would not only result in a wider bandwidth but also provide a 3 dB AR over a broader angle. This flexibility and scalability make the proposed antenna design suitable for a variety of applications.

CONCLUSION

A novel CP antenna design incorporates a nonuniform MS. The primary component is a corner-cut patch featuring an etched rectangle slot at its core and an off-centered coaxial feed known to enhance CP. This is encompassed by corner-cut patches forming an MS. It achieves an IBW of 2.2 GHz, equating to 40 percent from 4.4 to 6.6 GHz, with a 3 dB ARBW of 1 GHz, equating to 19 percent from 4.7 to 5.7 GHz. ■

References

1. K. Li, Y. Liu, Y. Jia and Y. J. Guo, "A Circularly Polarized High Gain Antenna with Low RCS Over a Wideband Using Chessboard Polarization Conversion Metasurfaces," *IEEE Transactions on Antennas and Propagation*, Vol. 65, No. 8, August 2017, pp. 4288–4292.
2. Y. Huang, L. Yang, J. Li, Y. Wang and G. Wen, "Polarization Conversion of Metasurface for the Application of Wide Band Low-Profile Circular Polarization Slot Antenna," *Applied Physics Letters*, Vol. 109, No. 5, August 2016.
3. X. Gao, S. Yin, G. Wang, C. Xue and X. Xie, "Broadband Low-RCS Circularly Polarized Antenna Realized by Nonuniform Metasurface," *IEEE Antennas and Wireless Propagation Letters*, Vol. 21, No. 12, December 202, pp. 2417–2421.
4. J. Cui, X. Zhao and W. Sheng, "Low Profile and Broadband Circularly Polarized Metasurface Antenna Based on Nonuniform Array," *AEU-International Journal of Electronics and Communications*, Vol. 156, August 2022.
5. N. Hussain, S. I. Naqvi, W. A. Awan and T. T. Le, "A Metasurface-Based Wideband Bidirectional Same Sense Circularly Polarized Antenna," *International Journal of RF and Microwave Computer Aided Engineering*, Vol. 30, No. 8, August 2020.
6. Y. Cheng and Y. Dong, "Bandwidth Enhanced Circularly Polarized Fabry-Perot Cavity Antenna Using Metal Strips," *IEEE Access*, Vol. 8, March 2020, pp. 60189–60198.
7. F. Qin, S. Gao, G. Wei, Q. Luo, C. Mao, C. Gu, J. Xu and J. Li, "Wideband Circularly Polarized Fabry-Perot Antenna [Antenna Applications Corner]," *IEEE Antennas and Propagation Magazine*, Vol. 57, No. 5, October 2015, pp. 127–135.
8. N. Hussain, M. Jeong, J. Park and N. Kim, "A Broadband Circularly Polarized Fabry-Perot Resonant Antenna Using a Single-Layered PRS for 5G MIMO Applications," *IEEE Access.*, Vol. 7, April 2019, pp. 42897–42907.

Low-Profile Compact Filtering Antenna Based on Characteristic Mode Analysis

Lingbu Kong, Yibo Wang, Zengjie Tao and Lin Lei
Hunan University of Information Technology, Changsha

A low-profile compact filtering antenna design is based on characteristic mode analysis (CMA). To attain a radiation null at the upper band, the antenna's TM20 mode is excited and to attain a radiation null at the lower band, its TM11 mode is excited. A new resonant mode is introduced through the introduction of an H-slot, which is referred to as the H-slot-improved TM20 mode. Analysis shows that the excitation of a TM01 mode and the improved TM20 mode contribute to the broadening of the antenna bandwidth. Measurements show a -10 dB impedance bandwidth of 10.13 percent from 3.09 to 3.42 GHz. A peak gain of 8.5 dBi is measured at 3.1 GHz. The antenna is suitable for various wireless communication systems due to its simple structure and ease of fabrication.

Prominent trends in modern communications systems include miniaturization, high integration and multifunctionality. Filters and antennas, as components of RF front ends, are typically designed independently and subsequently cascaded together using additional transmission lines to suppress undesired signals. However, this approach not only leads to increased system volume but also has the potential to degrade in-band performance due to mismatches and additional losses resulting from interconnec-

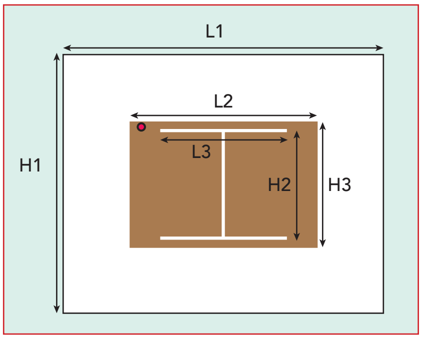

Fig. 1 Top view of the filtering antenna.

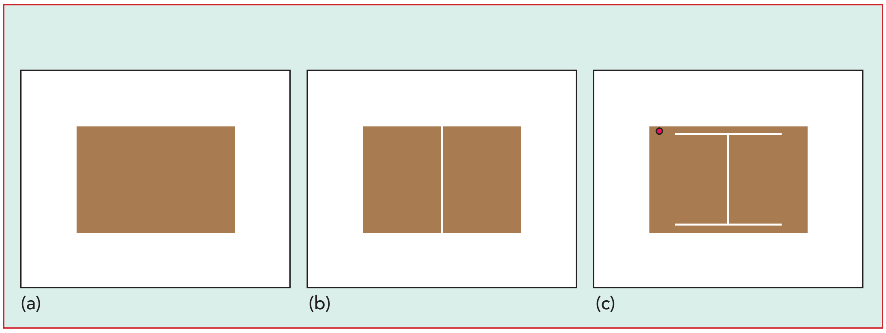

Fig. 2 Top view of the antenna design evolution: Antenna A (a), Antenna B (b) and Antenna C (c).

tions. To simplify the structure and minimize losses, researchers have shifted their focus toward developing filtering antennas that combine radiation and filtering capabilities. These antennas have attracted significant attention due to their ability to mitigate interference while providing compact form factors and optimized performance.[1-3]

In the traditional design approach, filters and antennas are designed independently and then the filtering circuitry is cascaded with the antenna. Good matching between the filter and antenna is attained through impedance transformation structures. Although this provides satisfactory filter performance, it limits integration and has high insertion loss.[4-9]

To overcome these disadvantages, filtering circuitry is integrated into the antenna feed network, where filtering performance is realized through the feed structure's design.[10-14] Parasitic elements such as branches and slots are introduced to prevent energy from radiating, thereby achieving the filtering performance. For example, transverse branch feed networks[15] and multiple branch feed networks have been employed.[16] While these antennas eliminate the need for additional filtering circuits and enhance integration, they also introduce complexity to the feed network.

In recent years, an alternative method to achieve filtering has been proposed that introduces specific structures on antennas that influence current distribution or impedance. This results in radiation nulls outside the desired frequency band. Various techniques have been studied, such as stacked patches,[17] loaded coplanar parasitic patches,[18,19] branches,[20] defected ground structures,[21] substrate-integrated waveguides with half-mode substrates[22] and fractal patches and shorting pins.[23]

The introduction of these structures not only broadens the antenna band-

TABLE 1

FILTERING ANTENNA PARAMETERS

Parameter	Value (mm)	Parameter	Value (mm)
H1	72.4	L1	91.1
H2	32.4	L2	56.1
H3	37.4	L3	38

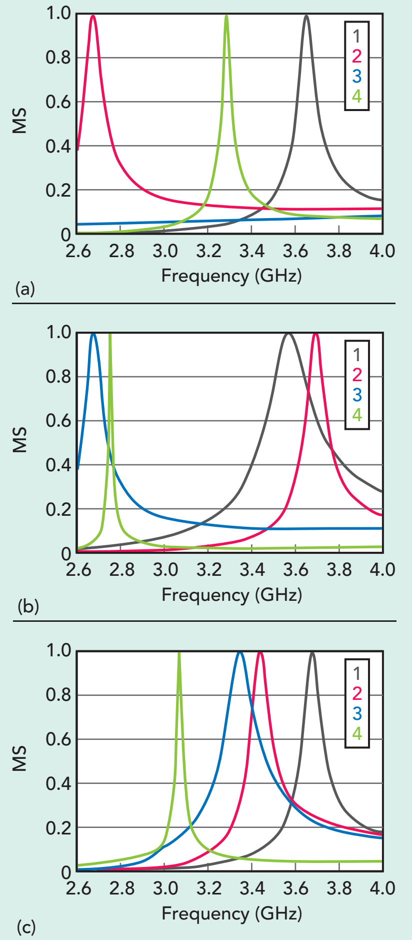

Fig. 3 Filtering antenna MS: Antenna A (a), Antenna B (b) and Antenna C (c).

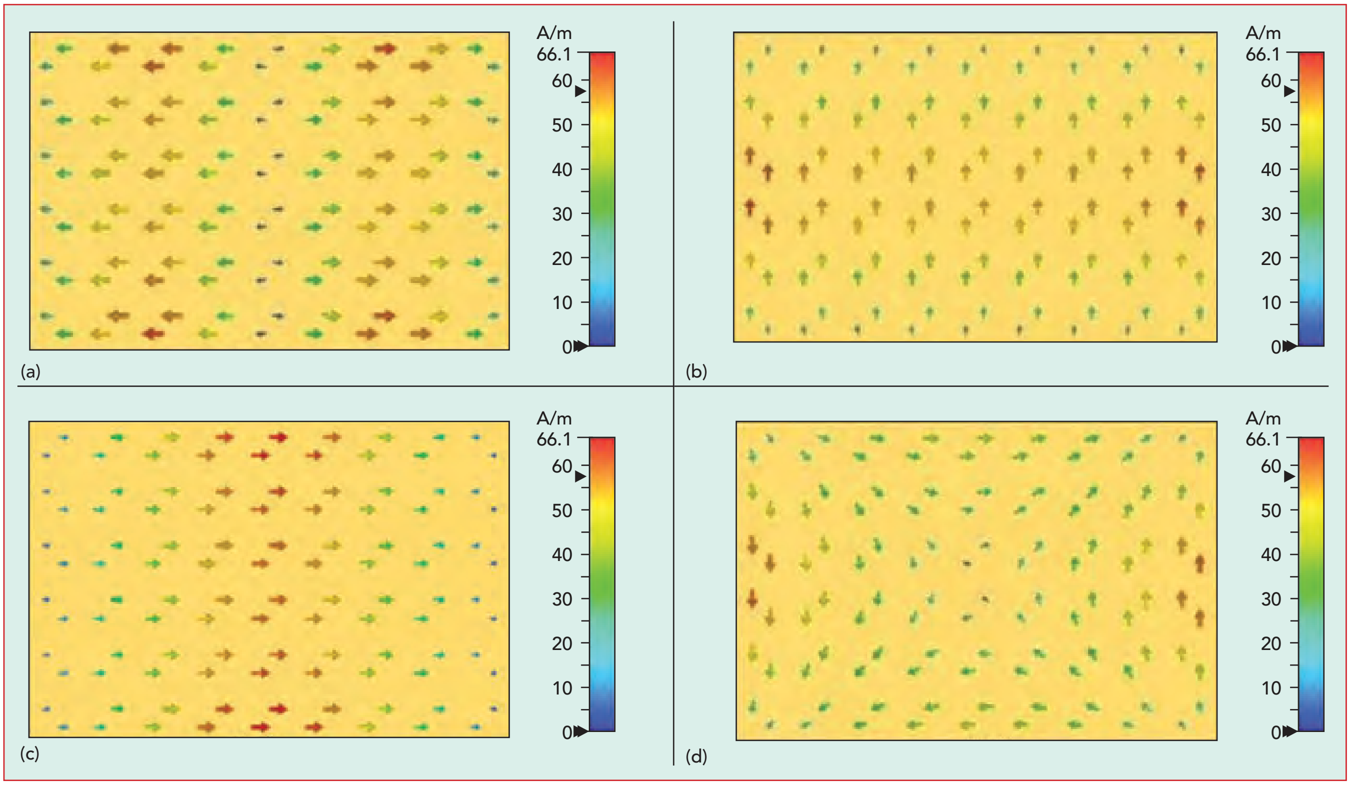

Fig. 4 Characteristic currents for Antenna A: Mode 1 (a), Mode 2 (b), Mode 3 (c) and Mode 4 (d).

width but also generates radiation nulls. However, it also leads to an increase in the antenna's physical area, profile height and complexity. For example, a filter antenna consisting of U-shaped microstrip resonators, a Γ-shaped antenna and a parallel-coupled line was proposed by Yan et al.,[24] having a low profile and a compact structure. However, the maximum gain was only 3.059 dBi.

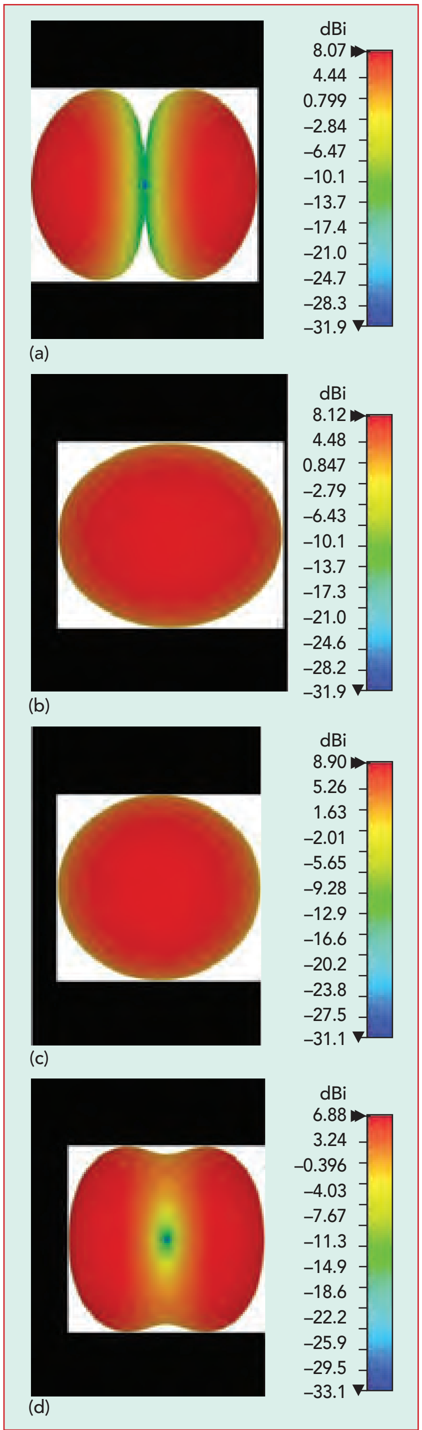

Fig. 5 Far-field patterns for Antenna A: Mode 1 (a), Mode 2 (b), Mode 3 (c) and Mode 4 (d).

In this work, a low-profile compact filtering antenna based on CMA is described. By strategically etching H-shaped slots at specific locations on the patch, four modes are generated. The TM20 mode generates radiation nulls at high frequencies, while the TM11 mode generates radiation nulls at lower frequencies. An improved TM20 mode is obtained by introducing a longitudinally oriented slot. Both the TM01 and improved TM20 modes are employed to broaden the bandwidth.

ANTENNA DESIGN AND ANALYSIS

Characteristic Mode Theory

The total current flowing on the surface of an obstacle can be decomposed into a linear superposition of orthogonal currents. ***Equation 1*** is used for determining the characteristic currents:

$$XJ_n = \lambda_n RJ_n \quad (1)$$

Where J_n denotes the nth eigenvector and λ_n represents the associated eigenvalue. The impedance operator is represented by R (real part) and X (imaginary part).

By characteristic mode theory, the expansion of the far field of the obstacle can be accomplished with characteristic fields, as shown in ***Equation 2***.

$$E = \sum_n \alpha_n E_n = \sum_n \frac{\left(E^i_{tan}(r), J_n\right)}{1 + j\lambda_n} E_n \quad (2)$$

The modal significance (MS_n) is defined in ***Equation 3*** as:

$$MS_n = \left| \frac{1}{1 + j\lambda_n} \right| \quad (3)$$

An MS_n value of 1 indicates that a specific mode is highly susceptible to excitation and conversely, an MS_n value of 0 implies that the mode is challenging to excite.

The far field is dependent on both the characteristic field and the complex weighting coefficients, α_n, as indicated by Equation 2. To generate radiation nulls, there are two methods. The first method involves generating a mode with zero characteristic fields in the desired direction. Alternatively, the other method is to choose the appropriate feed position to make $E^i_{tan}(r)$, J_n equal to zero.

In the design of filtering antennas, two types of modes are essential. The radiation mode generates a maximum radiation field in a certain direction, while the null radiation mode generates a zero-radiation field in a certain direction. As a result, it is possible to design an antenna structure in which the resonant frequency of the null radiation mode is distributed on both sides of the resonant frequency of the radiation mode.[25]

Antenna Structure Design

The antenna structure shown in ***Figure 1*** is composed of a rectangular patch etched with an H-shaped slot. A 50 Ohm SMA connector feeds the patch. The substrate material is Rogers RT5880, with a relative dielectric constant of 2.2 and a thickness of 1.5 mm. The optimized dimensions of the filtering antenna are given in ***Table 1***.

Evolution and Analysis of Filtering Antennas

The antenna evolution is shown in ***Figure 2***. In the beginning, the modal significance of the filtering antennas is simulated in CST Studio Suite 2022 and the corresponding results are shown in ***Figure 3***.

Subsequently, the characteristic currents and far-field patterns corresponding to the first four modes are shown in ***Figures 4*** through ***Figure 9***.

Figure 3a shows that Antenna A has four modes. However, Mode 3 is not considered because it is difficult to excite. The resonant frequencies of Modes 1, 2 and 4 are 3.65, 2.67 and 3.29 GHz, respectively. Figure 4 shows that Modes 1, 2 and 4 correspond to the TM20 mode, the TM01 mode and the TM11 modes, respectively. Additionally, Figure 5 shows that Mode 2 is a radiation mode, whereas Modes 1 and 4 are null radiation modes.

The resonance frequencies, listed from low to high, are Mode 2 (radiation mode), Mode 4 (null radiation mode) and Mode 1 (null radiation mode). According to the above analysis, Antenna A does not fulfill the condition of having the resonant frequency of the null radiation mode located on both sides

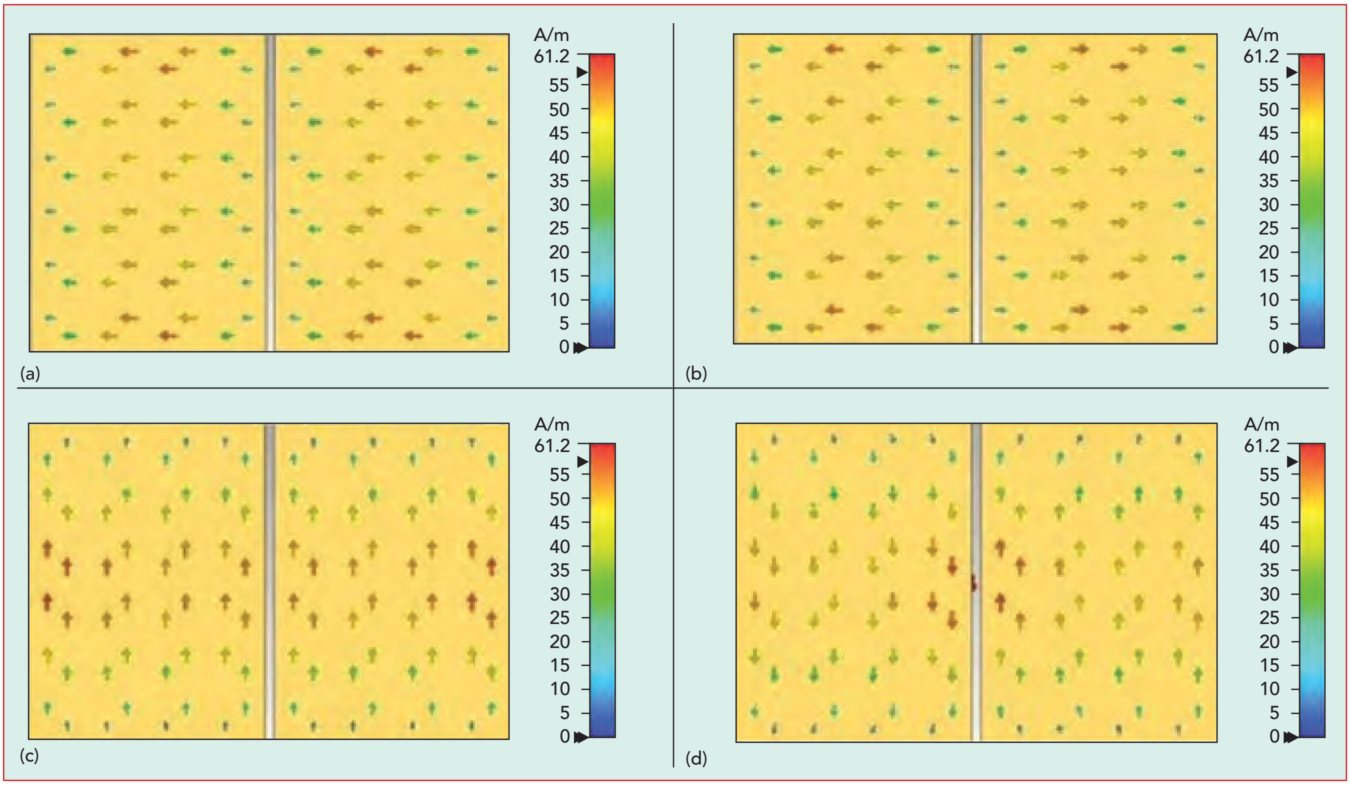

Fig. 6 **Characteristic currents for Antenna B: Mode 1 (a), Mode 2 (b), Mode 3 (c) and Mode 4 (d).**

of the radiation mode's resonance frequency. Consequently, it cannot achieve the filtering function.

From Figure 4b, it is seen that Antenna B not only has four modes but also that these four modes are easily excited. The resonant frequencies of Modes 1 through 4 are 3.56, 3.69, 2.67 and 2.75 GHz, respectively. From Figure 6, it is not difficult to find that Modes 2, 3 and 4 are the TM20 mode, TM01 mode and TM11 modes, respectively. From Figure 7, Modes 1 through 4 correspond to the radiation mode, the null radiation mode, the radiation mode and the null radiation mode, respectively.

The current distribution and far-field radiation characteristics of Mode 1 shown in Figure 6a and Figure 7a are the same as those of TM10 mode, but this mode is not TM10 mode. The electric field distribution of Mode 1 is shown in ***Figure 10*** and it is seen that the electric field directions on both sides of the longitudinal slot are opposite. Therefore, this mode is not the TM10 mode and is referred to here as the improved TM20 mode.

From Figures 6b and c, the discontinuity caused by the longitudinal slot does not affect the current distribution in Mode 2 (TM20) and Mode 3 (TM01). However, as shown in Figure 7d, the longitudinal slot does affect the current distribution of the TM11 mode. Interestingly, this effect is positive, as can be seen by comparing the far-field characteristics in Figure 5d and Figure 7d, where the longitudinal slot accentuates the zero-radiation characteristic of the TM11 mode, thus enhancing its filtering capability.

The modes for Antenna B, arranged in ascending order of resonant frequency, are Mode 3 (radiation mode), Mode 4 (null radiation mode), Mode 1 (radiation mode), and Mode 2 (null radiation mode). According to the above analysis, Antenna B satisfies the condition of having the resonant frequencies of the null radiation mode distributed on both sides of the resonant frequencies for the radiation modes. However, the resonant frequency of Mode 4 differs significantly from that of Mode 1, making it unable to achieve satisfactory filtering performance.

By adjusting the parameters of the H-slot etched on the radiating patch, the resonant frequencies of Modes 1 through 4 are tuned. From Figure 3c, it is observed that the resonant frequencies of Modes 1 through 4 are 3.65, 3.43, 3.34 and 3.05 GHz, respectively. According to the characteristic current distribution shown in Figure 8, Modes 1 through 4 correspond to the TM20 mode, the TM01 mode, an improved TM20 mode and the TM11 mode, respectively. The characteristic far-field patterns in Figure 9 show that Modes 1 through 4 correspond to null radiation, radiation, radiation and null radiation modes, respectively. For Antenna C, the modes are listed in ascending order of resonant frequencies as Mode 4 (null radiation mode), Mode 3 (radiation mode), Mode 2 (radiation mode), and Mode 1 (null radiation mode).

Based on the above analysis, Antenna C satisfies the condition of having the resonant frequencies of the null radiation modes distributed on both sides of the resonant frequencies for the radiation modes. The distribution pattern of the resonance frequencies in these four modes generates radiation nulls in the high and low frequency bands. It also simultaneously excites the TM01 mode and the improved TM20 mode, which effectively broadens the antenna's operating bandwidth.

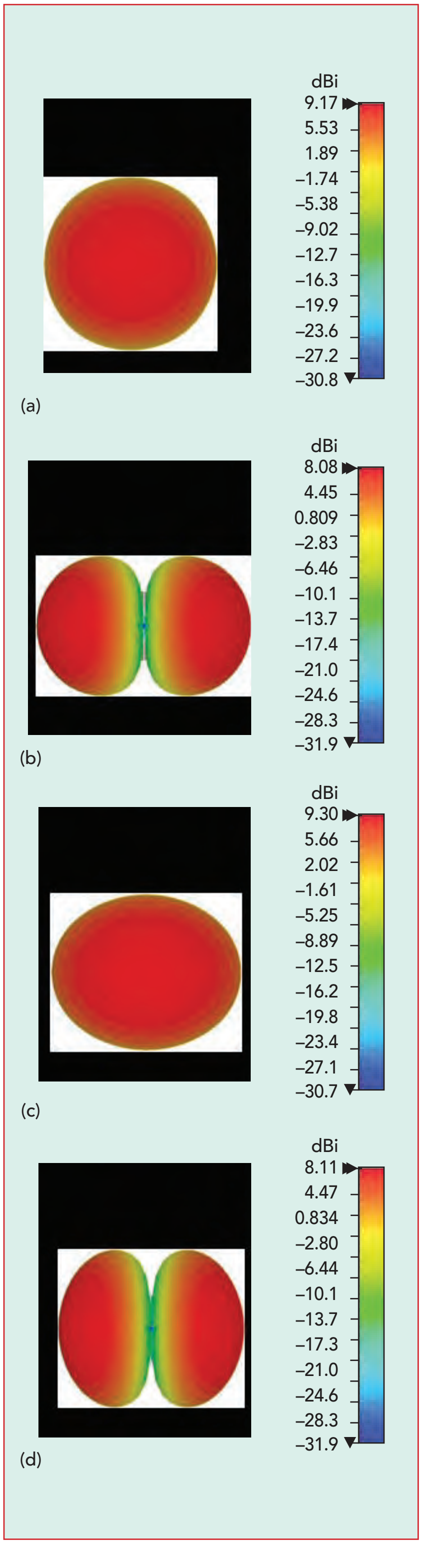

Fig. 7 Far-field patterns for Antenna B: Mode 1 (a), Mode 2 (b), Mode 3 (c) and Mode 4 (d).

ANTENNA MEASUREMENT AND DISCUSSION

The antenna prototype is shown in ***Figure 11***, with dimensions listed in Table 1. The SMA connector's outer conductor flange is soldered to the underside of the antenna, while the inner conductor is connected to the radiating patch through the substrate.

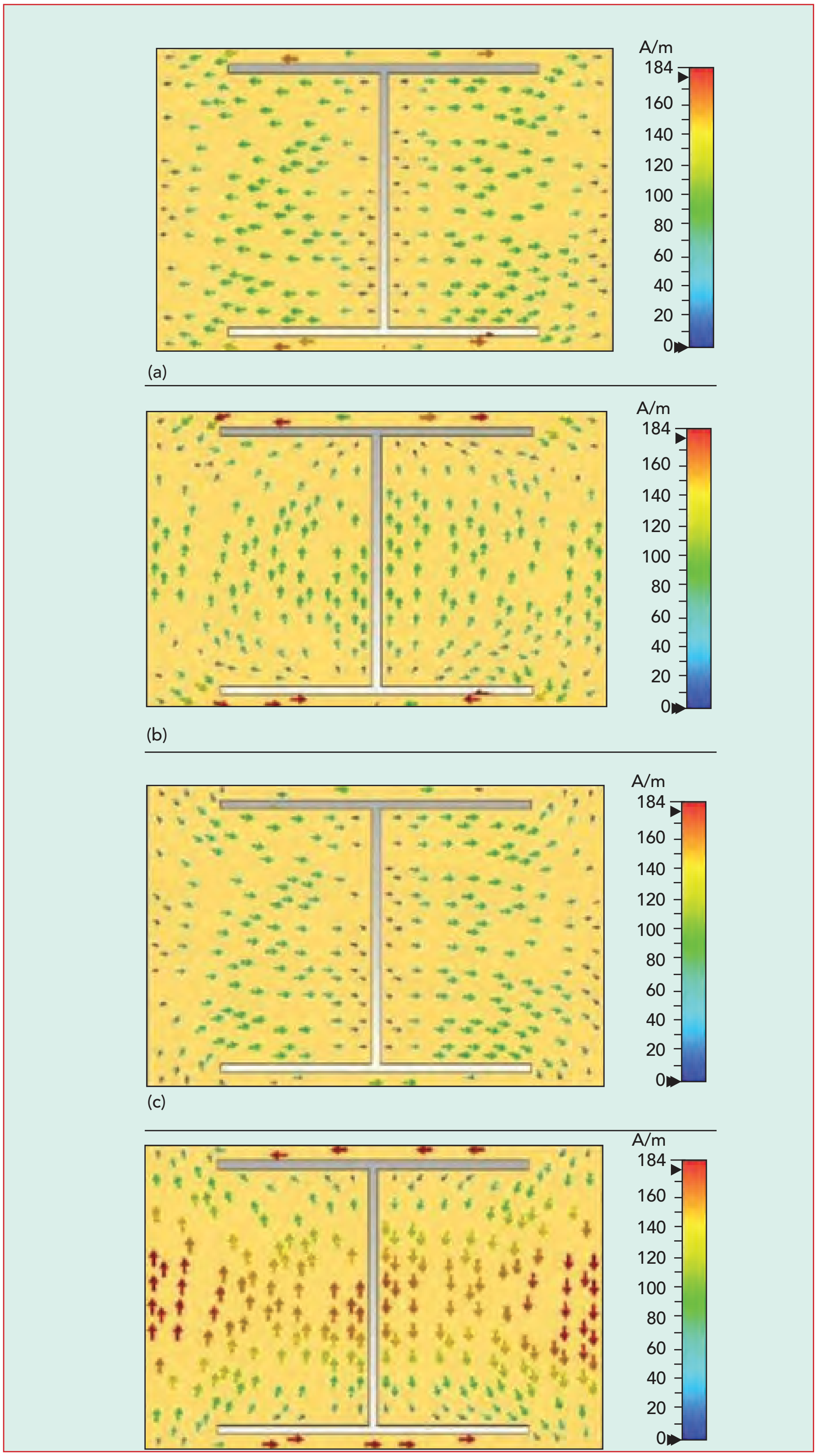

Fig. 8 Characteristic currents for Antenna C: Mode 1 (a), Mode 2 (b), Mode 3 (c) and Mode 4 (d).

$|S_{11}|$ and gain from simulations and measurements are shown in ***Figure 12***, showing close agreement. From the graph, it can be observed that there are two resonance frequencies within the passband, corresponding to Modes 2 and 3, respectively. The excitation of Modes 2 and 3 contributes to the expanded bandwidth of the antenna. The measured -10 dB impedance bandwidth is 10.13 percent (3.09 to 3.42 GHz) and the maximum antenna gain is 8.5 dBi at 3.1 GHz. Due to the excitation of Modes 1 and 4, two radiation nulls are formed at 3.51 and 2.98 GHz for out-of-band suppression in the upper and lower frequency bands. The resonances for Modes 3 and 4 occur at 3.30 and 3.19 GHz, respectively.

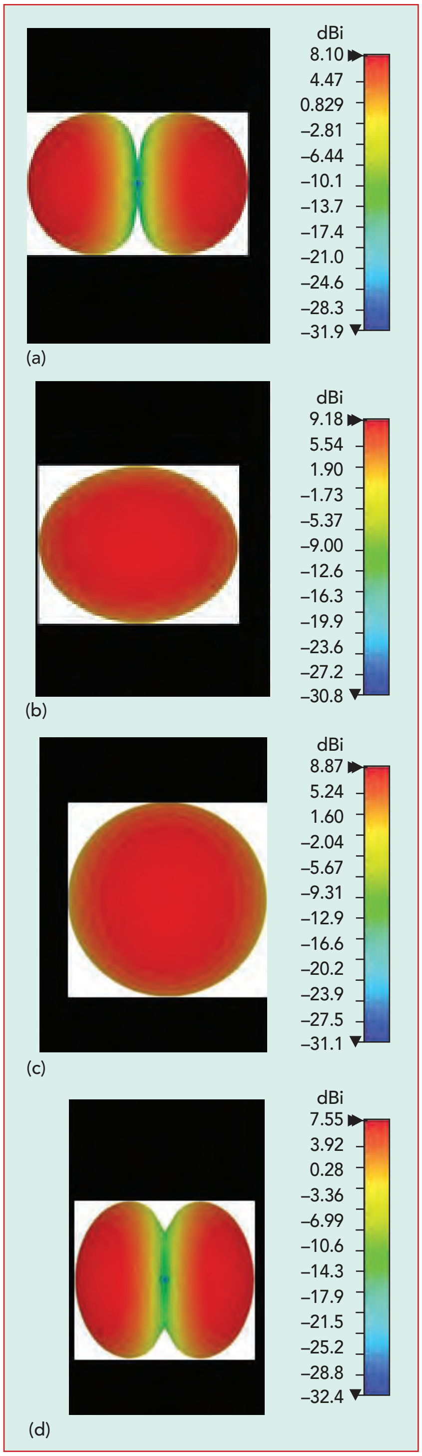

Fig. 9 **Far-field patterns for Antenna C: Mode 1 (a), Mode 2 (b), Mode 3 (c) and Mode 4 (d).**

Normalized radiation patterns of the measured and simulated filtering antenna are shown in ***Figure 13***. Figure 13a shows the E-plane results and Figure 13b the H-plane results at 3.1 GHz. Figure 13c shows the E-plane results and Figure 13d the H-plane results at 3.4 GHz. These results show good agreement between measurement and simulation. The co-polarized fields in the E- and H-planes are stronger than the cross-polarized fields by greater than 23 dB at boresight.

A comparison with other reported filtering patch antennas in ***Table 2*** shows that this antenna achieves an excellent filtering response without the need for extra filtering, consequently eliminating the additional loss associated with external filters while achieving a high gain of 8.5 dBi. Additionally, the antenna's design on a single-layer substrate enables the lowest profile.

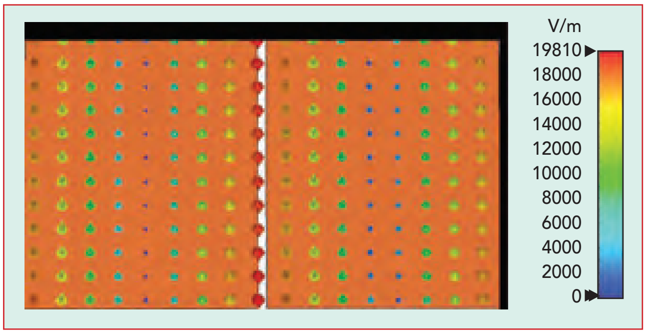

Fig. 10 **Mode 1 electric field distribution.**

Fig. 11 **Filtering antenna prototype.**

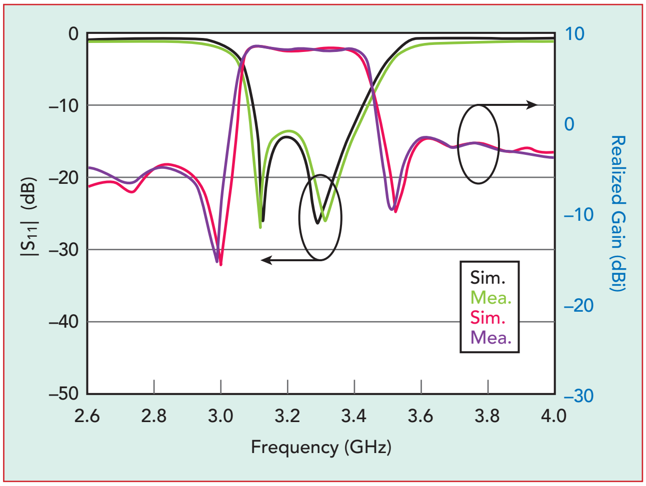

Fig. 12 **Simulated and measured $|S_{11}|$ and antenna gain.**

CONCLUSION

A low-profile compact filtering antenna is designed using the analysis of characteristic modes in the design evolution process. By adjusting the parameters of an H-shaped gap, the relative positions of radiation and null modes are controlled to achieve excellent filtering performance. The filtering antenna operates at 3.1 GHz with a gain of 8.5 dBi. Compared with previously reported antennas, it provides excellent performance in a simple, low-profile structure. ■

ACKNOWLEDGMENT

This work was supported by the Hunan Provincial Natural Science Foundation of China under Grant (2021JJ30478).

References

1. W. -J. Wu, Y. -Z. Yin, S. -L. Zuo, Z. -Y. Zhang and J. -J. Xie, "A New Compact Filter-Antenna for Modern Wireless Communication Systems," *IEEE Antennas and*

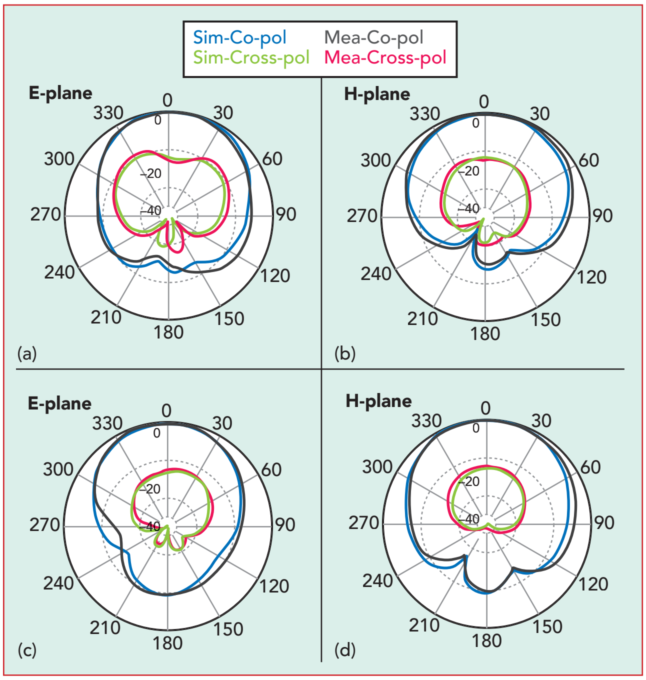

▲ **Fig. 13** **Simulated and measured radiation patterns of the filtering antenna.**

TABLE 2

PERFORMANCE COMPARISON WITH OTHER REPORTED WIDEBAND FILTERING ANTENNAS

Ref	Profile (λ_0)	Size ($\lambda_0 2$)	Peak Gain (dBi)	BW (percent)	*Roll-off (Lower/ Upper) (percent)
17	0.09	1 x 1	8.83	16	7.15/1.37
18	0.053	2.15 x 2.15	8.3	4.5	5.88/13.36
19	0.079	2.08 x 1.54	9.5	20.04	3.20/12.64
23	0.038	0.78 x 0.78	9.4	23.6	20.20/5.07
24	0.05	0.72 x 0.46	3.06	8	16.60/8.40
This Work	0.016	0.98 x 0.78	8.5	10.13	6.45/6.38

*Percent Roll-off = ($|f_{res} - f_{null}|$ / f_{res}) x 100 where f_{res} is the resonant mode frequency and f_{null} is the closest radiation null.

Wireless Propagation Letters, Vol. 10, October 2011, pp. 1131–1134.

2. J. -F. Qian, F. -C. Chen, Y. -H. Ding, H. -T. Hu and Q. -X. Chu, "A Wide Stopband Filtering Patch Antenna and its Application in MIMO System," *IEEE Transactions on Antennas and Propagation*, Vol. 67, No. 1, January 2019, pp. 654–658.
3. Y. Zhang, X. Y. Zhang and Q. H. Liu, "A Six-Port Dual-Function RF Device with Four-Element MIMO Antenna Array and Bandpass Filter Operations," *IEEE Transactions on Antennas and Propagation*, Vol. 68, No. 6, June 2020, pp. 4549–4559.
4. K. -Z. Hu, M. -C. Tang, D. Li, Y. Wang and M. Li, "Design of Compact, Single-Layered Substrate Integrated Waveguide Filtenna with Parasitic Patch," *IEEE Transactions on Antennas and Propagation*, Vol. 68, No. 2, February 2020, pp. 1134–1139.
5. J. -H. Lee, N. Kidera, S. Pinel, J. Laskar and M. M. Tentzeris, "Fully Integrated Passive Front-End Solutions for a V-band LTCC Wireless System," *IEEE Antennas and Wireless Propagation Letters*, Vol. 6, July 2007, pp. 285–288.
6. C. Lin and S. Chung, "A Filtering Microstrip Antenna Array," *IEEE Transactions on Microwave Theory and Techniques*, Vol. 59, No. 11, November 2011, pp. 2856–2863.
7. C. Yu, W. Hong, Z. Q. Kuai and H. M. Wang, "Ku-Band Linearly Polarized Omnidirectional Planar Filtenna," *IEEE Transactions on Antennas and Propagation*, Vol. 11, March 2012, pp. 310–313.
8. C. X. Mao, S. Gao, Y. Wang, B. S. Izquierdo, Z. P. Wang, F. Qin, Q. X. Chu, J. Li, G. Wei and J. Xu, "Dual-Band Patch Antenna with Filtering Performance and Harmonic Suppression," *IEEE Transactions on Antennas and Propagation*, Vol. 64, No. 9, September 2016, pp. 4074–4077.
9. C. X. Mao, L. Zhang, M. Khalily, Y. Gao and P. Xiao, "A Multiplexing Filtering Antenna," *IEEE Transactions on Antennas and Propagation*, Vol. 69, No. 8, August 2021, pp. 5066–5071.
10. M. -C. Tang, D. J. Li, Y. Wang, K. -Z. Hu and R. W. Ziolkowski, "Compact, Low-Profile, Linearly and Circularly Polarized Filtennas Enabled with Custom-Designed Feed-Probe Structures," *IEEE Transactions on Antennas and Propagation*, Vol. 68, No. 7, July 2020, pp. 5247–5256.
11. Y. Zhang, X. Y. Zhang and Y. M. Pan, "Low-Profile Planar Filtering Dipole Antenna with Omnidirectional Radiation Pattern," *IEEE Transactions on Antennas and Propagation*, Vol. 66, No. 3, March 2018, pp. 1124–1132.
12. P. F. Hu, Y. M. Pan, X. Y. Zhang and B. J. Hu, "A Filtering Patch Antenna with Reconfigurable Frequency and Bandwidth Using F-Shaped Probe," *IEEE Transactions on Antennas and Propagation*, Vol. 67, No. 1, January 2019, pp. 121–130.
13. Y. P. Li, Z. P. Zhao, Z. Y. Tang and Y. Z. Yin, "Differentially Fed, Dual-Band Dual-Polarized Filtering Antenna with High Selectivity for 5G Sub-6 GHz Base Station Applications," *IEEE Transactions on Antennas and Propagation*, Vol. 68, No. 4, April 2020, pp. 3231-3236.
14. H. -T. Hu, B. -J. Chen and C. H. Chan, "A Transparent Proximity-Coupled-Fed Patch Antenna with Enhanced Bandwidth and Filtering Response," *IEEE Access*, Vol. 9, February 2021.
15. P. F. Hu, Y. M. Pan and X. Y. Zhang, "Broadband Filtering Dielectric Resonator Antenna with Wide Stopband," *IEEE Transactions on Antennas and Propagation*, Vol. 65, No. 4, April 2017, pp. 2079–2084.
16. X. Y. Zhang, Y. Zhang, Y. -M. Pan and W. Duan, "Low-Profile Dual-Band Filtering Patch Antenna and Its Application to LTE MIMO System," *IEEE Transactions on Antennas and Propagation*, Vol. 65, No. 1, January 2017, pp. 103–113.
17. G. -Z. Liang, F. C. Chen, H. Yuan, K. -R. Xiang and Q. -X. Chu, "A High Selectivity and High Efficiency Filtering Antenna with Controllable Radiation Nulls Based on Stacked Patches," *IEEE Transactions on Antennas and Propagation*, Vol. 70, No. 1, January 2022, pp. 708–713.
18. W. -J. Yang, Y. -M. Pan and X. -Y. Zhang, "A Single-Layer Low-Profile Circularly Polarized Filtering Patch Antenna," *IEEE Antennas and Wireless Propagation Letters*, Vol. 20, No. 4, April 2021, pp. 602–606.
19. D. Yang, H. Q. Zhai, C. Z. Guo and H. K. Li, "A Compact Single-Layer Wideband Microstrip Antenna with Filtering Performance," *IEEE Antennas and Wireless Propagation Letters*, Vol. 19, No. 5, May 2020, pp. 801–805.
20. Y. -T. Liu, K. W. Leung and N. Yang, "Compact Absorptive Filtering Patch Antenna," *IEEE Transactions on Antennas and Propagation*, Vol. 68, No. 2, February 2020, pp. 633–642.
21. W. C. Yang, M. Z. Xun, W. Q Che, W. J. Feng, Y. Q. Zhang and Q. Xue, "Novel Compact High-Gain Differential-Fed Dual-Polarized Filtering Patch Antenna," *IEEE Transactions on Antennas and Propagation*, Vol. 67, No. 12, December 2019, pp. 7261–7271.
22. K. -Z. Hu, M. -C. Tang, D. J. Li, Y. Wang and M. Li, "Design of Compact, Single-Layered Substrate Integrated Waveguide Filtenna with Parasitic Patch," *IEEE Transactions on Antennas and Propagation*, Vol. 68, No. 2, February 2020, pp. 1134-1139.
23. J. C. Zhu, G. M. Zhang, Z. H. Li, Z. E. Che, J. Yue, Y. H. Feng, Q. Zhang and R. Qiu, "A High-Gain, Low-Profile Filtering Antenna Based on a Novel Metasurface," *The Applied Computational Electromagnetics Society Journal*, Vol. 37, No. 11, April 2023, pp. 1153–1161.
24. S. J. Yan, C. Q. Zhang, Q. Chen and M. S. Tong, "A Novel Compact Filtering Antenna for 5.0-GHz WLAN Communication System," *The Applied Computational Electromagnetics Society Journal*, Vol. 37, No. 09, February 2023, pp. 996–1004.
25. B. K. Lau, M. Capek and A. M. Hassan, "Characteristic Modes: Progress, Overview, and Emerging Topics," *IEEE Antennas & Propagation Magazine*, Vol. 64, No. 2, April 2022, pp. 14–22.